

The study of energy transport by consistent quantum histories

LI HUANAN

NATIONAL UNIVERSITY OF SINGAPORE

2013

The study of energy transport by consistent
quantum histories

LI HUANAN

(B.Sc., Sichuan University)

A THESIS SUBMITTED
FOR THE DEGREE OF DOCTOR OF PHILOSOPHY
DEPARTMENT OF PHYSICS
NATIONAL UNIVERSITY OF SINGAPORE
2013

©

Copyright by

HUANAN LI

2013

All rights reserved

Declaration

I hereby declare that the thesis is my original work and it has been written by me in its entirety. I have duly acknowledged all the sources of information which have been used in the thesis.

This thesis has also not been submitted for any degree in any university previously.

Li Huanan

Huanan Li

November 18, 2013

Acknowledgements

I always enjoy reading the acknowledgment when I read other students' Ph.D thesis, because it is usually considered as the most personal part, where I find myself today. The few pages of acknowledgments are not only an opportunity to say thank you to all the people who helped me selflessly, but more importantly also a chance to recall all the memories I had throughout this whole experience.

First and foremost I want to express my sincerest gratitude to my supervisor Professor Wang Jian-Sheng, who is a real 'teacher' teaching me how to overcome difficulties, how to do research. Without his guidance and selfless help, these works for the thesis could not have being done. My gratitude extends to Prof. Gong Jiangbin for his kindness on writing a recommendation letter for me.

I want to thank Dr. Yeo Ye and Dr. Wang Qinghai for their excellent teaching in the courses of advanced quantum mechanics and quantum field theory. I frequently remember the discussion after class with Dr. Yeo Ye.

I am grateful to my collaborators Dr. Bijay K. Agarwalla and Dr. Eduardo Cuansing.

I would like to thank our group members Dr. Jiang Jinwu, Dr Lan Jinghua, Dr.

Juzar Thingna, Dr. Zhang Lifa, Dr. Liu Sha, Dr. Leek Meng Lee, Dr. J. L. García-Palacios, Mr. Zhou Hangbo for the exciting and fruitful discussions.

I cherish the times in NUS with my friends Mr. Luo Yuan and Mr. Gong Li.

Last but not least, I would like to thank my parents and my fiancée Zeng Jing for their constant support and love.

Table of Contents

Acknowledgements	iii
Abstract	viii
List of Publications	xi
List of Figures	xii
1 Introduction	1
1.1 Energy transport	2
1.2 Probability distribution of energy transferred	5
1.3 Consistent quantum theory	6
1.3.1 Terminology	7
1.3.2 How to assign a probability to a quantum history?	9
1.3.3 How to assign probabilities to a family of histories?	11
1.4 Objectives	13
2 Nonequilibrium Green's function method	16
2.1 Pictures in quantum mechanics	17
2.2 Contour-ordered Green's Function	20

2.2.1	Motivation for closed-time contour	20
2.2.2	Exploring the definition	22
2.2.3	The basic formalism	25
2.2.4	The connection to conventional Green's functions	32
2.3	Transient and nonequilibrium steady state in NEGF	37
3	Energy transport in coupled left-right-lead systems	49
3.1	Formalism	52
3.1.1	Model system	52
3.1.2	Steady-state contour-ordered Green's functions	53
3.1.3	Generalized steady-state current formula	55
3.1.4	Recovering the Caroli formula and deriving an interface formula	58
3.2	An illustrative application	59
3.3	Explicit interface transmission function formula	63
3.4	Summary	65
4	Distribution of energy transport in coupled left-right-lead systems	66
4.1	Large deviation theory	67
4.2	Model and consistent quantum framework for the study of energy transport	71
4.3	Cumulant generating function (CGF)	74
4.4	The steady-state CGF	78
4.5	The steady-state fluctuation theorem (SSFT) and cumulants	81
4.6	Summary	83

4.7	Appendix: CGF of energy transport under quasi-classical approximation in harmonic networks	84
5	Distribution of energy transport across nonlinear systems	94
5.1	Model and the general formalism	95
5.2	Interaction picture on the contour	99
5.3	Application to molecular junction	104
5.4	Summary	108
5.5	Appendix: The Wick Theorem (Phonons)	109
6	Summary and future works	114
	References	117

Abstract

In this thesis, we consider energy transport or equivalently thermal transport in insulating lattice systems. We typically establish the nonequilibrium processes by sudden switching on the (linear) coupling between the leads and the junction, which are initially in their respective thermal equilibrium states. Since the leads are semi-infinite, the temperatures of the leads are maintained in their initial values.

We have first examined if, when, and how the onset of the steady-state thermal transport occurs by determining the time-dependent thermal current in a phonon system consisting of two linear chains, which are abruptly attached together at initial time. The crucial role of the on-site pinning potential in establishing the steady state of the heat transport was demonstrated both computationally and analytically. Also the finite-size effects on the thermal transport have been carefully studied. Furthermore, using this specific model, we have explicitly verified the subtle assumption employed in the nonequilibrium Green's function (NEGF) method that the steady-state thermal transport could be reached even for ballistic systems after long enough time.

The Landauer formula describing the steady-state thermal current assumes that

the two leads are decoupled. However, through modern nanoscale technology, a small junction is easily realized and frequently used in real experiments so that the coupling between the two leads is inevitable due to long-range interaction. Thus using the NEGF method, we have established a generalized Landauer-like formula explicitly taking the lead-lead coupling into account, which is computationally efficient to calculate steady-state heat current across various junctions.

To fully understand thermal transport, the distribution of heat transfer in a given time duration is desired. From consistent quantum history point of view, we have analytically obtained the cumulant generating function (CGF) formula of heat transfer in general coupled left-right-lead systems, which contains valuable information on microscopic transport process not available from current and considers transient and steady-state on an equal footing. It has been noticed that the coupling between the leads does not affect the validity of the Gallavotti-Cohen (GC) symmetry. In addition, the CGF can be directly used to obtain probability distribution of heat transfer based on the fundamental principle of the large deviation theory. Using the CGF formula, we have partly answered a question raised by Caroli et al. in 1971 regarding the (non)equivalence between the partitioned and partition-free approaches. Also, in the corresponding appendix, we have obtained the CGF formula under quasi-classical approximation, which ‘nearly’ match the pure quantum result to the second cumulant.

Finally, we have established a general formalism to study the distribution of heat transfer across arbitrary nonlinear junctions. Based on the nonequilibrium Feynman-Hellman method, we have related the CGF with the generalized contour-ordered Green’s function depending on the counting field in phononic systems. By

introducing the interaction picture defined on the contour, the closed equations for calculating the generalized contour-ordered Green's functions are obtained. This formalism is meaningful for the analysis of phononics involving the nonlinearity, which is the counterpart technology of electronics.

In conclusion, we have established a general formalism to study various aspects of quantum thermal transport using the unified language of consistent quantum theory. The study in this thesis may further our understanding on the statistical properties of quantum thermal transport and gives guidelines to experimentalists for devising transport devices at the nanoscale.

List of Publications

- [1] B. K. Agarwalla, H. Li, B. Li, and J.-S. Wang, “Heat transport between multi-terminal harmonic systems and exchange fluctuation theorem” (submitting).
- [2] J.-S. Wang, B. K. Agarwalla, H. Li, and J. Thingna, “Nonequilibrium Green’s function method for quantum thermal transport”, Front. Phys. (2013).
- [3] H. Li, B. K. Agarwalla, B. Li, and J.-S. Wang, “Cumulants of heat transfer in nonlinear quantum systems”, arXiv:1210.2798.
- [4] H. Li, B. K. Agarwalla, and J.-S. Wang, “Cumulant generating function formula of heat transfer in ballistic systems with lead-lead coupling”, Phys. Rev. B **86**, 165425 (2012).
- [5] H. Li, B. K. Agarwalla, and J.-S. Wang, “Generalized Caroli formula for the transmission coefficient with lead-lead coupling”, Phys. Rev. E **86**, 011141 (2012).
- [6] E. C. Cuansing, H. Li, and J.-S. Wang, “Role of the on-site pinning potential in establishing quasi-steady-state conditions in heat transport in finite quantum systems”, Phys. Rev. E **86**, 031132 (2012).
- [7] J.-S. Wang, B. K. Agarwalla, and H. Li, “Transient behavior of full counting statistics in thermal transport”, Phys. Rev. B **84**, 153412 (2011).

List of Figures

2.1	Contour C used to define the nonequilibrium Green's functions . . .	21
2.2	An illustration for the Dyson equation satisfied by $G_{LC}(\tau_2, \tau_1)$. . .	30
2.3	An illustration for the Dyson equation satisfied by $G_{CC}(\tau_2, \tau_1)$. . .	31
2.4	An illustration of combining two finite independent systems	37
2.5	Plots of the current as a function of time in the absence of on-site potential	44
2.6	Plots of the current as a function of time in the presence of on-site potential	45
3.1	An illustration of the model before (after) repartitioning the total Hamiltonian.	60
3.2	The transmission coefficient as a function of frequency	62
5.1	The first three steady-state cumulants with nonlinear strength . . .	107

Chapter 1

Introduction

Quantum thermal transport is an active research field in nonequilibrium statistical mechanics. In insulating lattice systems, the energy transport is carried mainly by phonons—quantized vibration modes, in the case of which we can equally well say heat transport or thermal transport. During the recent decades, it becomes feasible to manufacture devices with sizes of 10–100 nm. Thus we are now at a new stage of control energy and matter at nanoscale. At these scales quantum effects dominate almost all properties of such systems including their thermal conductivity and thermal fluctuation. For example, the quantized thermal conductance was observed at low temperatures [1], which showed conclusive phonon ballistic transport. Even in the electronic case, the real-time counting of electrons tunneling through a quantum dot has been performed [2], which involves the probability distribution of the transferred particle number. However, the phonon counting is a little tricky since the number of phonons is not a conserved quantity [3]. Therefore,

what we really care is the amount of energy, a continuous variable, transported out of a subsystem in a given time duration.

The study of energy transport involves not only the frequently calculated steady thermal current, but also the higher-order cumulants of the cumulant generating function (CGF) of the energy transferred or even the corresponding probability distribution, which satisfies certain ‘fluctuation theorem’ [4, 5]. All these problems will be studied by using the unified language of consistent quantum theory. In the following, we will introduce the research status of energy transport and the probability distribution of the energy transferred and the fundamental knowledge of consistent quantum theory separately.

1.1 Energy transport

In recent years there has been a huge increase in the research and development of nanoscale science and technology, with the study of energy and electron transport playing an important role. Focusing on thermal transport, Landauer-like results for the steady-state heat flow have been proposed earlier [6, 7]. Subsequently, based on the quantum Langevin equation approach, many authors successfully obtained a Landauer-type expression [8–10]. Alternatively, the nonequilibrium Green’s function (NEGF) method has been introduced to investigate mesoscopic thermal transport, which is particularly suited for the use with ballistic thermal transport and readily allows the incorporation of nonlinear interactions [11–13]. Generally speaking, in the lead-junction-lead system, the steady-state heat current

of ballistic thermal transport flowing from left lead to right lead has been described by the Landauer-like formula, which was derived first for electrical current, as

$$I = \int_0^\infty \frac{d\omega}{2\pi} \hbar\omega T[\omega] (f_L - f_R), \quad (1.1)$$

where $f_{\{L,R\}} = \{\exp(\hbar\omega/k_B T_{\{L,R\}}) - 1\}^{-1}$ is the Bose-Einstein distribution for phonons, and $T[\omega]$ is the transmission coefficient. Based on the NEGF method, $T[\omega]$ can be calculated through the Caroli formula in terms of the Green's functions of the junction and the self-energies of the leads,

$$T[\omega] = \text{Tr}(G^r \Gamma_R G^a \Gamma_L), \quad (1.2)$$

where $G^{r,a}$ is the Green's function of the junction, and

$$\Gamma_{\{L,R\}} = i(\Sigma_{\{L,R\}}^r - \Sigma_{\{L,R\}}^a), \quad (1.3)$$

where the self-energy terms $\Sigma_{\{L,R\}}^{r,a}$ are due to the semi-infinite leads on the left, L , and on the right, R , respectively. The superscript r and a denote retarded and advanced, respectively, both for the self-energies as well as for the Green's functions in the formula. We will recover this Caroli formula explicitly in the Subsec. 3.1.4 of the Chapter 3, by when all the relevant terminologies will automatically become clear. The specific form (1.2) was given from NEGF formalism by Meir and Wingreen [14] for the electronic case and later by Yamamoto and Watanabe for phonon transport [15], while Caroli *et al.* first obtained a formula for the electronic transport in a slightly more restricted case [16]. Also, Mingo *et al.* have derived a similar expression for transmission coefficient using an “atomistic Green's function” method [17, 18]. Very recently, Das and Dhar [19] derived the Landauer-like expression from the plane-wave picture using the Lippmann-Schwinger scattering approach.

The Landauer-like formula describes the situation in which the junction is small enough compared to the coherent length of the waves so that it could be treated as elastic scattering where the energy is conserved. Furthermore, it has been assumed that the two leads are decoupled, which physically means there is no direct tunneling between the two leads. Through modern nanoscale technology, a small junction is easily realized in certain nanoscale systems, for instance, a single molecule or, in general, a small cluster of atoms between two bulk electrodes. In that case, the electrode surfaces of the bulk conductors may be separated by just a few angstroms so that some finite electronic coupling between the two surfaces is inevitable, taking into account the long-range interaction. In order to solve this problem, Di Ventra suggested that [20] we can choose our “sample” region (junction) to extend several atomic layers inside the bulk electrodes, where screening is essentially complete, so that the above coupling could be negligible. This turns out to be correct when using this trick to avoid the interaction between the two leads, which will be discussed in the Chapter 3, even though we, to some limited extent, modify the initial condition necessary to derive a Landauer-like formula in NEGF formalism and repartition the total Hamiltonian. However, this procedure could not be always done, due to some topological reason, such as studying heat current in the Rubin model [21], in which the other end of the two semi-infinite leads is connected (a ring problem). Actually this somewhat trivial example is not so artificial since it is equivalent to using a periodic boundary condition in the Rubin model. Furthermore, the modification of the initial product state will certainly affect the behavior of the transient heat current. If we want to study the transient and steady heat current [22] in a unified way, the repartitioning procedure, which changes the model, is not acceptable.

1.2 Probability distribution of energy transferred

The physics of nonequilibrium many-body systems is one of the most rapidly expanding areas of theoretical physics. In the combined field of non-equilibrium states and statistics, the distribution of transferred charges in the electronic case or heat in the phononic case, the so-called full counting statistics (FCS), plays an important role, according to which we could understand the general features of currents and their fluctuations. Also, it is well known that the noise generated by nanodevices contains valuable information on microscopic transport processes not available from only transient or steady current. In FCS, the key object we need to study is the CGF, which presents high-order correlation information of the corresponding system for the transferred quantity.

The study of the FCS started from the field of electronic transport pioneered by Levitov and Lesovik, who presented an analytical result for the CGF in the long-time limit [23]. After that, many works followed in electronic FCS [4, 24–26], while much less attention is given to phonon transport. Saito and Dhar were the first ones to borrow this concept for thermal transport [27]. Later, Ren and co-workers gave results for two-level systems [28]. And very recently, transient behavior and the long-time limit of CGF have been obtained in lead-junction-lead harmonic networks both classically and quantum-mechanically using the Langevin equation method and NEGF method, respectively [29–31]. Experimentally, the FCS in the electronic case has been carefully studied, and the cumulants to very high orders have been successfully measured in quantum-dot systems [2, 32]. In principle, similar measurements could be carried out for thermal transport, e.g., in

a nanoresonator system. Again, whether Di Ventra’s trick that repartitioning the total Hamiltonian for the case of small junctions applies to all the higher cumulants of heat transfer in steady state is still a question, which we will discuss in Chapter 4. Obviously, this trick can not be applied to study the transient behavior of all the cumulants of heat transfer. On the other hand, although some works have already been devoted to the analysis of fluctuation considering the effect of nonlinearity in the classical limit through Langevin simulations [27], or approximately in a restricted electronic transport case, such as the FCS in molecular junctions with electron-phonon interaction [33], the present works are mainly restricted to noninteracting systems [26, 30, 34]. Also, so far the developed approaches dealing with nonlinear FCS problems mainly focus on single-particle systems, such as Ref. [35].

1.3 Consistent quantum theory

In this section, we briefly introduce the consistent quantum theory due to Griffiths, which will be used to properly assign probabilities to certain sequences of quantum events in a closed system while probability distribution of heat transferred is our main concern in this thesis. The consistent histories approach was first proposed by Robert Griffiths in 1984 [36], and further developed by Roland Omnès in 1988 [37], and by Murray Gell-Mann and James Hartle, who used the term “decoherent histories”, in 1990 [38]. For more detail about the consistent quantum theory, one may refer to Ref. [39].

1.3.1 Terminology

Physical property refers to something which can be said to be either true or false for a particular physical system. And a physical property of a quantum system is associated with a subspace \mathcal{P} of the quantum Hilbert space \mathcal{H} , onto which the (orthogonal) projector P plays a key role. The projector P satisfies two conditions

$$P^\dagger = P, P^2 = P, \quad (1.4)$$

where the superscript \dagger means hermitian conjugate.

If the state $|\Psi\rangle$ describing the quantum system lies in the subspace \mathcal{P} so that $P|\Psi\rangle = |\Psi\rangle$, one can say the quantum system has the property P ; On the other hand, if $P|\Psi\rangle = 0$, then one say the quantum system does not have the property P . When the state $|\Psi\rangle$ is not an eigenstate of P , we will say that the property P is undefined for the quantum system, which does not have the classical counterpart.

Considering two different quantum properties P and Q , we can have three *logical operations*:

Negation of \tilde{P} : $\tilde{P} \equiv I - P$ is defined as the property which is true if and only if P is false, and false if and only if P is true.

Conjunction of P and Q : $P \wedge Q \equiv PQ$ in the case of $[P, Q] = 0$. Furthermore, If $PQ = QP = 0$, i.e., P and Q are mutually orthogonal, the corresponding properties are said to be *mutually exclusive*.

Disjunction of P and Q : $P \vee Q \equiv P + Q - PQ$ in the case of $[P, Q] = 0$.

One can easily verify that the results after logical operations are still projectors. We must point out that if the two projectors P and Q do not commute with each other, the two properties of any quantum system are *incompatible* and it makes no sense to ascribe both properties to a single system at the same instant of time so that $P \wedge Q$ and $P \vee Q$ are meaningless.

A decomposition of the identity was defined to be a collection of mutually orthogonal projectors P_j , which sum to the identity, i.e., $I = \sum_j P_j$. Then a *Quantum sample space* is taken as any decomposition of the identity, corresponding to which the *quantum event algebra* consists of all projectors of the form $R = \sum_j \pi_j P_j$ with each π_j equal to 0 or 1. Certainly, the decomposition of the identity is not unique.

As we know, a quantum physical variable is represented by a Hermitian operator on the Hilbert space. For every Hermitian operator, there is a unique decomposition of the identity $\{P_j\}$, determined by the Hermitian operator A so that

$$A = \sum_j a_j P_j, \tag{1.5}$$

where the $\{a_j\}$ are the eigenvalues of A and $a_j \neq a_k$ for $j \neq k$. In this case, the collection $\{P_j\}$ is the natural quantum sample space for the physical variable A .

Perhaps the most important concept in consistent quantum theory is quantum histories, a realization of which consists of a sequence of quantum events occurred at successive times. A quantum event at a particular time can be any quantum property of the system so that it can be represented by a projector. Therefore, given a finite set of times $t_1 < t_2 < \dots < t_f$, a specific quantum history can be

specified by a collection of projectors $\{P_1, P_2, \dots, P_f\}$, which is expressed by

$$Y = P_1 \odot P_2 \odot \dots \odot P_f, \quad (1.6)$$

where \odot is a variant of the tensor product symbol \otimes , emphasizing that the factors in the quantum history refer to different times. Thus $Y^\dagger = Y = Y^2$ and Y itself is also a projector. So we can define a history Hilbert space as a tensor product

$$\check{\mathcal{H}} = \mathcal{H}_1 \odot \mathcal{H}_2 \odot \dots \odot \mathcal{H}_f, \quad (1.7)$$

where \mathcal{H}_j is a copy of the Hilbert space \mathcal{H} used to describe the system at a single time t_j . Then the quantum history Y is just a single element in the history Hilbert space $\check{\mathcal{H}}$. Also all the logical operations are equally well suited to quantum histories.

Next we can similarly define a sample space of quantum histories, which is a decomposition of the identity on the history Hilbert space $\check{\mathcal{H}}$:

$$\check{I} = \sum_{\alpha} Y^{\alpha}. \quad (1.8)$$

Here, the superscript α label a specific quantum history of the form Eq. (1.6). Associated with a sample space of histories is a quantum history algebra, called a *family of histories*, consisting of projectors of the form

$$Y = \sum_{\alpha} \pi^{\alpha} Y^{\alpha} \quad (1.9)$$

with each π^{α} equal to 0 or 1.

1.3.2 How to assign a probability to a quantum history?

In standard quantum mechanical textbooks, see Eg. [40], the Born rule is the unique way to assign the probability to a quantum event. Now let us consider a

simple situation in which the initial state is specified by a normalized ket $|\psi_0\rangle$ at time t_0 . And the system evolves to time t_1 according to the Schrödinger equation, when the physical variable A is measured. Then the probability $P(a_n)$ of obtaining the eigenvalue a_n is

$$P(a_n) = \sum_{i=1}^{g_n} |\langle u_n^i | U(t_1, t_0) |\psi_0\rangle|^2, \quad (1.10)$$

where $U(t_1, t_0)$ is the evolution operator, $|u_n^i\rangle$, $i = 1, 2, \dots, g_n$ are orthonormalized eigenvectors associated with the eigenvalue a_n of the physical variable A and g_n is the degree of degeneracy of a_n . The (orthogonal) projector onto the subspace associated with the eigenvalue a_n is expressed as

$$P_1^{a_n} = \sum_{i=1}^{g_n} |u_n^i\rangle \langle u_n^i|. \quad (1.11)$$

By virtue of this projector $P_1^{a_n}$, the normalized state after the measurement at time t_1 is simply

$$|\psi(t_1^+)\rangle = \frac{P_1^{a_n} U(t_1, t_0) |\psi_0\rangle}{\sqrt{\langle \psi_0 | U(t_0, t_1) P_1^{a_n} U(t_1, t_0) | \psi_0 \rangle}}. \quad (1.12)$$

This state $|\psi(t_1^+)\rangle$ continues to evolve unitarily until the next measurement is performed, corresponding to which is another projector $P_2^{b_m}$ onto the subspace associated with the eigenvalue b_m of another quantum variable B .

Actually the whole process can be re-expressed by the compact language in the consistent quantum theory. What we study here is the join probability of the quantum event

$$Y = |\psi_0\rangle \langle \psi_0| \odot P_1^{a_n} \odot P_2^{b_m}. \quad (1.13)$$

For convenience, we can introduce the *chain operator* $K(Y)$ and its adjoint $K^\dagger(Y)$,

given by

$$K^\dagger(Y) = |\psi_0\rangle \langle\psi_0| U(t_0, t_1) P_1^{a_n} U(t_1, t_2) P_2^{b_m}, \quad (1.14)$$

which is obtained by replacing \odot s with the corresponding evolution operators inside the expression for the quantum event Y . Then the joint probability of the quantum event Y is just

$$\Pr(Y) = \text{Tr} (K^\dagger(Y) K(Y)), \quad (1.15)$$

which is easily verified using the standard quantum mechanical language shown above.

In more general case, the initial state is specified by a density matrix ρ^{ini} instead of pure state $|\psi_0\rangle$. One can similarly show that the joint distribution for the quantum history $Y = I \odot P_1^{a_n} \odot P_2^{b_m}$ is

$$\Pr(Y) = \text{Tr} (\rho^{ini} K^\dagger(Y) K(Y)), \quad (1.16)$$

In the quantum history Y , I is the identity operator since we have not performed any measurement at initial time t_0 and have already explicitly written down the initial condition ρ^{ini} in the right-hand side of Eq. (1.16). In addition, one can convince himself that this approach can be applied to any quantum history.

1.3.3 How to assign probabilities to a family of histories?

At first glance, one might consider this section to be the same as the last section. However, the focus of the attention of this section is completely different. According to the probability theory, probabilities should be assigned to a sample space and satisfy three fundamental axioms [41]:

1. The probability of an event is a non-negative real number.
2. The probability that some elementary event in the entire sample space will occur is 1.
3. Any countable sequence of mutually exclusive events satisfies additive rule.

We can easily verify that the probabilities assigned to any quantum sample space satisfy the first and second axiom. However the third axiom require much more attention, which impose strong restrictions on the choice of the family of histories. Mathematically, this restrictions turn out to be *consistency conditions* which we will discuss now.

Suppose the quantum sample space we are considering is a decomposition of $\{Y^\alpha\}$ of the history identity. Then any quantum history in this sample space can be expressed as

$$Y = \sum_{\alpha} \pi^{\alpha} Y^{\alpha}, \quad (1.17)$$

with each π^{α} equal to 0 or 1. According to the third axiom of probability theory, the probability of the quantum history Y is equal to

$$\Pr(Y) = \sum_{\alpha} \pi^{\alpha} \Pr(Y^{\alpha}) = \sum_{\alpha} \pi^{\alpha} \text{Tr}(\rho^{ini} K^{\dagger}(Y^{\alpha}) K(Y^{\alpha})) \quad (1.18)$$

However, the joint probabilities assigned to the quantum histories according to the Born rule, see Eq. (1.16), do not necessarily satisfy Eq. (1.18). With the chain operator being a linear map, according to Eq. (1.17) we know that

$$K(Y) = \sum_{\alpha} \pi^{\alpha} K(Y^{\alpha}) \quad (1.19)$$

Thus, employing the general formula for the probability of a quantum history Eq. (1.16), we have

$$\Pr(Y) = \sum_{\alpha} \sum_{\beta} \pi^{\alpha} \pi^{\beta} \text{Tr} \left(\rho^{ini} K^{\dagger}(Y^{\alpha}) K(Y^{\beta}) \right). \quad (1.20)$$

We observe that Eq. (1.18) and Eq. (1.20), coming from the third axiom of probability theory and the Born rule respectively, are generally not equal. And we immediately realized that a sufficient condition for probabilities in a quantum sample space satisfying the axiom of probability theory is

$$\text{Tr} \left(\rho^{ini} K^{\dagger}(Y^{\alpha}) K(Y^{\beta}) \right) = 0, \quad \forall \alpha \neq \beta, \quad (1.21)$$

which are known as consistency conditions. A quantum sample space which fulfills consistency conditions will be referred as a *consistent quantum framework*, and the approach of consistent quantum theory is to limit ourselves to consistent quantum frameworks.

Before the ending of this section, we want to clarify several points: first, the consistency conditions Eq. (1.21) are by no means necessary conditions; second, the probability assigned to a specific quantum history does not depend on the choice of the quantum sample space; third, according to the probability theory *inconsistent* quantum frameworks turn out to be meaningless.

1.4 Objectives

In this thesis, we aim to develop a rigorous and systematic formalism to study the thermal current and probability distribution of the heat transfer in a given

time duration for both ballistic systems and nonlinear systems in terms of unified language of consistent quantum theory. Specifically, both the main objective of this thesis and the contributions are

1. to examine if, when, and how the onset of the steady-state thermal transport occurs incorporating finite-size effects of the leads [42];
2. to establish generalized Landauer-like formula explicitly taking the lead-lead coupling into account [43];
3. to derive the CGF formula of the heat transfer in coupled left-right-lead ballistic systems [44];
4. to extend the study regarding the CGF formula of heat transfer to nonlinear quantum systems [45].

The results of the present research may have significance on the systematic understanding of the quantum thermal transport carried by phonons, which can be readily extended to the transport by other kinds of particles such as electrons and photons. This research may provide insights into statistics aspect of the quantum thermal transport by using microphysics model to approach the fluctuation theorem. Also, the analytical results obtained in this thesis could give guidelines to experimentalists for devising transport devices at the nanoscale.

The structure of the thesis is as follows: we introduce the nonequilibrium Green's function (NEGF) method in Chapter 2, which will be used throughout the thesis, followed by the study on the steady-state thermal current in coupled left-right-lead systems in Chapter 3. In Chapter 4, the study is extended to the probability

distribution of energy transport in a given time duration. In Chapter [5](#), we consider the probability distribution of energy transport across nonlinear quantum systems. Finally, the summary of the study and future works are given in Chapter [6](#).

Chapter 2

Nonequilibrium Green's function method

In this thesis, we focus on the study of various aspect of energy transport from quantum histories point of view. As is known, the nonequilibrium Green's function (NEGF) method is a powerful and compact tool to study energy transport. Therefore, as a preliminary step this chapter is largely devoted to develop the NEGF method self-containedly using an insulating lattice system as a typical model, where energy transport is due to atomic vibrations (phonons).

The NEGF method was initiated by Schwinger for a treatment of Brownian motion of a quantum oscillator [46]. Later Kadanoff and Baym used the NEGF method to derive quantum kinetic equations [47]. Further, Keldysh introduced the concept of contour order to perform diagrammatic expansion for nonequilibrium processes

[48]. For the first time, Caroli, *et al.* gave an explicitly formula for the transmission coefficient in terms of Green's functions when studying transport [16], whose modern form is due to Meir and Wingreen [14]. For a thorough understanding of the NEGF method to quantum thermal transport, one can resort to the review article in Ref. [49] and a updated one [50].

In the first section, we will briefly recall three different pictures in quantum mechanics: Schrödinger picture, Heisenberg picture, and interaction (Dirac) picture, emphasizing the convention used throughout the thesis such as the choice of the synchronization time. In the second section, we discuss the basic formalism of the NEGF method around the contour-ordered Green's function. Finally, we explore the subtle conditions employed in the NEGF method for the existence of the steady-state thermal transport.

2.1 Pictures in quantum mechanics

Let us consider the total Hamiltonian $H_{tot}(t)$ in the Schrödinger picture of a quantum system, which can be separated to a noninteracting solvable part H_0 and a generally time-dependent interacting part $V(t)$, namely

$$H_{tot}(t) = H_0 + V(t). \quad (2.1)$$

Here, the 'solvable' simply means all the eigenfunctions and eigenvalues of H_0 are explicitly known.

Suppose that at the initial time t_0 , the normalized state of the quantum system is

specified by $|\psi(t_0)\rangle_S$, then the Schrödinger equation

$$i\hbar \frac{\partial |\psi(t)\rangle_S}{\partial t} = H_{tot}(t) |\psi(t)\rangle_S \quad (2.2)$$

govern the subsequent evolution of the state. Equivalently,

$$|\psi(t)\rangle_S = U_S(t, t_0) |\psi(t_0)\rangle_S, \quad t \geq t_0 \quad (2.3)$$

since Eq. (2.2) is a first-order differential equation with respect to time. Here $U_S(t, t_0)$ is just the evolution operator mentioned in the Eq. (1.10) of the last chapter, formally expressed as

$$U_S(t, t_0) = T \exp \left[-\frac{i}{\hbar} \int_{t_0}^t H_{tot}(t') dt' \right], \quad (2.4)$$

where T is time-order super-operator arranging the position of the operator at earlier time to the right. Similarly, the evolution operator $U_S(t_1, t_2)$ when $t_1 < t_2$ can be shown to be

$$U_S(t_1, t_2) = U_S^{-1}(t_2, t_1) = U_S^\dagger(t_2, t_1) = \bar{T} \exp \left[-\frac{i}{\hbar} \int_{t_2}^{t_1} H_{tot}(t') dt' \right], \quad (2.5)$$

where \bar{T} is anti-time-order super-operator arranging the position of the operator at earlier time to the left. Frequently, what we are concerned is the quantum average of some observable $A_S(t)$, which might be explicitly time-dependent due to a presumed protocol such as the power operator $\frac{\partial H_{tot}}{\partial t}$. The quantum average at arbitrary time t is experimentally verifiable, defined to be

$$\langle \psi(t) |_S A_S(t) | \psi(t) \rangle_S \quad (2.6)$$

in the Schrödinger picture.

Until now, what we discussed is the quantum language in the Schrödinger picture, labeled by the subscript 'S'. Alternatively, we can use the Heisenberg picture

to study the quantum system. We choose the synchronization time between the Heisenberg picture and the Schrödinger picture to be the time t_0 when the initial state of the quantum system is known, which means

$$|\psi(t)\rangle_H = U_S(t_0, t) |\psi(t)\rangle_S = |\psi(t_0)\rangle_S \quad (2.7)$$

so that we can freely set the synchronization time t_0 to be 0 or $-\infty$ or any value, whichever is much more convenient. Since the experimentally measurable quantum average should not depend on the picture we used, the operator in the Heisenberg picture is correspondingly defined as

$$A_H(t) = U_S(t_0, t) A_S(t) U_S(t, t_0), \quad (2.8)$$

so that

$$\langle \psi(t) |_H A_H(t) |\psi(t)\rangle_H = \langle \psi(t) |_S A_S(t) |\psi(t)\rangle_S. \quad (2.9)$$

As far as I am concerned, the interaction (Dirac) picture is just a calculation tool, much simpler much better. Thus the reference time for the interaction picture in this thesis is always chosen to be 0 except when explicitly mentioned so that

$$|\psi(t)\rangle_I = e^{\frac{i}{\hbar} H_0 t} |\psi(t)\rangle_S \quad (2.10)$$

$$A_I(t) = e^{\frac{i}{\hbar} H_0 t} A_S(t) e^{-\frac{i}{\hbar} H_0 t}. \quad (2.11)$$

Typically the operator in the interaction picture is quite easy to deal with, while the calculation of the ket in the interaction picture satisfying

$$i\hbar \frac{\partial |\psi(t)\rangle_I}{\partial t} = V_I(t) |\psi(t)\rangle_I \quad (2.12)$$

require much more effort. The Schrödinger equation in the interaction picture Eq (2.12) can be formally solved as

$$|\psi(t)\rangle_I = U_I(t, t_0) |\psi(t_0)\rangle_I \quad (2.13)$$

with the interaction-picture evolution operator $U_I(t, t_0)$ to be

$$U_I(t, t_0) = e^{\frac{i}{\hbar} H_0 t} U_S(t, t_0) e^{-\frac{i}{\hbar} H_0 t_0} \quad (2.14)$$

$$= T \exp \left[-\frac{i}{\hbar} \int_{t_0}^t V_I(t') dt' \right]. \quad (2.15)$$

It is helpful to relate the Heisenberg-picture operator with the corresponding interaction-picture form using the interaction-picture evolution operator, which turns out to be

$$A_H(t) = e^{-\frac{i}{\hbar} H_0 t_0} U_I(t_0, t) A_I(t) U_I(t, t_0) e^{\frac{i}{\hbar} H_0 t_0} \quad (2.16)$$

under our convention by Eqs. (2.8), (2.11) and (2.14).

2.2 Contour-ordered Green's Function

In the NEGF formalism, contour-ordered Green's functions are the central quantities. On restricting the variation of the arguments of the contour-ordered Green's functions to the separate branches of the contour, one can get four conventional Green's functions: the greater, lesser, time-ordered, and anti-time ordered Green's functions.

2.2.1 Motivation for closed-time contour

Those familiar with ground-state quantum field theory might consider it to be strange to introduce the forward-backward contour, see Fig. 2.1. So in this subsection, let us see what really happened in the ground-state formalism.

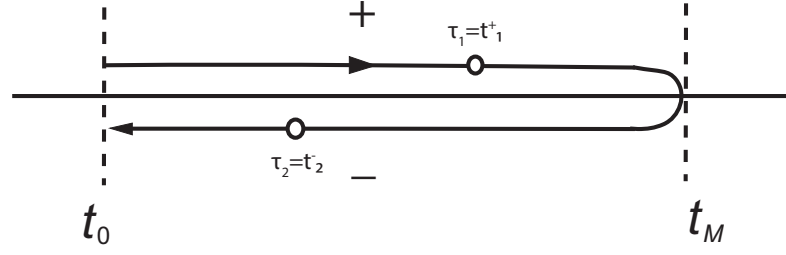


Figure 2.1: Contour C used to define the nonequilibrium Green's functions. The upper branch is called $+$ and lower one $-$ so that a particular time point τ_1 on the upper branch is denoted by t_1^+ while τ_2 on the lower one by t_2^- . The time order follows the direction of the arrows.

In the ground-state quantum field theory, the time-dependence of the interacting Hamiltonian $V(t)$ is only due to an adiabatic switch-on factor $e^{-\varepsilon|t|}$, $\varepsilon \rightarrow 0^+$, which fully switches the interaction on at time $t = 0$. It should be noted that in the ground-state quantum field theory the synchronization time t_0 between the Heisenberg and the Schrödinger picture is chosen to be 0, so that the quantum average at time t of the operator $A_S(t)$ with respect to the initial interacting ground state $|GS\rangle$ at time $t = 0$ is

$$\begin{aligned}
 & \langle GS | A_H(t) | GS \rangle \\
 &= \langle GS | U_I(0, t) A_I(t) U_I(t, 0) | GS \rangle \\
 &= \langle 0 | U_I(-\infty, 0) U_I(0, t) A_I(t) U_I(t, 0) U_I(0, -\infty) | 0 \rangle \\
 &= \langle 0 | U_I(-\infty, \infty) U_I(\infty, t) A_I(t) U_I(t, 0) U_I(0, -\infty) | 0 \rangle,
 \end{aligned}
 \tag{2.17}$$

where in the second equality we have employed the Gell-Mann and Low theorem [51], which says that

$$|GS\rangle = U_I(0, -\infty) |0\rangle \quad (2.18)$$

with $|0\rangle$ to be the ground state of non-interacting Hamiltonian H_0 . It is worth mentioning that $U_I(0, -\infty) |0\rangle$ is usually but not necessarily the interacting ground state. The key trick comes now that the state $U_I(\infty, -\infty) |0\rangle$ is equal to $|0\rangle$ up to an infinite phase factor when $\varepsilon \rightarrow 0^+$, namely

$$U_I(\infty, -\infty) |0\rangle = e^{iL} |0\rangle, \quad (2.19)$$

due to the adiabatic switch-on and subsequent switch-off process, which can be also considered as a corollary of the Gell-Mann and Low theorem. Therefore,

$$\langle GS | A_H(t) | GS \rangle = \frac{\langle 0 | U_I(\infty, t) A_I(t) U_I(t, -\infty) | 0 \rangle}{e^{iL}} \quad (2.20)$$

$$= \frac{\langle 0 | U_I(\infty, t) A_I(t) U_I(t, -\infty) | 0 \rangle}{\langle 0 | U_I(\infty, -\infty) | 0 \rangle}. \quad (2.21)$$

Now we realized that the reason why the backward contour is eliminated is due to the fact that in some restricted situation the state in future may be identified as a state in the past, see Eq. (2.19). However, for some general initial states and general evolution processes it is hopeless to expect this ‘good luck’ to happen again. In that case, we really need to consider both the forward and the backward branch of the closed-time contour, which will be studied in the following sections.

2.2.2 Exploring the definition

Let us consider a general lattice system described by vibrational displacement u_j , where the single subscript index j runs over all the relevant degrees of freedom.

For example, j may refer to the l -th atom shifting in the x direction in a three-dimensional lattice model. Thus the formalism we are introducing can be used to study a general network.

The contour C is explicitly defined to be going forward from the initial time t_0 in the upper branch, up to a maximum time t_M relevant to the problem (which actually could be ∞), then returning backward to the time t_0 from the lower branch, see Fig. 2.1. Typically we use τ to denote a particular position on the contour, and $\tau = t_1^+$ denotes the position at time t_1 on the upper branch while $\tau = t_2^-$ at time t_2 on the lower branch.

For clarity, we introduce a new evolution operator $U_S(\tau_2, \tau_1)$ which is defined on the contour C . Assuming that $\tau_2 \succ \tau_1$, namely τ_2 succeeds τ_1 on the contour, we will encounter three different situations depending on the relative position of the arguments τ_2 and τ_1 :

$$U_S(\tau_2, \tau_1) = \begin{cases} U_S^+(t_2, t_1), & (\tau_2 = t_2^+) > (\tau_1 = t_1^+) \\ U_S^-(t_2, t_M) U_S^+(t_M, t_1), & \tau_2 = t_2^-, \tau_1 = t_1^+ \\ U_S^-(t_2, t_1). & (\tau_2 = t_2^-) < (\tau_1 = t_1^-) \end{cases} \quad (2.22)$$

Where in the second situation we need not specify the relative magnitude of t_2^- and t_1^+ , since the time on the lower branch always succeeds the time on the upper branch along the contour. Also we should notice that the superscript $+$ or $-$ for the evolution operator simply tell us that the ordinary Schrödinger evolution operator is for the upper branch or the lower branch, respectively. Because frequently the Hamiltonian determining the evolution does not depend on the branch of the contour, the superscript $+$ or $-$ for the evolution operator is completely redundant

and finally $U_S(\tau_2, \tau_1) = U_S^\pm(t_2, t_1)$. However, for me in a formalism it is always much better to tolerate extra freedoms and the real value of allowing a branch-dependent Hamiltonian will be appreciated when we deal with the nonlinear case in Chapter 5, where due to the measurement procedure the convenient effective Hamiltonian depends on the branch of the contour through the counting field parameter. Compactly, the evolution operator defined on the contour $U_S(\tau_2, \tau_1)$ could be written as

$$U_S(\tau_2, \tau_1) = T_\tau \exp \left(-\frac{i}{\hbar} \int_{C[\tau_2, \tau_1]} H_{tot}(\tau) d\tau \right), \quad \tau_2 \succ \tau_1. \quad (2.23)$$

Where T_τ is contour-ordered super-operator arranging the position of the operator at later contour time to the left, and $C[\tau_2, \tau_1]$ denotes part of the whole contour C from earlier contour time τ_1 to the later contour time τ_2 along the contour. In order to keep group properties of the evolution operator, the evolution operator $U_S(\tau_1, \tau_2)$, $\tau_2 \succ \tau_1$ is defined to be

$$U_S(\tau_1, \tau_2) = U_S(\tau_2, \tau_1)^{-1} = U_S(\tau_2, \tau_1)^\dagger, \quad \tau_2 \succ \tau_1. \quad (2.24)$$

By virtue of the evolution operator defined on the contour, we can define a generalized Heisenberg-picture operator which is given as

$$A_H(\tau) = U_S(t_0^+, \tau) A_S U_S(\tau, t_0^+). \quad (2.25)$$

One can easily verify by himself that the generalized Heisenberg-picture operator $A_H(\tau)$ agrees with the usual one if the Hamiltonian determining the evolution of the system does not depend on the branch of the contour, which normally is. But, nonetheless, employing Heisenberg-picture operators defined on the contour, the component form of contour-ordered Green's function will be quite clearly defined

as

$$G_{jk}(\tau_2, \tau_1) = -\frac{i}{\hbar} \text{Tr} [\rho^{ini}(t_0) T_\tau u_j^H(\tau_2) u_k^H(\tau_1)]. \quad (2.26)$$

2.2.3 The basic formalism

Basically, there are two approaches to study the contour-ordered Green's function: the equation of motion method and the perturbation expansion method.

We first consider how to obtain the equation of motion satisfied by the the contour-ordered Green's function. At the beginning, we need to solve several technical problems. The first one is on the precise meaning of the time derivative of contour-time dependent functions, which is shown below:

$$\frac{df(\tau)}{d\tau} = \lim_{\Delta\tau \rightarrow 0} \frac{f(\tau + \Delta\tau) - f(\tau)}{\Delta\tau} \quad (2.27)$$

$$= \begin{cases} \frac{df^+(t)}{dt}, & \tau = t^+ \\ \frac{df^-(t)}{dt}, & \tau = t^- \end{cases} \quad (2.28)$$

where the function $f(\tau)$ is equal to $f^+(t)$ or $f^-(t)$, when the argument contour-time τ is on the upper branch t^+ or lower branch t^- , respectively. Equipped well with the contour-time derivative, we can develop a generalized Heisenberg equation of motion for the Heisenberg-picture operator on the contour $A_H(\tau)$, which turns out to be

$$i\hbar \frac{d}{d\tau} A_H(\tau) = [A_H(\tau), H_{tot}^H(\tau)]. \quad (2.29)$$

The second one is the definition of Heaviside step function $\theta(\tau, \tau')$ on the contour,

which is given below:

$$\theta(\tau, \tau') = \begin{cases} 1, & \tau \succ \tau' \\ \frac{1}{2}, & \tau = \tau' \\ 0, & \tau \prec \tau' \end{cases} \quad (2.30)$$

Since we want to keep the identity $\theta(\tau, \tau') + \theta(\tau', \tau) = 1$ for arbitrary value of τ and τ' , the special case $\theta(\tau, \tau)$ is set to be $1/2$. In addition, the δ function on the contour is defined to be

$$\delta(\tau, \tau') \equiv \frac{\partial \theta(\tau, \tau')}{\partial \tau} = -\frac{\partial \theta(\tau, \tau')}{\partial \tau'}. \quad (2.31)$$

In order to get a feeling about what the equation of motion for the contour-ordered Green's function looks like, we give a simple example, in which the total Hamiltonian is

$$H_{tot} = \frac{1}{2} p^T p + \frac{1}{2} u^T K u, \quad K^T = K, \quad (2.32)$$

where K is a symmetric, positive definite spring constant matrix, the superscript T stands for matrix transpose, u is a column vector with component u_j and p is the conjugate momentum vector. It is easily verified that the standard commutation relation for $u_H(\tau)$ and $p_H(\tau)$ on the contour still holds, namely,

$$[u_H(\tau), p_H^T(\tau)] = i\hbar I \quad (2.33)$$

with I to be an identity matrix. In this simple case, $H_{tot}^H(\tau) = H_{tot}$ and all the Heisenberg-picture operators on the contour are completely equivalent to the usual Heisenberg-picture ones, since the total Hamiltonian H_{tot} is contour-time

independent. After noticing that

$$\begin{aligned}
 G(\tau_2, \tau_1) &= -\frac{i}{\hbar} \langle T_\tau u_H(\tau_2) u_H^T(\tau_1) \rangle \\
 &= -\frac{i}{\hbar} \theta(\tau_2, \tau_1) \langle u_H(\tau_2) u_H^T(\tau_1) \rangle - \frac{i}{\hbar} \theta(\tau_1, \tau_2) \langle u_H(\tau_1) u_H^T(\tau_2) \rangle^T
 \end{aligned} \tag{2.34}$$

with $\langle \dots \rangle$ denoting $\text{Tr}[\rho^{ini}(t_0) \dots]$, $\frac{du_H(\tau)}{d\tau} = p_H(\tau)$ and $\frac{dp_H(\tau)}{d\tau} = -K u_H(\tau)$, we can obtain the equation of motion for the contour-ordered Green's function using contour-time derivative:

$$\frac{\partial^2 G(\tau_2, \tau_1)}{\partial \tau_2^2} + K G(\tau_2, \tau_1) = -\delta(\tau_2, \tau_1) I. \tag{2.35}$$

The δ function appearing on the right-hand side of this equation of motion justifies the name of the 'Green's function'. Also this equation of motion is generally true for arbitrary initial density matrix $\rho^{ini}(t_0)$. Just due to this fact, this equation is generally hard to solve directly which requires the careful specification of boundary conditions. We do not pursue to conquer this difficulty here and readers interested in this problem can refer to Ref. [52].

Now we try to use the perturbation expansion method to study contour-ordered Green's function. The main idea will be illustrated by a typical ballistic-transport model, which consists of three parts: a left lead (L), a right lead (R) and a center part (C) and the two couplings between the two leads and the center are both bilinear with respect to displacement operators in the leads and the center part. Explicitly, the total Hamiltonian is

$$H_{tot} = H_L + H_C + H_R + H_{LC} + H_{CR}, \tag{2.36}$$

where $H_\alpha = \frac{1}{2} p_\alpha^T p_\alpha + \frac{1}{2} u_\alpha^T K^\alpha u_\alpha$, $\alpha = L, C, R$ represents coupled harmonic oscillators, $u_\alpha = \sqrt{m} x_\alpha$ and p_α are column vectors of transformed coordinates and

corresponding conjugate momenta in region α . The coupling between the center and the two leads are $H_{LC} = u_L^T V^{LC} u_C$ and $H_{CR} = u_C^T V^{CR} u_R$. Essentially, this model can be taken account as a specific partition of the harmonic network considered above with K in Eq. (2.32) to be

$$K = \begin{bmatrix} K^L & V^{LC} & 0 \\ V^{CL} & K^C & V^{CR} \\ 0 & V^{RC} & K^R \end{bmatrix}. \quad (2.37)$$

A natural question will immediately come about the effects of the different partition of the total Hamiltonian on thermal transport, which will be discussed in the later Chapters 3 and 4. The relevant contour-ordered Green's functions to this model are

$$G_{\alpha\beta}(\tau_2, \tau_1) = -\frac{i}{\hbar} \text{Tr} \left[\rho_{prod}^{ini}(t_0) T_\tau u_\alpha^H(\tau_2) u_\beta^{H,T}(\tau_1) \right], \quad \alpha, \beta = L, C, R. \quad (2.38)$$

Where the initial density state at time t_0 is specified by the direct product state, i.e.,

$$\rho_{prod}^{ini}(t_0) = \rho_L \otimes \rho_C \otimes \rho_R, \quad \rho_\alpha = \frac{e^{-\beta_\alpha H_\alpha}}{\text{Tr}[e^{-\beta_\alpha H_\alpha}]} \quad \text{for } \alpha = L, C, R \quad (2.39)$$

with $\beta_\alpha = \frac{1}{k_B T_\alpha}$, $\alpha = L, C, R$ to be the inverse temperature. The first step is to transform the Heisenberg-picture operators appearing in the contour-ordered Green's function to the interaction-picture ones with respect to $H_0 = H_L + H_C + H_R$, which can be readily done as

$$G_{\alpha\beta}(\tau_2, \tau_1) = -\frac{i}{\hbar} \text{Tr} \left[\rho_{prod}^{ini}(t_0) T_\tau u_\alpha^I(\tau_2) u_\beta^{I,T}(\tau_1) e^{-\frac{i}{\hbar} \int_C V_I(\tau) d\tau} \right], \quad (2.40)$$

where

$$V_I(\tau) = e^{\frac{i}{\hbar} H_0 \tau} (H_{LC} + H_{CR}) e^{-\frac{i}{\hbar} H_0 \tau} = u_L^{I,T}(\tau) V^{LC} u_C^I(\tau) + u_C^{I,T}(\tau) V^{CR} u_R^I(\tau), \quad (2.41)$$

after noticing that the commutator $[\rho_{prod}^{ini}(t_0), H_0] = 0$. The contour variables such as τ only influence the ordering of the operators under T_τ , and $e^{\frac{i}{\hbar}H_0\tau}$ has the same meaning as $e^{\frac{i}{\hbar}H_0t}$ with real time t after ordering. For a better treatment of this contour-time interaction picture, please refer to the Sec. 5.2 of the Chapter 5.

Observing the exponent of Eq. (2.40), we know that there are only two kinds of 2-connector bare vertices V^{LC} and V^{CR} in this simple model, which describe the possible interactions allowed to take place. Then the second step is try to group the diagrams using Wick's theorem and the basic rule that a particle has two options: to interact or not to interact, see Chapter 9 of the Ref. [53]. Since, roughly speaking, the initial density state is quadratic, the Wick Theorem is justified for the interaction-picture form of the contour-ordered Green's function and for a detailed discussion about the Wick theorem, please refer to the Sec. 5.5 of the chapter 5. The goal of the perturbation expansion method is try to build nonequilibrium contour-ordered Green's functions from the known ones, which in this model are equilibrium contour-ordered Green's functions, namely,

$$\begin{aligned} g_{\alpha\alpha'}(\tau, \tau') &= -\frac{i}{\hbar} \text{Tr} \left[\rho_{prod}^{ini}(t_0) T_\tau u_\alpha^I(\tau) u_{\alpha'}^{I,T}(\tau') \right] \\ &= \delta_{\alpha\alpha'} g_\alpha(\tau, \tau'), \quad \alpha = L, C, R \end{aligned} \quad (2.42)$$

Let us first give a plausible reasoning for the perturbation study of $G_{LC}(\tau_2, \tau_1)$. On the one hand, the external leg $u_L^I(\tau_2)$ can not be directly connected with the other external leg $u_C^{I,T}(\tau_1)$ since $g_{LC}(\tau_2, \tau_1) = 0$. Instead, it can be connected to just one of the two vertices V^{LC} and the summation of all the remaining connected part simply contribute to a factor $G_{CC}(\tau, \tau_1)$. On the other hand, the summation of all the disconnected diagrams is equivalent to $\text{Tr} \left[\rho_{prod}^{ini}(t_0) T_\tau e^{-\frac{i}{\hbar} \int_C V_I(\tau) d\tau} \right]$, which is simply 1. Taken together, see Fig. 2.2, the Dyson equation for $G_{LC}(\tau_2, \tau_1)$ can

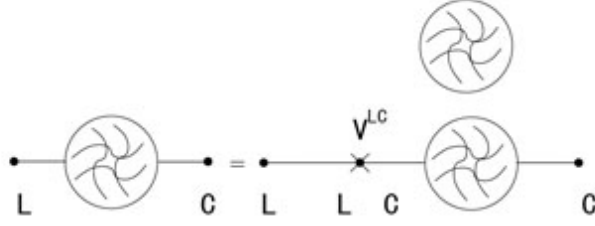


Figure 2.2: An illustration for the Dyson equation satisfied by $G_{LC}(\tau_2, \tau_1)$.

be written as

$$G_{LC}(\tau_2, \tau_1) = \int_C d\tau g_L(\tau_2, \tau) V^{LC} G_{CC}(\tau, \tau_1). \quad (2.43)$$

Similarly, $G_{RC}(\tau_2, \tau_1)$ satisfies the Dyson equation

$$G_{RC}(\tau_2, \tau_1) = \int_C d\tau g_R(\tau_2, \tau) V^{LC} G_{CC}(\tau, \tau_1). \quad (2.44)$$

One should notice that the above equation Eq. (2.43) and Eq. (2.44) are also true for the nonlinear center, since the extra nonlinear vertices introduced for the center such as 3-connector vertex does not change the above reasoning.

More importantly, we can obtain a closed Dyson equation for $G_{CC}(\tau_2, \tau_1)$. The reasoning is like the following: on the one hand, the external leg $u_C^I(\tau_2)$ can be directly connected with the other external leg $u_C^{I,T}(\tau_1)$ to contribute a separate term $g_C(\tau_2, \tau_1)$. Also, it can be connected to both 2-connector vertex V^{CL} and V^{RC} and the summation of all the remaining connected part simply contribute to a factor $G_{LC}(\tau, \tau_1)$ and $G_{RC}(\tau, \tau_1)$ respectively. On the other hand, the summation of all the disconnected diagrams is equivalent to $\text{Tr} \left[\rho_{prod}^{ini}(t_0) T_\tau e^{-\frac{i}{\hbar} \int_C V_I(\tau) d\tau} \right]$ and

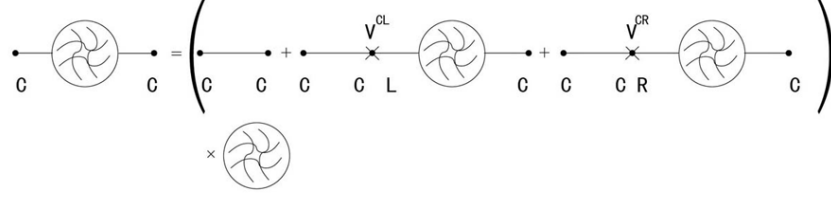


Figure 2.3: An illustration for the Dyson equation satisfied by $G_{CC}(\tau_2, \tau_1)$.

contribute to a factor 1. Thus, see Fig. 2.3, $G_{CC}(\tau_2, \tau_1)$ satisfies

$$G_{CC}(\tau_2, \tau_1) = g_C(\tau_2, \tau_1) + \int_C d\tau g_C(\tau_2, \tau) (V^{CL} G_{LC}(\tau, \tau_1) + V^{CR} G_{RC}(\tau, \tau_1)). \quad (2.45)$$

Combining Eq. (2.43), Eq. (2.44) and Eq. (2.45), an important closed Dyson equation for $G_{CC}(\tau_2, \tau_1)$ is given as

$$G_{CC}(\tau_2, \tau_1) = g_C(\tau_2, \tau_1) + \int_C d\tau \int_C d\tau' g_C(\tau_2, \tau) \Sigma(\tau, \tau') G_{CC}(\tau', \tau_1) \quad (2.46)$$

with the total self energy to be

$$\Sigma(\tau, \tau') = \Sigma_L(\tau, \tau') + \Sigma_R(\tau, \tau') \quad (2.47)$$

$$= V^{CL} g_L(\tau, \tau') V^{LC} + V^{CR} g_R(\tau, \tau') V^{RC}. \quad (2.48)$$

It is worth mentioning that the above three Dyson equations Eq. (2.43) and Eq. (2.44) and Eq. (2.46) could be also obtained by equation of motion method, in which the boundary conditions need to be properly considered, see, Eg. Ref. [54].

2.2.4 The connection to conventional Green's functions

After obtaining the contour-ordered Green's function relevant to the problem and specifying the ranges of variation of its arguments as mentioned before, we can get four conventional Green's functions: greater ($>$), lesser ($<$), time-ordered (t), and anti-time-ordered (\bar{t}) Greens functions, the respective component forms of which are shown as:

$$G_{jk}^>(t_2, t_1) = G_{jk}(t_2^-, t_1^+) = -\frac{i}{\hbar} \langle u_j^H(t_2) u_k^H(t_1) \rangle \quad (2.49)$$

$$G_{jk}^<(t_2, t_1) = G_{jk}(t_2^+, t_1^-) = -\frac{i}{\hbar} \langle u_k^H(t_1) u_j^H(t_2) \rangle \quad (2.50)$$

$$\begin{aligned} G_{jk}^t(t_2, t_1) &= G_{jk}(t_2^+, t_1^+) = -\frac{i}{\hbar} \langle T u_j^H(t_2) u_k^H(t_1) \rangle \\ &= \theta(t_2 - t_1) G_{jk}^>(t_2, t_1) + \theta(t_1 - t_2) G_{jk}^<(t_2, t_1) \end{aligned} \quad (2.51)$$

$$\begin{aligned} G_{jk}^{\bar{t}}(t_2, t_1) &= G_{jk}(t_2^-, t_1^-) = -\frac{i}{\hbar} \langle \bar{T} u_j^H(t_2) u_k^H(t_1) \rangle \\ &= \theta(t_2 - t_1) G_{jk}^<(t_2, t_1) + \theta(t_1 - t_2) G_{jk}^>(t_2, t_1), \end{aligned} \quad (2.52)$$

where $\langle \dots \rangle = \text{Tr} [\rho^{ini}(t_0) \dots]$ with respect to arbitrary initial density matrix $\rho^{ini}(t_0)$, the ordinary step function $\theta(t) = 1$ if $t > 0$ and 0 if $t < 0$ and 1/2 if $t = 0$ inherited from the step function on the contour defined in Eq. (2.30). Notice that when transforming from contour-ordered Green's function to the four conventional Green's functions by specifying the range of variation of the contour-time arguments, we have implicitly assumed that the total Hamiltonian does not depend on the branch of the contour so that $U_S^+(t_2, t_1) = U_S^-(t_2, t_1)$ appearing on the Eq. (2.22). Thus the Heisenberg-picture operators on the real time in the above definition for $G^>$, $G^<$, G^t , $G^{\bar{t}}$ are exactly the same as the definition in Eq. (2.8).

Using the greater and lesser Green's functions, we can define additional two conventional Green's functions, which are retarded (r) and advanced (a) Green's functions shown below:

$$G_{jk}^r(t_2, t_1) = \theta(t_2 - t_1) (G_{jk}^>(t_2, t_1) - G_{jk}^<(t_2, t_1)) \quad (2.53)$$

$$= -\frac{i}{\hbar} \theta(t_2 - t_1) \langle [u_j^H(t_2), u_k^H(t_1)] \rangle, \quad (2.54)$$

$$G_{jk}^a(t_2, t_1) = -\theta(t_1 - t_2) (G_{jk}^>(t_2, t_1) - G_{jk}^<(t_2, t_1)) \quad (2.55)$$

$$= \frac{i}{\hbar} \theta(t_1 - t_2) \langle [u_j^H(t_2), u_k^H(t_1)] \rangle. \quad (2.56)$$

In the case of equilibrium or nonequilibrium steady state for the initial density matrix, the six conventional Green's functions only depend on the time difference such as $G^>(t_2, t_1) = G^>(t_2 - t_1)$. Therefore it is helpful to introduce the Fourier-transformation pair of Green's functions, the convention of which throughout the thesis is shown below:

$$G[\omega] = \int_{-\infty}^{+\infty} dt G(t) e^{i\omega t}, \quad (2.57)$$

$$G(t) = \int_{-\infty}^{+\infty} \frac{d\omega}{2\pi} G[\omega] e^{-i\omega t}. \quad (2.58)$$

By virtue of the definitions of all the six conventional Green's function, we can show that

$$G^t = G^r + G^< = G^> + G^a, \quad (2.59)$$

$$G^{\bar{t}} = G^< - G^a = G^> - G^r. \quad (2.60)$$

Since these relations are true in both frequency and time domains, we do not specify the arguments of the Green's functions. Notice that generally out of the six Green's functions, only three of them are linearly independent.

If the system admits time translational invariance, retarded Green's function and advanced Green's function are hermitian conjugate of each other, namely,

$$G^a[\omega] = (G^r[\omega])^\dagger. \quad (2.61)$$

Then in this case only two conventional Green's functions are independent, which can be taken as $G^r[\omega]$ and $G^<[\omega]$. Since we have the relations

$$G^r[-\omega] = G^r[\omega]^*, \quad (2.62)$$

$$G^<[-\omega] = -G^<[\omega]^* + G^r[\omega]^T - G^r[\omega]^*, \quad (2.63)$$

the positive frequency part of the Green's functions $G^r[\omega]$ and $G^<[\omega]$ are completely sufficient.

Furthermore, in thermal equilibrium, fluctuation-dissipation theorem holds, which says

$$G^<[\omega] = f(\omega) (G^r[\omega] - G^a[\omega]), \quad (2.64)$$

where $f(\omega) = \frac{1}{e^{\beta\hbar\omega} - 1}$ is the Bose-Einstein distribution function at inverse temperature $\beta = \frac{1}{k_B T}$. So in equilibrium, there is really one independent Green's function.

It has been already realized from Dyson equation that in dealing with the contour-ordered Green's functions, we often encounter convolution of the form

$$C(\tau, \tau') = \int_C d\tau'' A(\tau, \tau'') B(\tau'', \tau'). \quad (2.65)$$

The transformation rules from contour-time convolution equations to real-time ones are generally named as the Langreth theorem. Corresponding to Eq. (2.65),

the following rules are commonly used:

$$C^{<, >} (t, t') = \int_{t_0}^{t_M} dt'' A^r (t, t'') B^{<, >} (t'', t') + \int_{t_0}^{t_M} dt'' A^{<, >} (t, t'') B^a (t'', t') \quad (2.66)$$

$$C^{r, a} (t, t') = \int_{t_0}^{t_M} dt'' A^{r, a} (t, t'') B^{r, a} (t'', t') \quad (2.67)$$

Here we only show a sample proof:

$$C^< (t, t') = C (t^+, t'^-) = \int_C d\tau'' A (t^+, \tau'') B (\tau'', t'^-) \quad (2.68)$$

$$= \int_{t_0}^{t_M} dt'' A (t^+, t''^+) B (t''^+, t'^-) + \int_{t_M}^{t_0} dt'' A (t^+, t''^-) B (t''^-, t'^-) \quad (2.69)$$

$$= \int_{t_0}^{t_M} dt'' A^t (t, t'') B^< (t'', t') - \int_{t_0}^{t_M} dt'' A^< (t, t'') B^{\bar{t}} (t'', t') \quad (2.70)$$

$$= \int_{t_0}^{t_M} dt'' [A^r (t, t'') + A^< (t, t'')] B^< (t'', t') - \int_{t_0}^{t_M} dt'' A^< (t, t'') [B^< (t'', t') - B^a (t'', t')] \quad (2.71)$$

$$= \int_{t_0}^{t_M} dt'' A^r (t, t'') B^< (t'', t') + \int_{t_0}^{t_M} dt'' A^< (t, t'') B^a (t'', t') \quad (2.72)$$

$$C^t(t, t') = C(t^+, t'^+) = \int_C d\tau'' A(t^+, \tau'') B(\tau'', t'^+) \quad (2.73)$$

$$= \int_{t_0}^{t_M} dt'' A(t^+, t''^+) B(t''^+, t'^+) + \int_{t_M}^{t_0} dt'' A(t^+, t''^-) B(t''^-, t'^+) \quad (2.74)$$

$$= \int_{t_0}^{t_M} dt'' A^t(t, t'') B^t(t'', t') - \int_{t_0}^{t_M} dt'' A^<(t, t'') B^>(t'', t') \quad (2.75)$$

$$C^r = C^t - C^< \quad (2.76)$$

$$\begin{aligned} &= (A^t B^t - A^< B^>) - (A^r B^< + A^< B^a) \\ &= A^t B^t - A^< (B^> + B^a) - A^r B^< \\ &= A^t B^t - A^< B^t - A^r B^< \\ &= (A^t - A^<) B^t - A^r B^< \\ &= A^r B^t - A^r B^< \\ &= A^r B^r \end{aligned} \quad (2.77)$$

In the final piece of proof, we have used self-explanatory short-hand notations. And in the whole sample proof, the general relations between the six conventional Green's functions are heavily used. Moreover, we want to point out that the Langreth theorem shown above can be readily extended to the frequency domain and the case of the convolution integral involving more than two contour-ordered Green's function by method of induction.

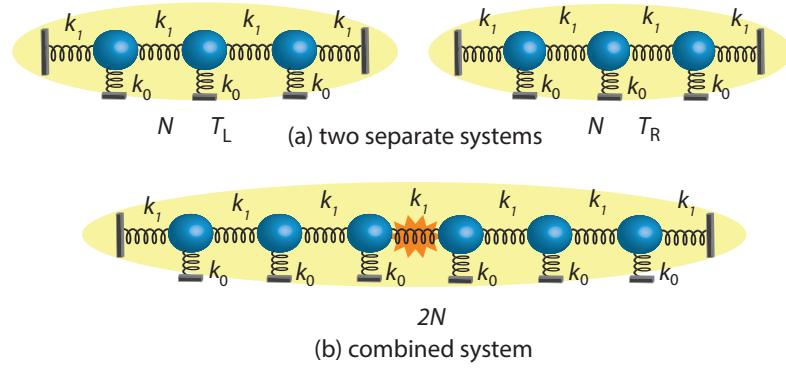


Figure 2.4: An illustration of how two finite independent systems at temperature T_L and T_R , both containing N particles are abruptly combined at $t = 0$ into a composite system containing $2N$ particles. The interparticle spring constant is k_1 and the on-site spring constant is k_0 .

2.3 Transient and nonequilibrium steady state in NEGF

In the early stage, NEGF is mainly applied to study steady-state current. When studying steady-state current using NEGF method, two heat baths at different temperature driving the heat current are typically modeled by collections of infinite harmonic oscillators. Frequently, see Ref. [49], we assume that steady-state thermal transport could be dynamically reached from initial product state after sudden switch-on of the coupling between the two heat baths. In this section we want to explicitly examine this subtle assumption using a straightforward Heisenberg equation of motion method.

We examine if, when, and how the onset of the steady-state transport occurs by

determining the time-dependent thermal current in a phonon system consisting of two linear chains, which are abruptly attached together at time $t = 0$ [42]. The analytical analysis appearing in the appendix of the Ref. [42] is my contribution, much more detail of which will be given in the following.

Shown in Fig. 2.4(a) are the two separate linear chains. The interparticle spring constant is k_1 and the on-site spring constant is k_0 . The left and right chains are initially in their respective thermal equilibrium with inverse temperature $\beta_L = 1/(k_B T_L)$ and $\beta_R = 1/(k_B T_R)$ and both contain N sites. In addition, fixed boundary conditions are used, wherein particles at the left and right edges are attached to fixed walls. At time $t = 0$ the chains are abruptly coupled with spring constant k_1 , as shown in Fig. 2.4(b). Then the total Hamiltonian is written as

$$\hat{\mathbf{H}}_{tot} = \hat{H}_L + \hat{H}_R + \hat{H}_{LR}$$

with

$$\begin{aligned} \hat{H}_L &= \sum_{n=1}^N \frac{\hat{p}_n^2}{2} + \left\{ \frac{1}{2} k_1 \sum_{n=1}^{N-1} (\hat{x}_{n+1} - \hat{x}_n)^2 + \frac{1}{2} k_1 \hat{x}_1^2 + \frac{1}{2} k_1 \hat{x}_N^2 \right\} \\ &+ \frac{1}{2} k_0 \sum_{n=1}^N \hat{x}_n^2, \end{aligned} \quad (2.78)$$

$$\begin{aligned} \hat{H}_R &= \sum_{n=N+1}^{2N} \frac{\hat{p}_n^2}{2} + \left\{ \frac{1}{2} k_1 \sum_{n=N+1}^{2N-1} (\hat{x}_{n+1} - \hat{x}_n)^2 + \frac{1}{2} k_1 \hat{x}_1^2 + \frac{1}{2} k_1 \hat{x}_{2N}^2 \right\} \\ &+ \frac{1}{2} k_0 \sum_{n=N+1}^{2N} \hat{x}_n^2, \end{aligned} \quad (2.79)$$

$$\hat{H}_{LR} = -k_1 \hat{x}_N \hat{x}_{N+1}. \quad (2.80)$$

And the initial density matrix is specified by

$$\hat{\rho}^{ini}(0) = \hat{\rho}_L \otimes \hat{\rho}_R = \frac{e^{-\beta_L \hat{H}_L}}{\text{Tr}(e^{-\beta_L \hat{H}_L})} \otimes \frac{e^{-\beta_R \hat{H}_R}}{\text{Tr}(e^{-\beta_R \hat{H}_R})}. \quad (2.81)$$

Now we introduce a new notation system to simplify the whole calculation:

$$\langle k|n\rangle^\dagger = \langle n|k\rangle \equiv \sqrt{\frac{2}{2N+1}} \sin(kn), \quad (2.82)$$

$$\langle n|\hat{x}\rangle \equiv \hat{x}_n, \langle \hat{x}^\dagger|n\rangle \equiv \hat{x}_n^\dagger, \langle \hat{p}|n\rangle \equiv \hat{p}_n, \langle n|\hat{p}^\dagger\rangle \equiv \hat{p}_n^\dagger, \quad (2.83)$$

$$\langle k|\hat{x}\rangle \equiv \hat{x}_k, \langle \hat{x}^\dagger|k\rangle \equiv \hat{x}_k^\dagger, \langle \hat{p}|k\rangle \equiv \hat{p}_k, \langle k|\hat{p}^\dagger\rangle \equiv \hat{p}_k^\dagger, \quad (2.84)$$

where $n = 1, 2, \dots, 2N$ and $k = \frac{\pi j}{2N+1}$ $j = 1, 2, \dots, 2N$. According to these definitions, we have some useful results:

$$\sum_n \langle k|n\rangle \langle n|k'\rangle = \delta_{kk'} \quad (2.85)$$

$$\sum_k \langle n|k\rangle \langle k|n'\rangle = \delta_{nn'} \quad (2.86)$$

$$\sum_{n=1}^{2N-1} (\langle k|n+1\rangle \langle n|k'\rangle + \langle k|n\rangle \langle n+1|k'\rangle) = 2 \cos k \delta_{kk'} \quad (2.87)$$

Or equivalently,

$$\sum_n |n\rangle \langle n| = \hat{I}, \quad \langle n|n'\rangle = \delta_{nn'}, \quad (2.88)$$

$$\sum_k |k\rangle \langle k| = \hat{I}, \quad \langle k|k'\rangle = \delta_{kk'}, \quad (2.89)$$

$$\sum_{n=1}^{2N-1} |n+1\rangle \langle n| + |n\rangle \langle n+1| = 2 \cos \hat{k}, \quad (2.90)$$

where $\hat{k}|k\rangle = k|k\rangle$, $k = \frac{\pi j}{2N+1}$, $j = 1, 2, \dots, 2N$.

In addition,

$$\begin{aligned}\hat{\mathbf{H}}_{tot} &= \sum_{n=1}^{2N} \frac{1}{2} \langle \hat{p} | n \rangle \langle n | \hat{p}^\dagger \rangle + \frac{1}{2} (2k_1 + k_0) \sum_{n=1}^{2N} \langle \hat{x}^\dagger | n \rangle \langle n | \hat{x} \rangle \\ &\quad - \frac{1}{2} k_1 \langle \hat{x}^\dagger | \left(\sum_{n=1}^{2N-1} |n+1\rangle \langle n| + |n\rangle \langle n+1| \right) | \hat{x} \rangle\end{aligned}\quad (2.91)$$

$$= \frac{1}{2} \langle \hat{p} | \hat{p}^\dagger \rangle + \frac{1}{2} (2k_1 + k_0) \langle \hat{x}^\dagger | \hat{x} \rangle - \frac{1}{2} k_1 \langle \hat{x}^\dagger | 2 \cos \hat{k} | \hat{x} \rangle \quad (2.92)$$

$$= \frac{1}{2} \langle \hat{p} | \hat{p}^\dagger \rangle + \frac{1}{2} \langle \hat{x}^\dagger | \hat{\omega}^2 | \hat{x} \rangle \quad (2.93)$$

with $\hat{\omega} \equiv \sqrt{2k_1 (1 - \cos \hat{k})} + k_0$.

Solving Heisenberg equation of motion, we could obtain

$$|\hat{x}(t)\rangle = \cos(\hat{\omega}t) |\hat{x}\rangle + \frac{\sin(\hat{\omega}t)}{\hat{\omega}} |\hat{p}^\dagger\rangle \quad (2.94)$$

$$\langle \hat{p}(t) | = -\langle \hat{x}^\dagger | \hat{\omega} \sin(\hat{\omega}t) + \langle \hat{p} | \cos(\hat{\omega}t), \quad (2.95)$$

where $\langle n | \hat{x}(t) \rangle \equiv \hat{x}_n^H(t)$ and $\langle \hat{p}(t) | n \rangle \equiv \hat{p}_n^H(t)$.

Moreover, we specify the initial correlation according to initial product state $\hat{\rho}^{ini}(0)$, which turns out to be

$$\langle \hat{x}_{n_1}^\alpha \hat{x}_{n_2}^\beta \rangle = \delta_{\alpha\beta} \langle n_1 | \frac{\hbar}{2\hat{\omega}} (1 + 2\hat{f}^\alpha) | n_2 \rangle \quad (2.96)$$

$$\langle \hat{p}_{n_1}^\alpha \hat{p}_{n_2}^\beta \rangle = \delta_{\alpha\beta} \langle n_1 | \frac{\hbar\hat{\omega}}{2} (1 + 2\hat{f}^\alpha) | n_2 \rangle \quad (2.97)$$

$$\langle \hat{x}_{n_1}^\alpha \hat{p}_{n_2}^\beta \rangle = \frac{i\hbar}{2} \delta_{\alpha\beta} \delta_{n_1 n_2} \quad (2.98)$$

$$\langle \hat{p}_{n_1}^\alpha \hat{x}_{n_2}^\beta \rangle = -\frac{i\hbar}{2} \delta_{\alpha\beta} \delta_{n_1 n_2} \quad (2.99)$$

where,

$$\hat{x}_{n_1} = \begin{cases} \hat{x}_{n_1}^L & 1 \leq n_1 \leq N \\ \hat{x}_{(n_1-N)}^R & N+1 \leq n_1 \leq 2N \end{cases} \quad (2.100)$$

$$\hat{p}_{n_1} = \begin{cases} \hat{p}_{n_1}^L & 1 \leq n_1 \leq N \\ \hat{p}_{(n_1-N)}^R & N+1 \leq n_1 \leq 2N \end{cases} \quad (2.101)$$

$$\begin{aligned} \hat{\omega} |\tilde{k}\rangle &= \sqrt{2k_1 (1 - \cos \tilde{k}) + k_0} |\tilde{k}\rangle, \\ \tilde{k} &= \frac{\pi \tilde{j}}{N+1}, \tilde{j} = 1, 2, \dots, N \end{aligned} \quad (2.102)$$

$$\hat{f}^\alpha = \frac{1}{e^{\beta_\alpha \hbar \hat{\omega}} - 1}, \alpha = L, R \quad (2.103)$$

$$\langle n | \tilde{k} \rangle = \sqrt{\frac{2}{N+1}} \sin(\tilde{k}n), n = 1, 2, \dots, N. \quad (2.104)$$

We try to group the terms into two parts. The first part, which involves terms that are proportional to the difference between the Bose distributions of the left and right leads, becomes steady current in the proper limit specified later. The rest of the terms constitutes the other part and are interpreted to be the fluctuating contribution around the steady-current. The detailed steps are shown below:

$$\begin{aligned} I_L(t) &= - \left\langle \frac{d\hat{H}_L(t)}{dt} \right\rangle \\ &= -k_1 \left\langle \langle \hat{p}(t) | N \rangle \langle N+1 | \hat{x}(t) \rangle \right\rangle \end{aligned} \quad (2.105)$$

$$\begin{aligned} &= -k_1 \left\langle \left\{ -\langle \hat{x}^\dagger | \hat{\omega} \sin(\hat{\omega}t) | N \rangle + \langle \hat{p} | \cos(\hat{\omega}t) | N \rangle \right\} \right. \\ &\quad \cdot \left. \left\{ \langle N+1 | \cos(\hat{\omega}t) | \hat{x} \rangle + \langle N+1 | \frac{\sin(\hat{\omega}t)}{\hat{\omega}} | \hat{p}^\dagger \rangle \right\} \right\rangle \end{aligned} \quad (2.106)$$

Since

$$\begin{aligned}
 & \left\langle -\langle \hat{x}^\dagger | \hat{\omega} \sin(\hat{\omega}t) | N \rangle \langle N+1 | \frac{\sin(\hat{\omega}t)}{\hat{\omega}} | \hat{p}^\dagger \rangle \right. \\
 & \quad \left. + \langle \hat{p} | \cos(\hat{\omega}t) | N \rangle \langle N+1 | \cos(\hat{\omega}t) | \hat{x} \rangle \right\rangle \\
 &= \sum_{n_1=1}^{2N} \sum_{n_2=1}^{2N} \langle n_1 | \hat{\omega} \sin(\hat{\omega}t) | N \rangle \langle N+1 | \frac{\sin(\hat{\omega}t)}{\hat{\omega}} | n_2 \rangle \langle -\hat{x}_{n_1} \hat{p}_{n_2} \rangle \\
 & \quad + \sum_{n_1=1}^{2N} \sum_{n_2=1}^{2N} \langle n_1 | \cos(\hat{\omega}t) | N \rangle \langle N+1 | \cos(\hat{\omega}t) | n_2 \rangle \langle \hat{p}_{n_1} \hat{x}_{n_2} \rangle \\
 &= \sum_{n_1=1}^{2N} \langle n_1 | \hat{\omega} \sin(\hat{\omega}t) | N \rangle \langle N+1 | \frac{\sin(\hat{\omega}t)}{\hat{\omega}} | n_1 \rangle \left(-\frac{i\hbar}{2} \right) \\
 & \quad + \sum_{n_1=1}^{2N} \langle n_1 | \cos(\hat{\omega}t) | N \rangle \langle N+1 | \cos(\hat{\omega}t) | n_1 \rangle \left(-\frac{i\hbar}{2} \right) \\
 &= \left(-\frac{i\hbar}{2} \right) \langle N+1 | \left(\frac{\sin(\hat{\omega}t)}{\hat{\omega}} \hat{\omega} \sin(\hat{\omega}t) + \cos^2(\hat{\omega}t) \right) | N \rangle \\
 &= 0,
 \end{aligned}$$

two terms ' xp ' and ' px ' inside Eq. (2.106) can be exactly canceled.

Defining

$$\begin{aligned}
 \langle k | \tilde{k} \rangle^L &\equiv \sum_{n_1=1}^N \langle k | n_1 \rangle \langle n_1 | \tilde{k} \rangle \\
 \langle k | \tilde{k} \rangle^R &\equiv \sum_{n_1=N+1}^{2N} \langle k | n_1 \rangle \langle n_1 - N | \tilde{k} \rangle,
 \end{aligned} \tag{2.107}$$

we can directly verify that $\langle k | \tilde{k} \rangle^R = \langle k | \tilde{k} \rangle^L (-1)^{j+\tilde{j}}$, and $\langle \tilde{k} | k_2 \rangle^L \langle k_2 | N+1 \rangle = \langle \tilde{k} | k_2 \rangle^L \langle k_2 | N \rangle (-1)^{j_2+1}$.

Thus the expression for the current $I_L(t)$ can be separated into two parts, $I_{\text{fluct}}^L(t)$

and $I_{\text{stdy}}^L(t)$, where the fluctuating contribution is

$$\begin{aligned}
 I_{\text{fluct}}^L(t) = & \hbar k_1 \sum_{\tilde{k}} (f_{\tilde{k}}^L + f_{\tilde{k}}^R + 1) \\
 & \times \sum_{k \text{ odd}} \left(\frac{\omega_k}{\omega_{\tilde{k}}} - \frac{\omega_{\tilde{k}}}{\omega_k} \right) \sin(\omega_k t) \langle N|k \rangle \langle k|\tilde{k} \rangle^L \\
 & \times \sum_{k_2 \text{ odd}} \cos(\omega_{k_2} t) \langle \tilde{k}|k_2 \rangle^L \langle k_2|N \rangle \\
 & - \hbar k_1 \sum_{\tilde{k}} (f_{\tilde{k}}^L + f_{\tilde{k}}^R + 1) \\
 & \times \sum_{k \text{ even}} \left(\frac{\omega_k}{\omega_{\tilde{k}}} - \frac{\omega_{\tilde{k}}}{\omega_k} \right) \sin(\omega_k t) \langle N|k \rangle \langle k|\tilde{k} \rangle^L \\
 & \times \sum_{k_2 \text{ even}} \cos(\omega_{k_2} t) \langle \tilde{k}|k_2 \rangle^L \langle k_2|N \rangle.
 \end{aligned} \tag{2.108}$$

and the steady-state contribution is

$$\begin{aligned}
 I_{\text{stdy}}^L(t) = & \hbar k_1 \sum_{\tilde{k}} (f_{\tilde{k}}^L - f_{\tilde{k}}^R) \\
 & \times \sum_{k \text{ even}} \left(\frac{\omega_k}{\omega_{\tilde{k}}} + \frac{\omega_{\tilde{k}}}{\omega_k} \right) \sin(\omega_k t) \langle N|k \rangle \langle k|\tilde{k} \rangle^L \\
 & \times \sum_{k_2 \text{ odd}} \cos(\omega_{k_2} t) \langle \tilde{k}|k_2 \rangle^L \langle k_2|N \rangle \\
 & - \hbar k_1 \sum_{\tilde{k}} (f_{\tilde{k}}^L - f_{\tilde{k}}^R) \\
 & \times \sum_{k \text{ even}} \cos(\omega_k t) \langle N|k \rangle \langle k|\tilde{k} \rangle^L \\
 & \times \sum_{k_2 \text{ odd}} \left(\frac{\omega_{\tilde{k}}}{\omega_{k_2}} + \frac{\omega_{k_2}}{\omega_{\tilde{k}}} \right) \sin(\omega_{k_2} t) \langle \tilde{k}|k_2 \rangle^L \langle k_2|N \rangle.
 \end{aligned} \tag{2.109}$$

In the above, the summation for \tilde{k} extends over all $\frac{\pi \tilde{j}}{N+1}$ for $\tilde{j} = 1, \dots, N$, the summation involving “ k even” is on $k \in \left\{ \frac{\pi j}{2N+1} \right\}_{j=1}^{2N}$, j is even, and the summation involving “ k_2 odd” is on $k_2 \in \left\{ \frac{\pi j_2}{2N+1} \right\}_{j_2=1}^{2N}$, j_2 is odd, and so on. The dispersion

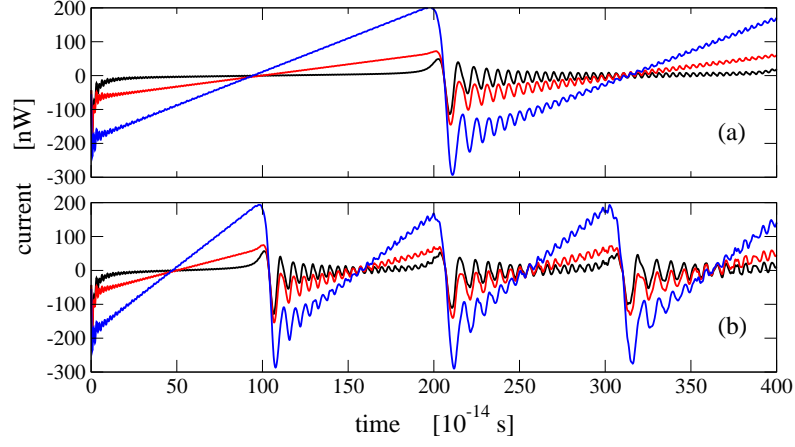


Figure 2.5: Plots of the current as a function of time when the left and right chains are finite with lengths (a) $N = 100$ and (b) $N = 50$. The average temperatures between the leads are $T = 10$ K (black line), $T = 100$ K (red (gray) line), and $T = 300$ K (blue (dark gray) line). The temperature bias between the leads $\alpha = 0.1$. There is no on-site potential, i.e., $k_0 = 0$, and the nearest-neighbor spring constant $k_1 = 1$ eV/Å²u.

relation satisfied is $\omega_q = \sqrt{2k_1(1 - \cos q) + k_0}$, and $f_k^\alpha = 1/(e^{\beta_\alpha \hbar \omega_k} - 1)$, $\alpha = \text{L, R}$. The sum in Eq. (2.107) can be carried out analytically, resulting in

$$\begin{aligned} \langle N|k\rangle \langle k|\tilde{k}\rangle^{\text{L}} &= \frac{-1}{(2N+1)\sqrt{2(N+1)}} \\ &\times \sin(\tilde{k}N) \frac{\cos k - (-1)^j}{\cos \tilde{k} - \cos k}. \end{aligned} \quad (2.110)$$

A similar expression can be derived for $\langle \tilde{k}|k_2\rangle^{\text{L}} \langle k_2|N\rangle$. Using Eqs. (2.108) to (2.110), the current can now be exactly calculated in computer time proportional to $\mathcal{O}(N^2)$.

Shown in Fig. 2.5 are plots of the current flowing out of the left lead when there is no on-site spring potential. The length of the leads are both $N = 100$ in Fig. 2.5(a)

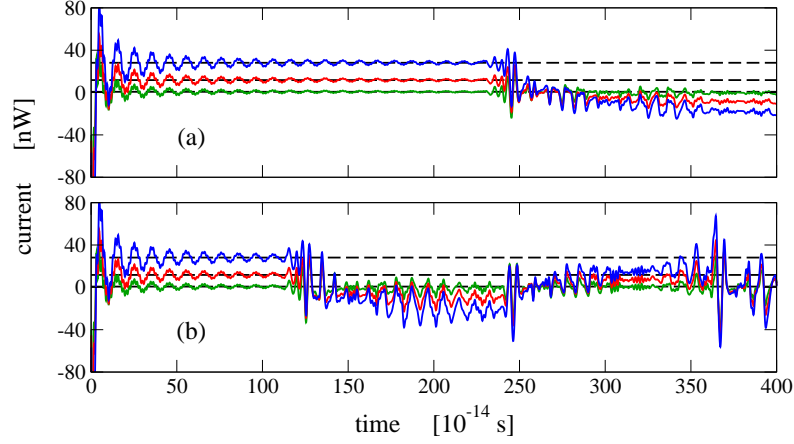


Figure 2.6: Plots of the current when the on-site spring constant is $k_0 = 0.1 \text{ eV/\AA}^2\text{u}$ at 10% of the value of $k_1 = 1 \text{ eV/\AA}^2\text{u}$. The left and right chains have lengths (a) $N = 100$ and (b) $N = 50$. the average temperature between the chains are $T = 100 \text{ K}$ (green (lowest gray) line), $T = 300 \text{ K}$ (red (middle gray) line), and $T = 500 \text{ K}$ (blue (upper gray) line). The temperature offset $\alpha = 10\%$. The dash lines are the values of the steady-state current, corresponding to $T = 100 \text{ K}$, 300 K , and 500 K , calculated independently from the Landauer-like formula.

and $N = 50$ in Fig. 2.5(b). The left lead initially has temperature $T_L = (1 + \alpha)T$, where $\alpha = 0.1$, while the right lead has initial temperature $T_R = (1 - \alpha)T$. The plots in Fig. 2.5 correspond to $T = 10 \text{ K}$, 100 K , and 300 K . Notice that the overall behavior is roughly periodic with a period proportional to the full length of the chain due to the finite size effect.

Shown in Fig. 2.6 are plots of the current when $k_0 = 0.1 \text{ eV/\AA}^2\text{u}$, i.e., at 10% of the value of $k_1 = 1 \text{ eV/\AA}^2\text{u}$. Also shown in the figure are dashed lines representing the steady-state current calculated using the Landauer-like formula. We now see that the current approaches a quasi-steady-state value and that this quasi-steady-state

lasts longer for longer leads. Note, however, that the quasi-steady-state does not last for more than $2t_m$ (t_m is defined to be the time when sound wave travels the left or right chain). After time $2t_m$, the waves or disturbances that have been reflected back at the hard walls, which is at the edges of the leads, have returned back to the interleads coupling and interfere with the other waves there. This results in the current to begin oscillating wildly.

In the following, we recover the Landauer-like formula for the thermal current in the large-size limit using Heisenberg equation of motion method directly. All of the expressions derived at this point are exact. We now make an approximation in order to extend our calculations for the steady-state contribution to large N and eventually arrive at the Landauer formula.

Notice that in Eq. (2.110) and the corresponding expression for k_2 that the terms involving $k \approx \tilde{k} \approx k_2$ would dominate the summation, especially when N approaches infinity. Consequently,

$$\begin{aligned}
 I_{\text{stdy}}^L(t) &\approx \hbar k_1 \frac{1}{N+1} \sum_{\tilde{k}} (f_{\tilde{k}}^L - f_{\tilde{k}}^R) \sin^4 \tilde{k} \\
 &\times \left\{ \frac{1}{2N+1} \frac{1}{2} \sum_{k_2} \frac{\sin(\omega_{\tilde{k}} - \omega_{k_2}) t}{\cos \tilde{k} - \cos k_2} \right\} \\
 &\times \left\{ \frac{1}{2N+1} \left\{ \sum_{k \text{ even}} \frac{-1}{\cos \tilde{k} - \cos k} \right. \right. \\
 &\quad \left. \left. + \sum_{k \text{ odd}} \frac{1}{\cos \tilde{k} - \cos k} \right\} \right\}.
 \end{aligned} \tag{2.111}$$

Let $N \rightarrow \infty$ and then followed by $t \rightarrow \infty$, we get

$$\begin{aligned}
 & \frac{1}{(2N+1)} \frac{1}{2} \sum_{k_2} \frac{\sin(\omega_{\tilde{k}} - \omega_{k_2}) t}{\left(\cos \tilde{k} - \cos k_2\right)} \\
 &= \frac{1}{(2N+1)} \sum_{k_2} \frac{\sin(\omega_{\tilde{k}} - \omega_{k_2}) t}{\omega_{k_2}^2 - \omega_{\tilde{k}}^2} \\
 &\approx \frac{1}{\pi} \int_0^\pi dk_2 \frac{\sin(\omega_{\tilde{k}} - \omega_{k_2}) t}{(\omega_{k_2} - \omega_{\tilde{k}})(\omega_{k_2} + \omega_{\tilde{k}})} \\
 &= - \int_{\sqrt{k_0}}^{\sqrt{4k_1+k_0}} d\omega_{k_2} \frac{\omega_{k_2}}{\sin k_2} \frac{1}{(\omega_{k_2} + \omega_{\tilde{k}})} \delta(\omega_{\tilde{k}} - \omega_{k_2}) \\
 &= - \frac{1}{2 \sin \tilde{k}}
 \end{aligned} \tag{2.112}$$

Furthermore, we have

$$\begin{aligned}
 \lim_{N \rightarrow \infty} \frac{1}{2N+1} \left\{ \sum_{k \text{ even}} \frac{-1}{\cos \tilde{k} - \cos k} \right. \\
 \left. + \sum_{k \text{ odd}} \frac{1}{\cos \tilde{k} - \cos k} \right\} = - \frac{1}{\sin^2 \tilde{k}}
 \end{aligned} \tag{2.113}$$

for some $\tilde{k} \in \left\{ \frac{\pi j}{N+1} \right\}_{j=1}^N$, which can be directly verified by the software Mathematica. We then recover the Landauer formula

$$\begin{aligned}
 I_{\text{stdy}}^L &= \frac{1}{2} \hbar k_1 \frac{1}{N+1} \sum_{\tilde{k}} (f_{\tilde{k}}^L - f_{\tilde{k}}^R) \sin \tilde{k} \\
 &= \frac{1}{2\pi} \int_{\sqrt{k_0}}^{\sqrt{4k_1+k_0}} d\omega \hbar \omega (f^L(\omega) - f^R(\omega)),
 \end{aligned} \tag{2.114}$$

the specific form of which can be also obtained from the application of Eq. (1.1) on this model. Note in the above that the discrete summation over wavevector \tilde{k} is converted into a continuous integration over the angular frequency ω . Furthermore, we want to emphasize that although the on-site constant k_0 appears in the expressions for both I_{stdy} and I_{fluct} , its presence in the steady-state contribution I_{stdy} does not prevent the contribution to approach a steady-state value in the long-time limit. In contrast, the value of k_0 is crucial for the fluctuating contribution

I_{fluct} to decay away. A zero k_0 would result in I_{trans} having a strong time-dependent zigzag-like behavior that dominates the total energy current at all times. There would be no steady current flow even when $N \rightarrow \infty$. However, even a small on-site potential, say $k_0/k_1 = 0.1$, would result in the fluctuating contribution to decay away in the long-time limit and leave only the contribution from the steady-state term.

Chapter 3

Energy transport in coupled left-right-lead systems

Generally in nonequilibrium state energy will transfer into or out of an open system H_L , the notation of which remind us of the left lead of the whole system $H_{tot} = H_L + H_C + H_R + H_{LC} + H_{CR}$ we discussed in the last chapter. In order to describe the energy transfer, we first consider the energy stored in the open system H_L at time t , which is

$$E_L(t) = \text{Tr} [\rho^{ini} H_L^H(t)] . \quad (3.1)$$

Then the energy current flowing out of the open system can be obtained as

$$I_L(t) = -\frac{dE_L(t)}{dt} = -\text{Tr} \left[\rho^{ini} \frac{dH_L^H(t)}{dt} \right] \equiv \text{Tr} \left[\rho^{ini} \hat{I}_L^H(t) \right] , \quad (3.2)$$

where correspondingly we have defined the current operator \hat{I}_L^S , whose Heisenberg-picture form is just $\hat{I}_L^H(t)$.

Now we try to understand the ensemble average defining the energy current from quantum histories point of view. With the specified initial density matrix ρ^{ini} , the quantum histories used to study the energy current shown in Eq. (3.2) simply consists of one-time events, which is expressed by the projectors onto the eigenstates of the current operator \hat{I}_L^S :

$$P^{i_L} = |i_L\rangle \langle i_L|, \quad \hat{I}_L^S |i_L\rangle = i_L |i_L\rangle, \quad (3.3)$$

$$\sum_{i_L} |i_L\rangle \langle i_L| = I, \quad (3.4)$$

where without loss of generality we assume the eigenstates are nondegenerate. A realization of the history relevant to the energy current is given as $Y = I \odot P_t^{i_L}$. Then the energy current at time t is obtained as

$$I_L(t) = \sum_{i_L} i_L \text{Pr}(Y) \quad (3.5)$$

$$= \sum_{i_L} i_L \text{Tr} \left[\rho^{ini} K(Y)^\dagger K(Y) \right] \quad (3.6)$$

$$= \sum_{i_L} i_L \text{Tr} \left[\rho^{ini} U(t_0, t) P_t^{i_L} P_t^{i_L} U(t, t_0) \right] \quad (3.7)$$

$$= \text{Tr} \left[\rho^{ini} U(t_0, t) \hat{I}_L^S U(t, t_0) \right] \quad (3.8)$$

$$= \text{Tr} \left[\rho^{ini} \hat{I}_L^H(t) \right] \quad (3.9)$$

which is consistent with the original definition in Eq. (3.2). In the derivation, we have used the spectrum decomposition of the current operator $\hat{I}_L^S = \sum_{i_L} i_L |i_L\rangle \langle i_L|$ and the property of the projector $P_t^{i_L} P_t^{i_L} = P_t^{i_L}$.

The family of the quantum histories we used to study the energy current is automatically consistent due to the orthogonality of different projectors defined in Eq. (3.3), which is briefly shown as below:

$$\text{Tr} \left[\rho^{ini} K(Y)^\dagger K(Y') \right] = \text{Tr} \left[\rho^{ini} U(t_0, t) P_t^{i_L} P_t^{i'_L} U(t, t_0) \right] = 0 \quad (3.10)$$

for $Y \neq Y'$.

Here for the simplicity of notations and discussion, we implicitly assume that the eigenstates of the current operator are discrete, which normally is not true in lattice systems. However for the case of continuous spectrum of the current operator, the projector can be written as $P_t^{i_L} = |i_L\rangle \langle i_L| di_L$, which generally depends on the accuracy of the ‘measurement’ di_L .

In this chapter, we study energy transport and present a generalized transmission coefficient formula for the lead-junction-lead system, in which interaction between the leads has been taken into account [43]. Based on this formula, the Caroli formula could be easily recovered and a transmission coefficient formula for interface problem in the ballistic system can be obtained. The condition of validity for the formula is carefully explored. Also, an illustrative example is given to clarify the precise meaning of the quantities used in the formula, such as the concept of the reduced interacting matrix in different situations. In addition, an explicit transmission coefficient formula for a general one-dimensional interface setup is obtained based on the derived interface formula.

3.1 Formalism

3.1.1 Model system

We consider the lead-junction-lead model initially prepared in product state $\hat{\rho}(t_0) = \frac{e^{-\beta_L H_L}}{\text{Tr}(e^{-\beta_L H_L})} \otimes \frac{e^{-\beta_C H_C}}{\text{Tr}(e^{-\beta_C H_C})} \otimes \frac{e^{-\beta_R H_R}}{\text{Tr}(e^{-\beta_R H_R})}$. We can imagine that left lead (L), center junction (C), and right lead (R) in this model were in contact with three different heat baths at the inverse temperatures $\beta_L = (k_B T_L)^{-1}$, $\beta_C = (k_B T_C)^{-1}$, and $\beta_R = (k_B T_R)^{-1}$, respectively, for time $t < t_0$. At time $t = t_0$, all the heat baths are removed, and coupling of the center junction with the leads and the interaction between the two leads are switched on abruptly. Now the total Hamiltonian of the lead-junction-lead system becomes

$$H_{tot} = H_L + H_C + H_R + H_{LC} + H_{CR} + H_{LR}, \quad (3.11)$$

where $H_\alpha = \frac{1}{2}p_\alpha^T p_\alpha + \frac{1}{2}u_\alpha^T K^\alpha u_\alpha$, $\alpha = L, C, R$ represents coupled harmonic oscillators, and $u_\alpha \equiv \sqrt{m}x_\alpha$ and p_α are column vectors of transformed coordinates and corresponding conjugate momenta in region α . The superscript T stands for matrix transpose. $H_{LC} = u_L^T V^{LC} u_C$ and $H_{CR} = u_C^T V^{CR} u_R$ are the usual couplings between the junction and the two leads, which are certainly necessary to establish the heat current. Now the new term representing interaction between two leads $H_{LR} = u_L^T V^{LR} u_R$ will greatly modify transmission coefficient, which is our main interest.

It is worth mentioning that nonlinear interaction could be added inside the center junction and dealt with using a self-consistent approach in the framework of NEGF, which has been done by some authors [12, 55, 56].

3.1.2 Steady-state contour-ordered Green's functions

As was mentioned in the previous Chapter, contour-ordered Green's functions are the central objects in the NEGF formalism, among which the directly derived relation, say, the Dyson equation, could be readily transformed to all kinds of relations among the real-time Green's functions by the Langreth theorem [57]. Many interesting quantities, such as the current we consider in the following subsection, could be easily related to the proper real-time Green's functions.

Steady-state contour-ordered Green's functions are defined as

$$G_{jk}^{\alpha\beta}(\tau_1, \tau_2) = -\frac{i}{\hbar} \text{Tr} \left\{ \hat{\rho}^{ss}(s) T_\tau \left[u_j^\alpha(\tau_1) u_k^\beta(\tau_2) \right] \right\}, \alpha, \beta = L, C, R, \quad (3.12)$$

where $\hat{\rho}^{ss}(s) = U(s, t_0) \hat{\rho}(t_0) U(t_0, s)$ is the steady-state density operator, in which time $s > t_0$ introduced for convenience in later discussion could take any finite time since the switch-on time t_0 will go to $-\infty$ at the end in order to establish steady-state heat current. $u_j^\alpha(\tau_1) = U(s, \tau_1) u_j^\alpha U(\tau_1, s)$ is the coordinate operator of j th degree of freedom in region α in the Heisenberg picture and similarly for $u_k^\beta(\tau_2)$. The variables τ_1 and τ_2 are on the contour from time s to ∞ and back from ∞ to time s . $U(t_0, s)$ are the time evolution operators of the full Hamiltonian. T_τ is the contour-ordering superoperator. There is a strong assumption here which is all we need in the whole derivation, where we assume steady state could be established from initial product state after infinite time so that all the steady-state real-time Green's functions depend only on the difference of the two-time arguments. This intuitively reasonable assumption is not always guaranteed and in the Sec. 2.3 of the last chapter we have carefully examined if, when, and how the onset of the steady-state occurs using a specific example.

After $t_0 \rightarrow -\infty$, $s \rightarrow t_0^+$, and transforming to the interaction picture, where the total Hamiltonian H_{tot} is separated into the free part $H_0 = H_L + H_C + H_R$ and the interaction part $H_{int} = H_{LC} + H_{CR} + H_{LR}$, we obtain

$$G_{jk}^{\alpha\beta}(\tau_1, \tau_2) = -\frac{i}{\hbar} \text{Tr} \left\{ \hat{\rho}(-\infty) T_\tau \left[e^{-\frac{i}{\hbar} \int_K H_{int}^I(\tau') d\tau'} u_{I,j}^\alpha(\tau_1) u_{I,k}^\beta(\tau_2) \right] \right\}, \quad (3.13)$$

where $u_{I,j}^\alpha(\tau_1) = e^{\frac{i}{\hbar} H_0 \tau_1} u_j^\alpha e^{-\frac{i}{\hbar} H_0 \tau_1}$ is the operator in the interaction picture and similarly for $u_{I,k}^\beta(\tau_2)$ and $H_{int}^I(\tau')$. Now the variables τ_1 and τ_2 are on the Keldysh contour [58, 59] K from $-\infty$ to ∞ and back from ∞ to $-\infty$. Expanding the exponential to perform a perturbation expansion and using Feynman diagrammatic technique, we can obtain Dyson equations for $G^{\alpha\beta}(\tau_1, \tau_2)$, $\alpha, \beta = L, C, R$ such as

$$G_{ij}^{CL}(\tau_1, \tau_2) = \sum_{l,n} \int_K d\tau g_{il}^C(\tau_1, \tau) V_{ln}^{CL} G_{nj}^{LL}(\tau, \tau_2) + \sum_{l,n} \int_K d\tau g_{il}^C(\tau_1, \tau) V_{ln}^{CR} G_{nj}^{RL}(\tau, \tau_2). \quad (3.14)$$

All these Dyson equations could be symbolically lumped into a compact matrix expression,

$$G = g + gVG = g + GVg, \quad (3.15)$$

where $G = \begin{bmatrix} G^{LL} & G^{LC} & G^{LR} \\ G^{CL} & G^{CC} & G^{CR} \\ G^{RL} & G^{RC} & G^{RR} \end{bmatrix}$, $g = \begin{bmatrix} g^L & 0 & 0 \\ 0 & g^C & 0 \\ 0 & 0 & g^R \end{bmatrix}$, $V = \begin{bmatrix} 0 & V^{LC} & V^{LR} \\ V^{CL} & 0 & V^{CR} \\ V^{RL} & V^{RC} & 0 \end{bmatrix}$
 ($V^T = V$), and

$$g_{jk}^\alpha(\tau_1, \tau_2) = -\frac{i}{\hbar} \text{Tr} \left\{ \frac{e^{-\beta_\alpha H_\alpha}}{\text{Tr}(e^{-\beta_\alpha H_\alpha})} T_c [u_{I,j}^\alpha(\tau_1) u_{I,k}^\alpha(\tau_2)] \right\}, \quad (3.16)$$

$\alpha = L, C, R$ are equilibrium contour-ordered Green's functions for the free subsystems, which are easy to calculate directly. No approximation is needed here, since the coupling H_{int} is quadratic.

3.1.3 Generalized steady-state current formula

Certainly, heat current flowing out of the left lead in steady state does not depend on time and based on its definition $I_L^{ss} \equiv -\text{Tr}[\hat{\rho}^{ss}(s) dH_L(t)/dt]$ for $t > s$, we could simply obtain

$$\begin{aligned} I_L^{ss} &= - \int_{-\infty}^{\infty} \frac{d\omega}{2\pi} \hbar\omega \text{Tr}[(VG^<[\omega])_{LL}] \\ &= - \int_{-\infty}^{\infty} \frac{d\omega}{2\pi} \hbar\omega \text{Tr}[(V_{red}G_{red}^<[\omega])_{LL}], \end{aligned} \quad (3.17)$$

where $(VG^<[\omega])_{LL}$ denotes the LL part submatrix of $VG^<[\omega]$.

Observing the structure of $\text{Tr}[(VG^<[\omega])_{LL}]$, we note that the size of the $G^<[\omega]$ making nonzero contribution to I_L^{ss} is completely determined by nonzero entries in the symmetric total coupling matrix V . So we do not need the full $G^<[\omega]$ which is an infinite matrix due to the two semi-infinite leads. According to this observation, we choose the reduced square matrix $G_{red}^<[\omega]$ to be the corresponding submatrix of $G^<[\omega]$ determined by the row indexes of nonzero row vectors of coupling matrices $V^{LC}, V^{LR}, V^{RC}, V^{RL}$ plus full center part row indexes inside the total coupling matrix V for the rows of $G_{red}^<[\omega]$, and the column indexes of nonzero column vectors of coupling matrices $V^{CL}, V^{RL}, V^{CR}, V^{LR}$ plus full center part column indexes inside the total coupling matrix V for the columns of $G_{red}^<[\omega]$.

In order to calculate the lesser Green's function $G_{red}^<[\omega]$, a closed Dyson equation for reduced contour-ordered Green's function $G_{red}(\tau_1, \tau_2)$ is needed. Equation (3.15) is the starting point, and it is also true that $G_{red} = g_{red} + g_{red}V_{red}G_{red}$, where g_{red} is similarly defined as G_{red} and V_{red} is the submatrix of original V after crossing out all the zero column and row vectors except for the possible zero vectors

whose row or column indexes are the center (junction) ones. Actually, G_{red} is the corresponding submatrix of G just like V_{red} .

From now on, for notational simplicity, we omit the subscript *red* of all the steady-state Green's functions and all the coupling matrices with the understanding that these matrices are of finite dimensions.

Using the Langreth theorem [57] and Fourier transforming the obtained real-time Green's functions, we can get

$$G^<[\omega] = G^r[\omega] \begin{pmatrix} -if_L \tilde{\Gamma}_L[\omega] & 0 & 0 \\ 0 & 0 & 0 \\ 0 & 0 & -if_R \tilde{\Gamma}_R[\omega] \end{pmatrix} G^a[\omega], \quad (3.18)$$

where

$$\tilde{\Gamma}_{\{L,R\}} \equiv i \left[\left(g_{\{L,R\}}^{sur,a} \right)^{-1} - \left(g_{\{L,R\}}^{sur,r} \right)^{-1} \right], \quad (3.19)$$

$g_L^{sur,a}$ is the advanced surface Green's function for the left lead coming from the corresponding part of the advanced reduced Green's function g_{red}^a , and similarly for the retarded one. This new function plays an important role for our generalized Caroli formula and for an interface formula, derived below. Here, fluctuation dissipation theorem $g_\alpha^<[\omega] = f_\alpha[\omega] (g_\alpha^r - g_\alpha^a)$, $\alpha = L, C, R$, has been used as well as $(g_C^a)^{-1} - (g_C^r)^{-1} = 0$, which is responsible for the vanishing of junction temperature dependence of the final steady-state current formula.

Substituting Eq. (3.18) into steady current expression (3.17), we easily obtain

$$I_L^{ss} = \int_{-\infty}^{\infty} \frac{d\omega}{2\pi} \hbar \omega \left(f_L T_1[\omega] + f_R T_2[\omega] \right), \quad (3.20)$$

where

$$T_1[\omega] = i\text{Tr} \left(V^{LC} G_{CL}^r \tilde{\Gamma}_L G_{LL}^a + V^{LR} G_{RL}^r \tilde{\Gamma}_L G_{LL}^a \right), \quad (3.21)$$

$$T_2[\omega] = i\text{Tr} \left(V^{LC} G_{CR}^r \tilde{\Gamma}_R G_{RL}^a + V^{LR} G_{RR}^r \tilde{\Gamma}_R G_{RL}^a \right). \quad (3.22)$$

Again applying Langreth theorem and Fourier transform to the corresponding reduced one of Eq. (3.15), we get $G_{LR}^a = G_{LL}^a V^{LR} g_R^{sur,a} + G_{LC}^a V^{CR} g_R^{sur,a}$ and $G_{LC}^a = G_{LL}^a V^{LC} g_C^a + G_{LR}^a V^{RC} g_C^a$. Using the relations such as $(G_{CL}^r)^\dagger = G_{LC}^a$, $(\tilde{\Gamma}_L)^\dagger = \tilde{\Gamma}_L$ (where the superscript \dagger stands for transpose conjugate), we obtain

$$T_1[\omega] + T_1^*[\omega] = \text{Tr} \left(G_{RL}^r \tilde{\Gamma}_L G_{LR}^a \tilde{\Gamma}_R \right), \quad (3.23)$$

In deriving it, the cyclic property of the trace was used. Following similar steps, we get

$$T_2[\omega] + T_2^*[\omega] = -\text{Tr} \left(G_{RL}^a \tilde{\Gamma}_L G_{LR}^r \tilde{\Gamma}_R \right), \quad (3.24)$$

Because $\tilde{\Gamma}_\alpha^T = \tilde{\Gamma}_\alpha$, $\alpha = L, R$, $(G_{RL}^r)^T = G_{LR}^r$, and $(G_{RL}^a)^T = G_{LR}^a$, it is easy to show that $T_1 + T_1^* = -(T_2 + T_2^*)$. Now we define the general transmission coefficient

$$T_G[\omega] \equiv T_1[\omega] + T_1^*[\omega] = \text{Tr} \left(G_{RL}^a \tilde{\Gamma}_L G_{LR}^r \tilde{\Gamma}_R \right). \quad (3.25)$$

Since current is certainly a real number, and this property has been kept in the whole derivation, we have $I_L^{ss} = \frac{1}{2} (I_L^{ss} + I_L^{ss*}) = \frac{1}{2} \int_{-\infty}^{\infty} \frac{d\omega}{2\pi} \hbar\omega T_G[\omega] (f_L - f_R)$.

According to the definitions of retarded and advanced Green's functions in the frequency domain, we know $G_{RL}^a[-\omega] = (G_{LR}^r[\omega])^T$ and $\tilde{\Gamma}_{\{L,R\}}[-\omega] = (-\tilde{\Gamma}_{\{L,R\}}[\omega])^T$. Together with $f_L[-\omega] - f_R[-\omega] = -f_L[\omega] + f_R[\omega]$, we see that the integrand is even in ω ; steady current I_L^{ss} can be simplified further to the final expression

$$I_L^{ss} = \int_0^\infty \frac{d\omega}{2\pi} \hbar\omega T_G[\omega] (f_L - f_R). \quad (3.26)$$

Thus, it is the same as expected that the Landauer-like formula still applies to this general case, taking lead-lead interaction into account. This Landauer-like formula with the explicit general transmission coefficient expression (3.25) is the contribution in the thesis.

Now we need to know how to calculate G_{LR}^r for specific applications. According to the corresponding reduced one of Eq. (3.15), we can obtain a closed equation for G_{LR}^r ,

$$G_{LR}^r = \tilde{g}_L^r \tilde{V}^{LR,r} \tilde{g}_R^r + \tilde{g}_L^r \tilde{V}^{LR,r} \tilde{g}_R^r \tilde{V}^{RL,r} G_{LR}^r, \quad (3.27)$$

where $\tilde{g}_\alpha^r \equiv ((g_\alpha^{sur,r})^{-1} - V^{\alpha C} g_C^r V^{C\alpha})^{-1}$, $\alpha = L, R$, and $(\tilde{V}^{RL,r})^T = \tilde{V}^{LR,r} = V^{LR} + V^{LC} g_C^r V^{CR}$. Since $G_{RL}^a = (G_{LR}^r)^\dagger$, now all the quantities necessary to obtain general transmission coefficient T_G could be expressed in terms of retarded or advanced form of submatrix of g_{red} and submatrix of V_{red} , which are both easily obtained.

3.1.4 Recovering the Caroli formula and deriving an interface formula

First, we recover the Caroli formula for transmission coefficient. In this case, coupling between the two leads V^{LR} has been assumed to be 0. Thus, similar to what we did in Subsec. 3.1.3, we could easily derived $G_{LR}^r = g_L^{sur,r} V^{LC} G_{CR}^r = g_L^{sur,r} V^{LC} G_{CC}^r V^{CR} g_R^{sur,r}$. Together with $G_{RL}^a = (G_{LR}^r)^\dagger$, we could immediately obtain from formula (3.25) that $T[\omega] = \text{Tr}(G_{CC}^r \Gamma_R G_{CC}^a \Gamma_L)$, where $\Gamma_L = iV^{CL}(g_L^{sur,r} - g_L^{sur,a})V^{LC}$, and similarly for Γ_R . Here, we should remember that all the quantities

inside the trace now are reduced ones. However, it is still equal to expression (1.2), in which all the quantities could be the full ones, taking the trace operation and the reducing procedure for G and V into account. Method for calculating $T[\omega]$ and applying this efficient formula to specific applications have been stated by many authors, e.g. [49].

Now we derive an interface formula still based on formula (3.25). By *interface* we simply mean that the left lead and right lead have been connected directly and the center junction has been removed. Mathematically, we know $V^{CL} = 0$ and $V^{CR} = 0$ in this situation. Consequently, $G_{LR}^r = g_L^{sur,r} V^{LR} G_{RR}^r$ and $G_{RL}^a = (G_{LR}^r)^\dagger = G_{RR}^a V^{RL} g_L^{sur,a}$. Straightforwardly, we get the transmission coefficient formula in this interface problem [60]

$$T_I[\omega] = \text{Tr} \left(G_{RR}^r \tilde{\Gamma}_R G_{RR}^a \Gamma_L \right). \quad (3.28)$$

In order to apply this formula, still we need a closed equation for G_{RR}^r , which could be simply obtained to be

$$G_{RR}^r = g_R^{sur,r} + g_R^{sur,r} \tilde{\Sigma}_L^r G_{RR}^r, \quad (3.29)$$

where the reduced retarded self-energy is given by $\tilde{\Sigma}_L^r = V^{RL} g_L^{sur,r} V^{LR}$.

3.2 An illustrative application

The illustrative example is a one-dimensional central ring problem, in which there is only one particle in the center junction connected with two semi-infinite spring chain leads, see Fig. 3.1(a). In this model, the interaction between the two nearest

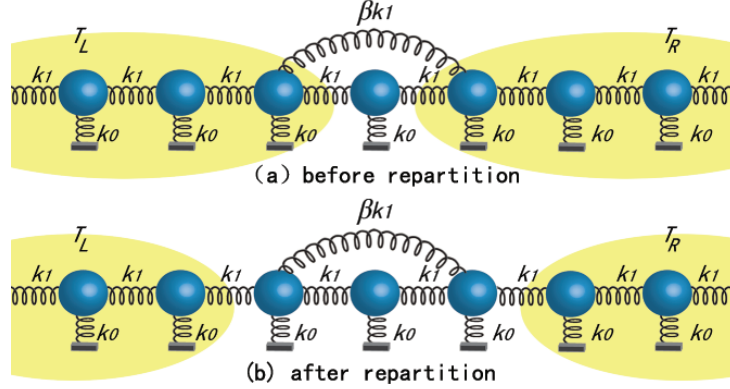


Figure 3.1: An illustration of the model (a) before and (b) after repartitioning the total Hamiltonian. The temperature of the left lead and the right lead are maintained in T_L and T_R respectively. The interparticle spring constant is $k_1 = \omega_1^2$ and the on-site spring constant is $k_0 = \omega_0^2$. The coupling between the two lead is $\beta k_1 = \beta \omega_1^2$.

particles inside the two leads also exists and is taken into account as V^{LR} . Thus, the form of the total Hamiltonian is the same as in Eq. (5.1) with K_0^α , $\alpha = L, R$ being the semi-infinite tridiagonal spring constant matrix consisting of $2\omega_1^2 + \omega_0^2$ along the diagonal and $-\omega_1^2$ along the two off-diagonals, $K^C = 2\omega_1^2 + \omega_0^2$, $V_{red}^{LC} = -\omega_1^2$, $V_{red}^{CR} = -\omega_1^2$, and $V_{red}^{LR} = -\beta\omega_1^2$, where β is the coupling strength between two leads. The on-site potential term ω_0^2 is necessary in establishing the steady-state current dynamically. In this simple case, there is an analytical expression for $g_{\alpha,0}^{sur,r}[\omega]$, $\alpha = L, R$, which is $g_{\alpha,0}^{sur,r} = -\lambda_1/\omega_1^2$, $\lambda_1 = (-\Omega \pm \sqrt{\Omega^2 - 4\omega_1^4})/(2\omega_1^2)$, where $\Omega = (\omega + i0^+)^2 - 2\omega_1^2 - \omega_0^2$ and the choice between the plus or minus sign depends on satisfying $|\lambda_1| < 1$. Also, $g_C^{sur,r}[\omega] = 1/\Omega$. After all these preparations, the transmission coefficient is simply calculated by the formula (3.25).

An alternative method to deal with this problem was suggested by Di Ventra. Essentially we repartition the total Hamiltonian so that interaction between leads is absent, see Fig. 3.1(b). Thus, in this model, the form of the total Hamiltonian is still the same as in Eq. (5.1) but with

$$K^C = \begin{bmatrix} 2\omega_1^2 + \omega_0^2 & -\omega_1^2 & -\beta\omega_1^2 \\ -\omega_1^2 & 2\omega_1^2 + \omega_0^2 & -\omega_1^2 \\ -\beta\omega_1^2 & -\omega_1^2 & 2\omega_1^2 + \omega_0^2 \end{bmatrix}, \quad (3.30)$$

$$V_{red}^{LC} = \begin{bmatrix} -\omega_1^2 & 0 & 0 \end{bmatrix}, \quad (3.31)$$

$$V_{red}^{CR} = \begin{bmatrix} 0 \\ 0 \\ -\omega_1^2 \end{bmatrix}. \quad (3.32)$$

Since now $V_{red}^{LR} = 0$, we can use either the Caroli formula (1.2) or the general one (3.25) to calculate the transmission coefficient. The results of the two methods are compared in Fig. 3.2. It turns out to be that the results of the two methods are the same, which justifies the suggestion of Di Ventra from the NEGF point of view in this example. For $\beta = 0$, perfect transmission ($T[\omega] = 1$) is reached. From Fig. 3.2, we notice that the transmission decreases with increasing coupling strength between the two leads, which is very typical for transmission with broken translational invariance. Also, roughly speaking, the new peak in Fig. 3.2(d) originates from the interference of the two waves coming from the two different paths.

Probably a much more efficient way to calculate the transmission coefficient in this type of noninteracting problem is to use the interface formula (3.28). Frequently, the surface Green's functions become complex when we separate the total system

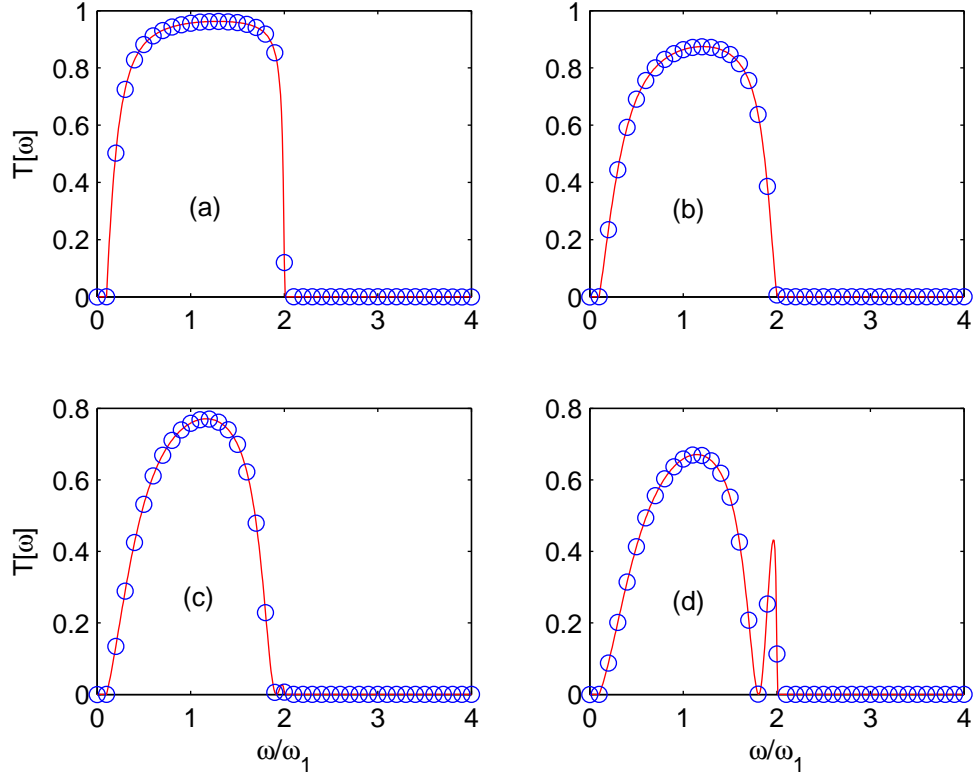


Figure 3.2: The transmission coefficient $T[\omega]$ as a function of frequency for coupling between leads (a) $\beta = 0.2$, (b) $\beta = 0.4$, (c) $\beta = 0.6$, and (d) $\beta = 0.8$. The results was calculated directly (red solid line), and by repartitioning the total Hamiltonian (blue circles). $\omega_0 = 0.1 \omega_1$ in all cases.

into two parts in order to apply the interface formula. However, there are some efficient algorithms for surface Green's functions see, for example, Ref. [49]. Now we show a specific application of the interface formula (3.28).

3.3 Explicit interface transmission function formula

In this section we derive an explicit expression for the transmission function $T_I[\omega]$ using Eq. (3.28) for the single interface setup; that is the left and right lead are directly connected and the center part is removed.

Let us consider that the normalized force constants for left and the right leads are ω_1^2 and ω_2^2 respectively and the normalized interface coupling strength is ω_{12}^2 . Also, on-site potential ω_0^2 to all the atoms exists to ensure that the steady state could be established dynamically. This is a quite general scenario for a one-dimensional harmonic chain, which is useful for the study of interface effects. One of the force constant matrix, say K^L , is equal to $K_0^L + \Delta K$, where ΔK is the semi-infinite matrix with only first element being nonzero $\Delta K_{11} = \omega_{12}^2 - \omega_1^2$ while K_0^L is the same as defined in the last application. The same holds for K^R with ω_1^2 replaced by ω_2^2 . In order to obtain the explicit form, only inputs that are required are retarded surface Green's function $g_\alpha^{sur,r}$ for both the leads. $G_{RR}^{\{r,a\}}$ in Eq. (3.28) can then be easily obtained from these expressions.

Let us calculate the surface Green's function for one of the leads, say, the left lead.

Then for the right lead it can be obtained by replacing ω_1^2 with ω_2^2 . The surface Green's function for a semi-infinite lead when all force constants are the same is given as before, that is $g_{L,0}^{sur,r}$. For this interface case, we can obtain the surface Green's function as follows. The retarded Green's function for the left lead satisfies the following equation

$$[(\omega + i0^+)^2 - K^L]g_L^r = I. \quad (3.33)$$

Taking $K^L = K_0^L + \Delta K$ into account, and using ΔK as a perturbation, we can write

$$g_L^r = g_{L,0}^r + g_{L,0}^r \Delta K g_L^r. \quad (3.34)$$

Since in this case only first atom of the left lead is connected with the first atom of the right lead, the retarded surface Green's function of the left lead is just the $(1, 1)$ -th element of g_L^r and we obtain

$$g_L^{sur,r} = \frac{1}{\omega_1^2 - \omega_{12}^2 - \omega_1^2/\lambda_1}, \quad (3.35)$$

and the self-energy for the lead is given by

$$\tilde{\Sigma}_L^r = \frac{\omega_{12}^4}{\omega_1^2 - \omega_{12}^2 - \omega_1^2/\lambda_1}. \quad (3.36)$$

Knowing this surface Green's function and self-energy, we can easily obtain $T_I[\omega]$ from Eq. (3.28), which can be written as

$$T_I[\omega] = -\frac{\omega_1^2 \omega_2^2 \omega_{12}^4 (\lambda_1 - \lambda_1^*)(\lambda_2 - \lambda_2^*)}{|(\omega_1^2 - \omega_{12}^2 - \omega_1^2/\lambda_1)(\omega_2^2 - \omega_{12}^2 - \omega_2^2/\lambda_2) - \omega_{12}^4|^2}, \quad (3.37)$$

where λ_2 is similarly defined as λ_1 with ω_1 replaced by ω_2 . We note that it matches exactly with the result in Ref. [61], where this expression is obtained from a wave-scattering method. Now if $\omega_1^2 = \omega_2^2 = \omega_{12}^2$, then we have perfect transmission (i.e., $T_I[\omega] = 1$ for ω within the phonon band $\omega_0^2 \leq \omega^2 \leq 4\omega_1^2 + \omega_0^2$ and 0 outside this region).

3.4 Summary

We examine the heat current in a lead-junction-lead quantum system, in which coupling between the leads has been taken into account. After assuming an ideal steady state could be established from initial product state, we rigorously derived a general Landauer-like formula in the NEGF framework, from which the corresponding transmission coefficient was obtained. Based on this general transmission coefficient formula, Caroli formula was recovered and a computationally efficient interface formula applicable to the case in which the total noninteracting Hamiltonian could be repartitioned was derived. Also an illustrative example was given as both verification of the validity of the repartitioning procedure which does not affect the steady current value, and clarification of the meaning of some quantities used in the formula, such as V_{red}^{LC} , in different situations. Finally, we derived an explicit transmission coefficient formula in a general one-dimensional interface situation based on the interface formula, which turned out to be perfectly consistent with result obtained by the wave-scattering method.

Chapter 4

Distribution of energy transport in coupled left-right-lead systems

In this chapter, we first briefly discuss the general theory of large deviations. Then based on two-time observation protocol (two-time quantum histories), we consider heat transfer in a given time interval t_M in lead-junction-lead system taking coupling between the leads into account. In view of the two-time quantum histories, consistency conditions are carefully verified in our specific family of quantum histories. Furthermore, its implication is briefly explored. Then using the nonequilibrium Green's function method, we obtain an exact formula for the cumulant generating function for heat transfer between the two leads valid in both transient and steady-state regimes. Also, a compact formula for the cumulant generating function in the long-time limit is derived, for which the Gallavotti-Cohen fluctuation symmetry is explicitly verified. In addition, we briefly discuss Di Ventra's

repartitioning trick regarding whether the repartitioning procedure of the total Hamiltonian affects the nonequilibrium steady-state current fluctuation. All kinds of properties of nonequilibrium current fluctuations, such as the fluctuation theorem in different time regimes, could be readily given according to these exact formulas.

4.1 Large deviation theory

The large deviation theory in terms of its mathematical version was initiated by Cramér [62] in the 1930s. Later several authors, such as Donsker and Freidlin [63, 64], contribute a lot to the development of this topic. For a thorough understanding of large deviation theory, one can resort to the books in Refs. [65, 66]. The brief discussion in this section mainly follows Touchette [67].

The theory of large deviations is concerned with the exponential decay of probabilities of large fluctuations in stochastic processes. The cornerstone of large deviation theory is the so-called large deviation principle. For our purpose, the large deviation principle is restricted to the situation as below: Let A_t be a random variable indexed by the positive integer t ¹, and let $\Pr(A_t = a)$ be the probability that A_t takes on a value a . In case that the value a the random variable A_t can take on is

¹The label t here stands for an integer number while for our purpose it means time, which certainly is real. The contradiction will be compromised when later t becomes very large.

continuous, then

$$\Pr(A_t = a) \equiv \Pr(A_t \in [a, a + da]) \quad (4.1)$$

$$= p(A_t = a) da \quad (4.2)$$

with $p(A_t = a)$ being the probability density of A_t . We say that $\Pr(A_t = a)$ satisfies a large deviation principle with rate function $I(a)$ if the limit

$$\lim_{t \rightarrow \infty} -\frac{1}{t} \ln \Pr(A_t = a) = I(a) \quad (4.3)$$

exists. For convenience, we introduce the sign “ \asymp ” and interpret it as expressing an equality relationship on a logarithmic scale; that is $a_t \asymp b_t$ means $\lim_{t \rightarrow \infty} \frac{1}{t} \ln a_t = \lim_{t \rightarrow \infty} \frac{1}{t} \ln b_t$. Thus, alternatively, we can use

$$\Pr(A_t = a) \asymp e^{-tI(a)} da \quad (4.4)$$

to mean that $\Pr(A_t = a)$ satisfy a large deviation principle, where we implicitly assume that A_t is a continuous random variable.

The theory of large deviations can be considered as a collection of methods developed to establish the large deviation principle for a given random variable if it exists and further derive the expression of the associated rate function. A fundamental result of large deviation theory known as the Gärtner-Ellis theorem can solve these two problems.

The Gärtner-Ellis Theorem

Consider a real continuous random variable A_t parameterized by the positive integer t , and define the (scaled) cumulant generating function of A_t by the limit

$$\lambda(k) = \lim_{t \rightarrow \infty} \frac{1}{t} \ln \langle e^{tkA_t} \rangle \quad (4.5)$$

and

$$\langle e^{tkA_t} \rangle \equiv \int_{-\infty}^{+\infty} e^{tkA_t} p(A_t = a) da \quad (4.6)$$

with the parameter k being real.

The Gärtner-Ellis theorem claims that, if $\lambda(k)$ exists and is differentiable for all $k \in \mathfrak{R}$, then A_t satisfies a large deviation principle, *i.e.*,

$$\Pr(A_t = a) \asymp e^{-tI(a)} da \quad (4.7)$$

with a rate function given by

$$I(a) = \sup_{k \in \mathfrak{R}} \{ka - \lambda(k)\}. \quad (4.8)$$

Where the mathematical symbol “sup” stands for “supremum of”.

In the following we give a plausible proof for the Gärtner-Ellis Theorem. Let us assume that the real random variable $A_t(\omega)$ is a function of t real random variables $\omega = (\omega_1, \omega_2, \dots, \omega_t)$. Denoting by $p(\omega)$ the probability density of ω , the probability density of A_t can be given as

$$p(A_t(\omega) = a) = \int_{\mathfrak{R}^t} \delta(A_t(\omega) - a) p(\omega) d\omega. \quad (4.9)$$

Employing the Laplace transform representation of Dirac’s delta function

$$\delta(a) = \frac{1}{2\pi i} \int_{b-i\infty}^{b+i\infty} e^{\xi a} d\xi, \quad \forall b \in \mathfrak{R}, \quad (4.10)$$

the probability density of A_t can be written as

$$p(A_t(\omega) = a) = \frac{1}{2\pi i} \int_{b-i\infty}^{b+i\infty} e^{-\xi a} d\xi \int_{\mathfrak{R}^t} e^{\xi A_t(\omega)} p(\omega) d\omega. \quad (4.11)$$

Performing the change of variable $\xi \rightarrow t\xi$, and notice that we have assumed

$$\int_{\mathfrak{R}^t} e^{t\xi A_t(\omega)} p(\omega) d\omega \equiv \langle e^{t\xi A_t(\omega)} \rangle \asymp e^{t\lambda(\xi)} \quad (4.12)$$

with $\lambda(\xi)$ being differentiable, we can write

$$p(A_t = a) \asymp \int_{b/t-i\infty}^{b/t+i\infty} d\xi e^{-t(\xi a - \lambda(\xi))}. \quad (4.13)$$

Choosing a proper parameter b so that the contour goes through the saddle-point ξ^* of $\xi a - \lambda(\xi)$, then using the saddle-point approximation, we can obtain

$$p(A_t = a) \asymp e^{-t(\xi^* a - \lambda(\xi^*))}. \quad (4.14)$$

Furthermore, assuming that $\lambda(\xi)$ is analytic, then ξ^* is both the unique minimum of $\xi a - \lambda(\xi)$ along the contour, which runs parallel to the imaginary axis from $\xi = \xi^* - i\infty$ to $\xi = \xi^* + i\infty$, and the maximum of $\xi a - \lambda(\xi)$ along the real axis. Therefore, we can get

$$\lim_{t \rightarrow \infty} -\frac{1}{t} \ln p(A_t = a) = \sup_{\xi \in \mathbb{R}} \{\xi a - \lambda(\xi)\}. \quad (4.15)$$

It is interesting to notice that the cumulant generating function $\lambda(k)$ is always convex: Considering Hölder's inequality

$$\sum_i |y_i z_i| \leq \left(\sum_i |y_i|^{1/p} \right)^p \left(\sum_i |z_i|^{1/q} \right)^q \quad (4.16)$$

with $0 \leq p, q \leq 1$, $p + q = 1$, and setting

$$y_i = [\Pr(a_i)]^\alpha e^{\alpha t k_1 a_i} \quad (4.17)$$

$$z_i = [\Pr(a_i)]^{1-\alpha} e^{(1-\alpha) t k_2 a_i} \quad (4.18)$$

$$p = \alpha \quad (4.19)$$

$$q = 1 - \alpha \quad (4.20)$$

$$\alpha \in [0, 1],$$

we can get

$$\begin{aligned} \sum_i \Pr(a_i) e^{t(\alpha k_1 a_i + (1-\alpha)k_2 a_i)} &\leq \left(\sum_i \Pr(a_i) e^{t k_1 a_i} \right)^\alpha \\ &\cdot \left(\sum_i \Pr(a_i) e^{t k_2 a_i} \right)^{1-\alpha} \end{aligned} \quad (4.21)$$

or

$$\ln \langle e^{t[\alpha k_1 + (1-\alpha)k_2]A_t} \rangle \leq \alpha \ln \langle e^{t k_1 A_t} \rangle + (1-\alpha) \ln \langle e^{t k_2 A_t} \rangle. \quad (4.22)$$

Hence,

$$\alpha \lambda(k_1) + (1-\alpha) \lambda(k_2) \geq \lambda(\alpha k_1 + (1-\alpha)k_2). \quad (4.23)$$

4.2 Model and consistent quantum framework for the study of energy transport

We consider the lead-junction-lead model initially prepared in product state $\rho^{ini} = \frac{e^{-\beta_L H_L}}{\text{Tr}(e^{-\beta_L H_L})} \otimes \frac{e^{-\beta_C H_C}}{\text{Tr}(e^{-\beta_C H_C})} \otimes \frac{e^{-\beta_R H_R}}{\text{Tr}(e^{-\beta_R H_R})}$. We can imagine that left lead (L), center junction (C), and right lead (R) in this model were in contact with three different heat baths at the inverse temperatures $\beta_L = (k_B T_L)^{-1}$, $\beta_C = (k_B T_C)^{-1}$, and $\beta_R = (k_B T_R)^{-1}$, respectively, for time $t < 0$. At time $t = 0$, all the heat baths are removed, and coupling of the center junction with the leads $H_{LC} = u_L^T V^{LC} u_C$ and $H_{CR} = u_C^T V^{CR} u_R$ and the lead-lead coupling term $H_{LR} = u_L^T V^{LR} u_R$ are switched on abruptly. Now the total Hamiltonian of the lead-junction-lead system becomes

$$H_{tot} = H_L + H_C + H_R + H_{LC} + H_{CR} + H_{LR}, \quad (4.24)$$

where $H_\alpha = \frac{1}{2} p_\alpha^T p_\alpha + \frac{1}{2} u_\alpha^T K^\alpha u_\alpha$, $\alpha = L, C, R$ represents coupled harmonic oscillators, and $u_\alpha = \sqrt{m} x_\alpha$ and p_α are column vectors of transformed coordinates

and corresponding conjugate momenta in region α . The superscript T stands for matrix transpose.

In order to extract information on heat transfer, we introduce a two-time observation protocol in the process of the evolution of the system; that is, at time $t = 0^-$, we carry out the measurement of energy of the left lead associated with the operator H_L , obtaining the result to be the eigenvalue a of H_L , and measure it again at time $t = t_M$, obtaining the eigenvalue b of H_L [68]. Here the measurement is in the sense of quantum measurement of von Neumann [69]. This quantum history [39], that is a sequence of quantum events at successive times, is represented by the product projector $Y = P_{0^-}^a \odot P_{t_M}^b$, where \odot is a variant of the tensor product symbol \otimes , emphasizing that the factors in the quantum history refer to different times, and $P_{0^-}^a$ is the projector on the energy eigenstate of H_L , with energy a measured at time $t = 0^-$, similarly for $P_{t_M}^b$. And the corresponding chain operator $K(Y)$ is given by the expression $K(Y) \equiv P_{t_M}^b U(t_M, 0^-) P_{0^-}^a$ in the case of a quantum history $Y = P_{0^-}^a \odot P_{t_M}^b$ involving just two times, where $U(t_M, 0^-)$ is the time evolution operator of the full Hamiltonian H_{tot} . Then according to the discussion in the Sec. 1.3 of the Chapter 1, the joint probability distribution for the quantum history Y is

$$\Pr(Y) = \langle K^\dagger K \rangle \equiv \text{Tr} \{ \rho^{ini} K^\dagger K \}, \quad (4.25)$$

where the superscript \dagger stands for the transpose conjugate and from now on the angle brackets $\langle \dots \rangle$ simply denotes an ensemble average with respect to ρ^{ini} . Here it is worth mentioning that this scheme for the joint probability distribution could be readily extended to many-time measurement.

Taking the commutator $[\rho^{ini}, P_{0-}^a] = 0$ into account, we can verify that consistency conditions $\langle K(Y), K(Y') \rangle_{\rho^{ini}} \equiv \text{Tr} \left\{ \rho^{ini} K(Y)^\dagger K(Y') \right\} = 0$ for all $Y \neq Y'$ are fulfilled, which guarantees that we are working with a consistent quantum framework. This observation, on the other hand, has explained why we prefer the initial direct product state ρ^{ini} in this thesis. The consistent quantum framework, combining the axiom of probability, especially the additivity of the probability of disjoint events, with the Born rule of the quantum theory, is crucial to understand the probability aspect of the quantum theory [39]. Now we want to gain some insight into the specific consistent quantum framework we study from the thermal transport point of view.

As we will consider later, in order to study the probability distribution function for the processing quantity heat transfer during the time t_M , we introduce the corresponding generating function (GF), defined as

$$\mathcal{Z}(\xi) \equiv \sum_{a,b} e^{i\xi(a-b)} \text{Pr} \left(P_{0-}^a \odot P_{t_M}^b \right), \quad (4.26)$$

where the summation for a and b extends over all the eigenvalues of H_L [4]. Then based on this definition, we simply take the derivative of $\mathcal{Z}(\xi)$ with respect to $i\xi$ and then set $\xi = 0$ to obtain the average heat transfer out of the left lead L ,

$$Q_L(t_M) = \sum_{a,b} (a-b) \text{Pr} \left(P_{0-}^a \odot P_{t_M}^b \right) \quad (4.27)$$

$$= \text{Tr} [\rho^{ini} H_L] - \text{Tr} [\rho^{ini} U(0^-, t_M) H_L U(t_M, 0^-)], \quad (4.28)$$

where the properties $(P_{0-}^a)^2 = P_{0-}^a$ and $\sum_a P_{0-}^a = 1$ for the projector P_{0-}^a , and similarly for $P_{t_M}^b$ are used. Also, we use the key relation $[\rho^{ini}, P_{0-}^a] = 0$, which assures that we are working with a consistent quantum framework. Thus, we

immediately realize that

$$\frac{dQ_L(t_M)}{dt_M} = - \left\langle \frac{dH_L(t_M)}{dt_M} \right\rangle, \quad (4.29)$$

of which the right-hand side is just the natural definition of thermal current I_L out of the left lead at time $t = t_M$. We must emphasize that, if the initial density matrix does not commute with P_{0-}^a , such as a steady-state density matrix, so that the framework we work with is not consistent, then the thermal current deriving from GF for the heat transfer will not be equal to the natural definition of it.

4.3 Cumulant generating function (CGF)

As was mentioned before, we proceed to study the GF for the heat transfer out of the left lead. According to the definition of the GF in Eq. (4.26), we can obtain

$$\mathcal{Z}(\xi) = \langle U_{\xi/2}(0^-, t_M) U_{-\xi/2}(t_M, 0^-) \rangle, \quad (4.30)$$

where $U_{-\xi/2}(t_M, 0^-)$ is an evolution operator associated with the modified total Hamiltonian $H_{tot}^{-\xi/2} = e^{i(-\xi/2)H_L} H_{tot} e^{-i(-\xi/2)H_L}$, and similarly for $U_{\xi/2}(0^-, t_M)$. Transforming to the interaction picture with respect to the free part of the modified total Hamiltonian $H_0 = H_L + H_C + H_R$, the GF for the heat transfer becomes

$$\begin{aligned} \mathcal{Z}(\xi) = & \left\langle T_\tau e^{-\frac{i}{\hbar} \int_C d\tau \hat{u}_L^T(\hbar x_\tau + \tau) (V^{LC} \hat{u}_C(\tau) + V^{LR} \hat{u}_R(\tau)) + \hat{u}_C^T(\tau) V^{CR} \hat{u}_R(\tau)} \right\rangle, \end{aligned} \quad (4.31)$$

where T_τ is a τ -ordering operator arranging operators with earliest τ on the contour C (from 0^- to t_M and back to 0^-) to the right, and a caret is put above operators

to denote their τ dependence with respect to the free Hamiltonian such as $\hat{u}_C(\tau) = e^{\frac{i}{\hbar}H_C\tau}u_Ce^{-\frac{i}{\hbar}H_C\tau}$, and $x_\tau = -\xi/2$ with $\tau = t^+$ on the upper branch of the contour C , while $x_\tau = +\xi/2$ with $\tau = t^-$ on the lower branch.

The key step to evaluate GF is to rewrite the exponent in Eq. (4.31) as

$$-\frac{i}{\hbar} \int_C d\tau_1 d\tau_2 \frac{1}{2} u^T(\tau_1) V(\tau_1, \tau_2) u(\tau_2), \quad (4.32)$$

where

$$u^T(\tau) = \begin{bmatrix} \hat{u}_L^T(\hbar x_\tau + \tau), & \hat{u}_C^T(\tau), & \hat{u}_R^T(\tau) \end{bmatrix}, \quad (4.33)$$

$$V(\tau_1, \tau_2) = \begin{bmatrix} 0 & V^{LC} & V^{LR} \\ V^{CL} & 0 & V^{CR} \\ V^{RL} & V^{RC} & 0 \end{bmatrix} \delta(\tau_1, \tau_2), \quad (4.34)$$

$$(V^T(\tau_1, \tau_2) = V(\tau_1, \tau_2)).$$

Here the generalized δ -function $\delta(\tau_1, \tau_2)$ is simply counterpart of the ordinary Dirac delta function on the contour C , see, for example, Ref. [49].

Then expanding the exponential to perform a perturbation expansion and employing Feynman diagrammatic technique, especially Wick's theorem and the linked cluster theorem, the CGF for the heat transfer can be obtained to be

$$\ln \mathcal{Z}(\xi) = \frac{1}{2} \sum_{n=1}^{\infty} \text{Tr}_{(j,\tau)} \left[\frac{1}{n} (V g^x)^n \right] \quad (4.35)$$

$$= \frac{1}{2} \sum_{n=1}^{\infty} \text{Tr}_{(j,\tau)} \left[\frac{1}{n} (V_{red} g_{red}^x)^n \right] \quad (4.36)$$

$$= -\frac{1}{2} \text{Tr} \ln \left(I - \tilde{V}_{red} \tilde{g}_{red}^x \right), \quad (4.37)$$

where in the first equality

$$g^x(\tau_1, \tau_2) = \begin{bmatrix} g^L(\hbar x_{\tau_1} + \tau_1, \hbar x_{\tau_2} + \tau_2) & 0 & 0 \\ 0 & g^C(\tau_1, \tau_2) & 0 \\ 0 & 0 & g^R(\tau_1, \tau_2) \end{bmatrix}, \quad (4.38)$$

with the equilibrium contour-ordered Green functions

$$g_{jk}^\alpha(\tau_1, \tau_2) = -\frac{i}{\hbar} \text{Tr} \left\{ \frac{e^{-\beta_\alpha H_\alpha}}{\text{Tr}(e^{-\beta_\alpha H_\alpha})} T_\tau [\hat{u}_j^\alpha(\tau_1) \hat{u}_k^\alpha(\tau_2)] \right\}, \quad (4.39)$$

$$\alpha = L, C, R$$

and the notation $\text{Tr}_{(j,\tau)}$ means trace both in real space index j and contour time τ such as $\text{Tr}_{(j,\tau)} [V g^x] = \int_C d\tau_1 \int_C d\tau_2 \text{Tr}_j [V(\tau_1, \tau_2) g^x(\tau_2, \tau_1)]$; in the second equality, considering the structure of the last expression, instead of the full matrix we only need the finite reduced ones, which make all the contribution to $\ln \mathcal{Z}(\xi)$, and

$$V_{red}(\tau_1, \tau_2) = \delta(\tau_1, \tau_2) \begin{bmatrix} 0 & V_{red}^{LC} & V_{red}^{LR} \\ V_{red}^{CL} & 0 & V_{red}^{CR} \\ V_{red}^{RL} & V_{red}^{RC} & 0 \end{bmatrix} \quad (4.40)$$

is the generalized δ -function $\delta(\tau_1, \tau_2)$ times the reduced total coupling matrix obtained by deleting all the zero column and row vectors of the full one except for the possible zero vectors whose row or column indexes are the center (junction) ones, and g_{red}^x is the corresponding submatrix of g^x just like V_{red} of V ; in the third equality a tilde above matrix means discretized contour-time version of the corresponding quantity such as $[\tilde{g}_{red}^x]_{\tau_i l, \tau_j n} = [g_{red}^x]_{ln}(\tau_i, \tau_j) d\tau_j$ with an evenly spaced grid τ_i and τ_j along the contour C and I is the identity matrix.

Introducing the Dyson equation

$$G(\tau, \tau') = g(\tau, \tau') + \int_C d\tau_1 \int_C d\tau_2 g(\tau, \tau_1) V(\tau_1, \tau_2) G(\tau_2, \tau') \quad (4.41)$$

$$= g(\tau, \tau') + \int_C d\tau_1 \int_C d\tau_2 G(\tau, \tau_1) V(\tau_1, \tau_2) g(\tau_2, \tau'), \quad (4.42)$$

which actually defines

$$G = \begin{bmatrix} G^{LL} & G^{LC} & G^{LR} \\ G^{CL} & G^{CC} & G^{CR} \\ G^{RL} & G^{RC} & G^{RR} \end{bmatrix} \quad (4.43)$$

based on $g(\tau, \tau') = g^{x \equiv 0}(\tau, \tau')$, we easily realized that

$$\tilde{G}_{red} = \tilde{g}_{red} + \tilde{g}_{red} \tilde{V}_{red} \tilde{G}_{red} \quad (4.44)$$

$$= \tilde{g}_{red} + \tilde{G}_{red} \tilde{V}_{red} \tilde{g}_{red} \quad (4.45)$$

still holds. From now on, for notational simplicity, we omit all the subscripts *red* with the understanding that these matrices are of finite dimensions in the real space domain. Thus, employing Eqs. (4.44) and (4.45) along with the equality $\text{Tr} \ln A = \ln \det A$, we obtain

$$\ln \mathcal{Z}(\xi) = -\frac{1}{2} \ln \det (I - d), \quad (4.46)$$

$$d \equiv \begin{bmatrix} \tilde{V}^{LC} & \tilde{V}^{LR} \end{bmatrix} \begin{bmatrix} \tilde{G}^{CC} & \tilde{G}^{CR} \\ \tilde{G}^{RC} & \tilde{G}^{RR} \end{bmatrix} \begin{bmatrix} \tilde{V}^{CL} \\ \tilde{V}^{RL} \end{bmatrix} \tilde{g}_L^A,$$

where \tilde{g}_L^A is the discretized contour-time version of $g_L^A(\tau_1, \tau_2) = g^L(\hbar x_{\tau_1} + \tau_1, \hbar x_{\tau_2} + \tau_2) - g^L(\tau_1, \tau_2)$.

If we introduce \tilde{g}_L^{-1} satisfying $\tilde{g}_L^{-1} \tilde{g}_L = I$ and employ Eqs. (4.44) and (4.45), we

can simplify the CGF for heat transfer further to be

$$\ln \mathcal{Z}(\xi) = -\frac{1}{2} \ln \det \left(I - \tilde{g}_L^{-1} \left(\tilde{G}^{LL} - \tilde{g}_L \right) \tilde{g}_L^{-1} \tilde{g}_L^A \right), \quad (4.47)$$

which is valid in both transient and steady-state regimes.

4.4 The steady-state CGF

Now, we proceed to evaluate the long-time limit of the CGF in Eq. (4.47) called the steady-state CGF. Transforming Eq. (4.47) from contour-time to real-time and then using the Keldysh rotation, which is essentially an orthogonal transformation that

$$\check{A}(t_1, t_2) = O^T \sigma_z \begin{bmatrix} A(t_1^+, t_2^+) & A(t_1^+, t_2^-) \\ A(t_1^-, t_2^+) & A(t_1^-, t_2^-) \end{bmatrix} O \quad (4.48)$$

$$\equiv \begin{bmatrix} A^r(t_1, t_2) & A^K(t_1, t_2) \\ A^{\bar{K}}(t_1, t_2) & A^a(t_1, t_2) \end{bmatrix} \quad (4.49)$$

with

$$O = \frac{1}{\sqrt{2}} \begin{bmatrix} 1 & 1 \\ -1 & 1 \end{bmatrix} \quad (4.50)$$

and the Pauli z matrix

$$\sigma_z = \begin{bmatrix} 1 & 0 \\ 0 & -1 \end{bmatrix} \quad (4.51)$$

appearing due to the transition from contour time to real time, see Ref. [31], we then obtain

$$\ln \mathcal{Z}(\xi) = \frac{1}{2} \sum_{n=1}^{\infty} \text{Tr}_{(j,t)} \left[\frac{1}{n} \left(\check{g}_L^{-1} \left(\check{G}^{LL} - \check{g}_L \right) \check{g}_L^{-1} \check{g}_L^A \right)^n \right] \quad (4.52)$$

where the notation $\text{Tr}_{(j,t)}$ means trace both in real space j and real time t , such as $\text{Tr}_{(j,t)}(\check{A}\check{B}) = \int_0^{t_M} dt_1 \int_0^{t_M} dt_2 \text{Tr}_j [\check{A}(t_1, t_2) \check{B}(t_2, t_1)]$.

Before proceeding, we must point out that all kinds of real-time versions of the contour-time Green's function $G(\tau, \tau')$ defined in Eqs. (4.41) or (4.42) are not necessarily time translationally invariant so that $\check{G}^{LL}(t, t')$ may not simply depend on the time difference $t - t'$. However, in the long-time limit, i.e., $t_M \rightarrow \infty$, the time translationally invariant part obtained from the lowest order of the Wigner transformation will dominate the CGF [57]. It is equivalent to saying that $\check{G}^{LL}(t, t') = \check{G}^{LL}(t - t')$ is time translationally invariant in the long-time limit (higher order terms of the product of the Wigner transformation have been ignored).

Consequently, by setting $t_M \rightarrow \infty$, and Fourier transforming Eq. (4.52), we get

$$\begin{aligned} \ln \mathcal{Z}(\xi) \\ = -\frac{1}{2} t_M \int_{-\infty}^{\infty} \frac{d\omega}{2\pi} \ln \det \left(I - \left(\check{g}_L^{-1} \check{G}^{LL} - I \right) \check{g}_L^{-1} \check{g}_L^A \right), \end{aligned} \quad (4.53)$$

where,

$$\check{g}_L = \begin{bmatrix} g_L^r & g_L^K \\ 0 & g_L^a \end{bmatrix}, \quad \check{G}^{LL} = \begin{bmatrix} G_{LL}^r & G_{LL}^K \\ 0 & G_{LL}^a \end{bmatrix}, \quad (4.54)$$

$$\check{g}_L^A = \frac{1}{2} \begin{bmatrix} a - b & a + b \\ -a - b & -a + b \end{bmatrix}, \quad (4.55)$$

$$a \equiv g_L^> (e^{-i\hbar\omega\xi} - 1), \quad b \equiv g_L^< (e^{i\hbar\omega\xi} - 1)$$

are all in frequency space.

To further simplify the steady-state CGF in Eq. (4.53), we use the formula

$$\det \begin{pmatrix} A & B \\ C & D \end{pmatrix} = \det (AD - BC) \quad (4.56)$$

in case of $[C, D] = 0$ to reduce the dimension of the matrix inside determinant by half. Therefore, the steady-state CGF is given by

$$\begin{aligned} \ln \mathcal{Z}(\xi) = & -t_M \int_{-\infty}^{\infty} \frac{d\omega}{4\pi} \ln \det \left\{ I - \mathcal{T}_G[\omega] \right. \\ & \left. \times \left[(e^{i\xi\hbar\omega} - 1) f_L (1 + f_R) + (e^{-i\xi\hbar\omega} - 1) f_R (1 + f_L) \right] \right\}, \end{aligned} \quad (4.57)$$

where $\mathcal{T}_G[\omega] \equiv G_{LR}^r \tilde{\Gamma}_R G_{RL}^a \tilde{\Gamma}_L$ with

$$\tilde{\Gamma}_{\{L,R\}} \equiv i \left[(g_{\{L,R\}}^a)^{-1} - (g_{\{L,R\}}^r)^{-1} \right] \quad (4.58)$$

is the transmission matrix and $f_{\{L,R\}} = \{\exp(\beta_{\{L,R\}}\hbar\omega) - 1\}^{-1}$ is the Bose-Einstein distribution function for phonons.

In deriving it, we have used the fluctuation dissipation theorem $e^{-\beta_L\hbar\omega} g_L^>[\omega] = g_L^<[\omega] = f_L (g_L^r - g_L^a)$ along with

$$\begin{aligned} & G_{LL}^< \\ &= G_{LL}^r \left(-if_L \tilde{\Gamma}_L \right) G_{LL}^a + G_{LR}^r \left(-if_R \tilde{\Gamma}_R \right) G_{RL}^a, \end{aligned} \quad (4.59)$$

$$\begin{aligned} & G_{LL}^r - G_{LL}^a - G_{LL}^r (g_L^{a-1} - g_L^{r-1}) G_{LL}^a \\ &= G_{LR}^r (g_R^{a-1} - g_R^{r-1}) G_{RL}^a, \end{aligned} \quad (4.60)$$

due to $(g_C^a)^{-1} - (g_C^r)^{-1} = 0$ and the Langreth theorem [57] acting on Eqs. (4.44) and (4.45). A computationally practical closed equation for G_{LR}^r could be found in Eq. (3.27). The formulas of Eq. (4.47) and Eq. (4.57) are the contributions in the thesis [44].

Now we recover the classical version of the CGF for the heat transfer in harmonic networks without the lead-lead coupling, which was first derived in Ref. [29] using the Langevin equation method. To this end we simply set the lead-lead coupling $V^{LR} = 0$ in Eqs. (4.44) and (4.45), then use the Langreth theorem and the Fourier transformation to obtain $G_{LR}^r = g_L^r V^{LC} G_{CR}^r = g_L^r V^{LC} G_{CC}^r V^{CR} g_R^r$ along with $G_{RL}^a = (G_{LR}^r)^\dagger$.

After setting $\hbar \rightarrow 0$ and employing $G_{RL}^a[-\omega] = (G_{LR}^r[\omega])^T$ and $\tilde{\Gamma}_{\{L,R\}}[-\omega] = -\tilde{\Gamma}_{\{L,R\}}[\omega]^T$, we can get

$$\lim_{t_M \rightarrow \infty} \frac{\ln \mathcal{Z}(\xi)}{t_M} = - \int_0^\infty \frac{d\omega}{2\pi} \ln \det \left\{ I - \mathcal{T}[\omega] \right. \\ \left. \times k_B^2 T_L T_R (i\xi) [i\xi + (\beta_R - \beta_L)] \right\}, \quad (4.61)$$

with

$$\mathcal{T}[\omega] \equiv G_{CC}^r \Gamma_R G_{CC}^a \Gamma_L, \quad (4.62)$$

$$\Gamma_{\{L,R\}} = i [\Sigma_{\{L,R\}}^r - \Sigma_{\{L,R\}}^a] \quad (4.63)$$

$$\Sigma_\alpha^{\{r,a\}} = V^{C\alpha} g_\alpha^{\{r,a\}} V^{\alpha C}, \quad \alpha = L, R.$$

4.5 The steady-state fluctuation theorem (SSFT) and cumulants

According to the steady-state CGF in Eq. (4.57), one could easily verify that the GC fluctuation symmetry [70] $\mathcal{Z}(\xi) = \mathcal{Z}(-\xi + i(\beta_R - \beta_L))$ is still satisfied in this general set-up with lead-lead coupling. And recall the definition of GF in Eq.

(4.26), we know that the probability distribution for the heat transferred Q_L is $\Pr(Q_L) = \frac{1}{2\pi\delta(0)} \int_{-\infty}^{\infty} d\xi \mathcal{Z}(\xi) e^{-i\xi Q_L}$. Therefore, following the GC symmetry is the SSFT $\Pr(Q_L) = e^{(\beta_R - \beta_L)Q_L} \Pr(-Q_L)$.

Also, the CGF can be used to evaluate cumulants. Here we only focus on steady-state cumulants of heat transfer. As illustrated in Sec. 4.2, the steady current is closed related to the first cumulant so that

$$\begin{aligned} I_L^{ss} &= \lim_{t_M \rightarrow \infty} \frac{d}{dt_M} \left(\frac{\partial \ln \mathcal{Z}(\xi)}{\partial (i\xi)} \Big|_{\xi=0} \right) \\ &= \int_0^\infty \frac{d\omega}{2\pi} \hbar\omega (f_L - f_R) \text{Tr} \mathcal{T}_{\mathcal{G}}[\omega], \end{aligned} \quad (4.64)$$

where, $\mathcal{Z}(0) = 1$ is used. This generalized Caroli formula with lead-lead coupling was previously given in Eq. (3.26) based on the definition of current directly. The second cumulant describing the fluctuation of the heat transferred is obtained by taking the second derivative of steady-state CGF with respect to $i\xi$ and then setting $\xi = 0$, which is

$$\begin{aligned} \langle\langle Q_L^2 \rangle\rangle &= \lim_{t_M \rightarrow \infty} t_M \int_{-\infty}^{\infty} \frac{d\omega}{4\pi} (\hbar\omega)^2 \left\{ (f_L + f_R + 2f_L f_R) \text{Tr} \mathcal{T}_{\mathcal{G}} \right. \\ &\quad \left. + (f_L - f_R)^2 \text{Tr} \mathcal{T}_{\mathcal{G}}^2 \right\}. \end{aligned} \quad (4.65)$$

Higher-order cumulants are also systematically given by corresponding higher-order derivatives.

After some experiences with the first few order cumulants of heat transfer, we want to discuss the trick suggested by Di Ventra that repartitioning the total Hamiltonian to avoid the inevitable coupling between leads in real nanoscale or mesoscopic systems when calculating steady current. Now whether this trick is applicable to the evaluation of higher-order cumulant (fluctuation) of the heat

transfer in steady state boils down to checking whether $\text{Tr}\mathcal{T}_{G,old}^n = \text{Tr}\mathcal{T}_{G,new}^n$ holds for all n less than or equal to the corresponding order of the cumulant one wants, where $\mathcal{T}_{G,old}(\mathcal{T}_{G,new})$ is the transmission matrix before (after) repartitioning the total Hamiltonian. Though giving a general verification is difficult, $\text{Tr}\mathcal{T}_{G,old}^n = \text{Tr}\mathcal{T}_{G,new}^n, \forall n$ is indeed true in a one-dimensional central ring model, in which there is only one particle in the center junction connected with two semi-infinite spring chain leads, and the interaction between the two nearest particles in the two leads respectively exists (in this case, both $\mathcal{T}_{G,old}$ and $\mathcal{T}_{G,new}$ are just a number). One step forward, if one thinks of CGF of heat transfer as the complete knowledge of the steady state, we can claim that the steady state is partition-independent after verification of $\text{Tr}\mathcal{T}_{G,old}^n = \text{Tr}\mathcal{T}_{G,new}^n, \forall n$ or equivalently, $\ln \mathcal{Z}_{old}(\xi) = \ln \mathcal{Z}_{new}(\xi)$ in Eq. (4.57). Then we can partly answer a question raised by Caroli *et al.* regarding the (non)equivalence between the partitioned and partition-free approaches [16], which recently was partly settled by explicitly constructing a nonequilibrium steady state through adiabatically turning on an electrical bias between the leads [71].

4.6 Summary

We examine the statistics of heat transfer during time t_M in a general lead-junction-lead quantum system, in which coupling between leads has been taken into account. To this end, a consistent quantum framework was introduced to derive the CGF, valid in both transient and long-time regimes using the NEGF method. Also, the implication of consistency of the quantum framework was discussed from a thermal transport point of view. After that, a compact form of the steady-state

CGF was obtained, following which the GC symmetry and the SSFT were verified. In addition, the first few cumulants were given and a generalized Caroli formula was recovered. Furthermore, some valuable hints with respect to the rigorous proof for whether fluctuation of heat transfer in steady state is partition-independent have been offered.

4.7 Appendix: CGF of energy transport under quasi-classical approximation in harmonic networks

In this appendix, we consider energy transport across an arbitrary harmonic networks connected to two heat baths modeled by coupled harmonic oscillators at different temperatures. We are interested in the effects of semiclassical approximation on the cumulant generating function (CGF) of energy transport, which is my present work. It is meaningful to notice that quantum molecular dynamics (QMD) [72] employing quasi-classical approximation can even give ‘nearly’ correct results for second cumulant of energy transport in ballistic systems, the precise meaning of which will be clarified later. We mainly extend the method used by Saito etc [29].

First, we specify the total Hamiltonian, which is written as

$$H_{tot} = \sum_{i=L,C,R} H_i + (u^L)^T V^{LC} u^C + (u^C)^T V^{CR} u^R, \quad (4.66)$$

where $H_i = \frac{1}{2} (p^i)^T p^i + \frac{1}{2} (u^i)^T K^i u^i$, $i = L, C, R$ and the meaning of the notations

we use here are the same as before. This setup consists of a central junction H_C connected to two semi-infinite harmonic lattices H_L and H_R which serve as heat baths and in respective thermal equilibrium at temperature T_L and T_R . The Heisenberg equations of motion for the center and the baths are of the form:

$$\ddot{u}^C = -K^C u^C - V^{CR} u^R - V^{CL} u^L, \quad (4.67)$$

$$\ddot{u}^\alpha = -K^\alpha u^\alpha - V^{\alpha C} u^C, \quad \alpha = L, R \quad (4.68)$$

We solve the equation of motions for the baths in terms of center degrees of freedom, given as

$$u^\alpha(t) = \int_0^\infty g_\alpha^r(t-t') V^{\alpha C} u^C(t') dt' + u_0^\alpha(t), \quad \alpha = L, R, \quad (4.69)$$

where $g_\alpha^r(t)$ is the retarded Green's function of the free heat bath α and $u_0^\alpha(t)$ satisfies the homogenous equation of the free heat bath α :

$$\ddot{u}_0^\alpha + K^\alpha u_0^\alpha = 0. \quad (4.70)$$

The “free” here means that the relevant dynamics is simply due to Hamiltonian H_α , $\alpha = L, R$.

Now we eliminate the baths degrees of freedom u^L and u^R by substituting the general solution for the baths Eq. (4.69) back into the equation of motion for the center Eq. (4.67). We obtain

$$\ddot{u}^C(t) = -K^C u^C(t) - \int_0^\infty \Sigma^r(t-t') u^C(t') dt' + \xi(t), \quad (4.71)$$

where $\Sigma^r = \Sigma_L^r + \Sigma_R^r$, $\Sigma_\alpha^r = V^{C\alpha} g_\alpha^r V^{\alpha C}$ is the self energy of the baths, and the noise $\xi = \xi_L + \xi_R$ with $\xi_\alpha(t) = -V^{C\alpha} u_0^\alpha(t)$. Notice that throughout the discussion we implicitly assume the initial time is $t = 0$ so that Eq. (4.71) is valid for $t > 0$.

For later convenience, the Eq. (4.71) is separated to two equations with the subscript C being omitted:

$$\dot{u}(t) = v(t), \quad (4.72)$$

$$\dot{v}(t) = -K^C u(t) - \int_0^\infty \Sigma^r(t-t') u(t') dt' + \xi(t). \quad (4.73)$$

The quasi-classical approximation partially take into account the quantum effect by employing quantum heat baths, which are Gaussian noise specified by

$$\langle \xi_\alpha(t) \rangle = 0, \quad (4.74)$$

$$\begin{aligned} \langle \xi_\alpha(t) \xi_\beta(t') \rangle &= \delta_{\alpha\beta} i\hbar \frac{1}{2} [\Sigma_\alpha^>(t-t') + \Sigma_\alpha^<(t-t')], \\ &= \delta_{\alpha\beta} \int_{-\infty}^\infty \frac{d\omega}{2\pi} \left(f_\alpha(\omega) + \frac{1}{2} \right) \hbar \Gamma_\alpha[\omega] e^{-i\omega(t-t')}, \\ \alpha, \beta &= L, R. \end{aligned} \quad (4.75)$$

where $f_\alpha(\omega) = 1/[e^{\hbar\omega/(k_B T_\alpha)} - 1]$ is the Bose distribution function, and $\Gamma_\alpha[\omega] = i(\Sigma_\alpha^r[\omega] - \Sigma_\alpha^a[\omega])$.

Notice that the two baths are independent and we have used a symmetrized noise after considering that the quantum operators $\xi_\alpha(t)$ do not commute in general. The other aspect of quasi-classical approximation is to replace all operators, *i.e.*, u^C , v^C and ξ_α , by numbers from now on. The linear equations Eq. (4.72) and Eq. (4.73) can be solved by introducing discrete Fourier transforms and the corresponding inverses as follows:

$$\begin{aligned} \left\{ \tilde{u}_n, \tilde{v}_n, \tilde{\xi}_{L,n}, \tilde{\xi}_{R,n} \right\} &= \frac{1}{t_M} \int_0^{t_M} dt \{ u(t), v(t), \xi_L(t), \xi_R(t) \} e^{i\omega_n t}, \\ \{ u(t), v(t), \xi_L(t), \xi_R(t) \} &= \sum_{n=-\infty}^\infty \left\{ \tilde{u}_n, \tilde{v}_n, \tilde{\xi}_{L,n}, \tilde{\xi}_{R,n} \right\} e^{-i\omega_n t}, \\ \omega_n &= \frac{2\pi n}{t_M}, \quad n = (\dots, -2, -1, 0, 1, 2, \dots). \end{aligned} \quad (4.76)$$

Setting $t_M \rightarrow \infty$ and employing

$$\lim_{t_M \rightarrow \infty} \int_0^{t_M} dt e^{-it(\omega - \omega_n)} = 2\pi \delta(\omega - \omega_n), \quad (4.77)$$

we get

$$\begin{aligned} \tilde{v}_n &= i\omega_n G_n^r \left(\tilde{\xi}_{L,n} + \tilde{\xi}_{R,n} \right) \\ &\quad - \frac{1}{t_M} G_n^r \left\{ i\omega_n \Delta v + (K^C + \Sigma_n^r) \Delta u \right\}, \end{aligned} \quad (4.78)$$

$$\begin{aligned} \tilde{u}_n &= -G_n^r \left(\tilde{\xi}_{L,n} + \tilde{\xi}_{R,n} \right) \\ &\quad + \frac{1}{t_M} G_n^r \left\{ \Delta v - i\omega_n \Delta u \right\} \end{aligned} \quad (4.79)$$

with $G_n^r \equiv [\omega_n^2 - K^C - \Sigma_n^r]^{-1}$. Where $\Sigma_n^r = \int_{-\infty}^{+\infty} \Sigma^r(t) e^{i\omega_n t} dt$, $\Delta v = v(t_M) - v(0)$ and $\Delta u = u(t_M) - u(0)$. Actually the second terms in both \tilde{v}_n and \tilde{u}_n are smaller compared with the first terms due to the factor $\frac{1}{t_M}$. Thus from now on we drop the second terms and simply use the leading-order solution $\tilde{v}_n = i\omega_n G_n^r (\tilde{\xi}_{L,n} + \tilde{\xi}_{R,n})$ and $\tilde{u}_n = -G_n^r (\tilde{\xi}_{L,n} + \tilde{\xi}_{R,n})$.

In frequency space, the noise such as $\{\xi_L(t) : 0 < t < t_M\}$ can be equivalently described by the infinite independent random variables $\{\tilde{\xi}_{L,0} = \tilde{\xi}_{L,0}^*, \tilde{\xi}_{L,n}, \tilde{\xi}_{L,n}^* : n = 1, 2, \dots\}$ (* denotes complex conjugate), which are still Gaussian specified by

$$\langle \tilde{\xi}_{L,m} \rangle = \langle \tilde{\xi}_{L,m}^* \rangle = 0, \quad (4.80)$$

$$\langle \tilde{\xi}_{L,n} \tilde{\xi}_{L,n'}^T \rangle = \langle \tilde{\xi}_{L,n}^* \tilde{\xi}_{L,n'}^{*T} \rangle = 0, \quad (4.81)$$

$$\langle \tilde{\xi}_{L,m} \tilde{\xi}_{L,m'}^{*T} \rangle = \delta_{mm'} \frac{\hbar}{t_M} \left(f_{L,m} + \frac{1}{2} \right) \Gamma_{L,m} \quad (4.82)$$

with $f_{L,m} = f_L(\omega_m)$ and $\Gamma_{L,m} = \Gamma_L[\omega_m]$ and $m = 0, 1, 2, \dots$ coming from Eq. (4.74) and Eq. (4.75) and the observation $\tilde{\xi}_{L,m}^* = \tilde{\xi}_{L,-m}$. The similar is true for the other noise $\{\xi_R(t) : 0 < t < t_M\}$. Precisely, the probability density of the total noise is

written as

$$\begin{aligned}
 p \left[\tilde{\xi}_L, \tilde{\xi}_R, \tilde{\xi}_L^*, \tilde{\xi}_R^* \right] &= \prod_{m \geq 0} \frac{\det C_{1,m} \det C_{2,m}}{\pi^{2N_C}} \\
 &\cdot \exp \left[- \left(\tilde{\xi}_{L,m}^T, \tilde{\xi}_{R,m}^T \right) \begin{pmatrix} C_{1,m} & 0 \\ 0 & C_{2,m} \end{pmatrix} \begin{pmatrix} \tilde{\xi}_{L,m}^* \\ \tilde{\xi}_{R,m}^* \end{pmatrix} \right] \quad (4.83)
 \end{aligned}$$

with

$$C_{1,m} = \left[\frac{\hbar}{t_M} \left(f_{L,m} + \frac{1}{2} \right) \Gamma_{L,m} \right]^{-1}, \quad (4.84)$$

$$C_{2,m} = \left[\frac{\hbar}{t_M} \left(f_{R,m} + \frac{1}{2} \right) \Gamma_{R,m} \right]^{-1}, \quad (4.85)$$

where N_C is the total degrees of freedom in the central junction.

The interested quantity in this appendix is the total amount of energy Q_L , transferred out of the left heat bath into the central junction, from the initial time $t = 0$ to the maximum time $t = t_M$. It can be obtained based on the following argument: the total rate of energy transport into the central junction is

$$\frac{dH_C(t)}{dt} = \dot{Q}_L(t) + \dot{Q}_R(t) \quad (4.86)$$

with

$$\begin{aligned}
 \dot{Q}_\alpha(t) &= v^T(t) \left[\xi_\alpha(t) - \int_0^\infty \Sigma_\alpha^r(t-t') u(t') dt \right], \\
 \alpha &= L, R.
 \end{aligned} \quad (4.87)$$

Thus

$$\begin{aligned}
 Q_L &= \int_0^{t_M} \dot{Q}_L(t) dt \\
 &= t_M \sum_{n=-\infty}^{\infty} \tilde{v}_n^T \left(\tilde{\xi}_{L,-n} - \Sigma_{L,-n}^r \tilde{u}_{-n} \right) \\
 &= t_M \sum_{n=-\infty}^{\infty} i\omega_n \left(\tilde{\xi}_{L,n}^T, \tilde{\xi}_{R,n}^T \right) \begin{pmatrix} G_n^r + G_n^r \Sigma_{L,n}^a G_n^a & G_n^r \Sigma_{L,n}^a G_n^a \\ G_n^r + G_n^r \Sigma_{L,n}^a G_n^a & G_n^r \Sigma_{L,n}^a G_n^a \end{pmatrix} \begin{pmatrix} \tilde{\xi}_{L,n}^* \\ \tilde{\xi}_{R,n}^* \end{pmatrix} \\
 &= t_M \sum_{n=1}^{\infty} \left(\tilde{\xi}_{L,n}^T, \tilde{\xi}_{R,n}^T \right) \omega_n \begin{pmatrix} G_n^r \Gamma_{R,n} G_n^a & -iG_n^a - G_n^r \Gamma_{L,n} G_n^a \\ iG_n^r - G_n^r \Gamma_{L,n} G_n^a & -G_n^r \Gamma_{L,n} G_n^a \end{pmatrix} \begin{pmatrix} \tilde{\xi}_{L,n}^* \\ \tilde{\xi}_{R,n}^* \end{pmatrix}.
 \end{aligned} \tag{4.88}$$

In the second equality, we express the total amount of energy Q_L in the frequency space; in obtaining the third equality, we have employed the leading-order solution for \tilde{v}_n and \tilde{u}_n and the properties $G_n^{r,T} = G_n^r$, $\Sigma_{L,-n}^r = \Sigma_{L,n}^a$ and $G_{-n}^r = G_n^a$; In obtaining the fourth equality, the observation is that $\omega_0 = 0$ and recall that $G_n^a - G_n^r = iG_n^r (\Gamma_{L,n} + \Gamma_{R,n}) G_n^a$.

We proceed to the calculation of the characteristic function $\mathcal{Z}(\xi) \equiv \langle e^{i\xi Q_L} \rangle$ using the multi-dimensional Gaussian integral of complex variables, which is obtained to be

$$\begin{aligned}
 \mathcal{Z}(\xi) &= \int d[\tilde{\xi}_L, \tilde{\xi}_R, \tilde{\xi}_L^*, \tilde{\xi}_R^*] p[\tilde{\xi}_L, \tilde{\xi}_R, \tilde{\xi}_L^*, \tilde{\xi}_R^*] e^{i\xi Q_L} \\
 &= \prod_{n \geq 1} \frac{\det C_{1,n} \det C_{2,n}}{\pi^{2N_C}} \pi^{2N_C} \frac{1}{\det A_n}
 \end{aligned} \tag{4.89}$$

with

$$\begin{aligned}
 \det A_n &= \det \left\{ \begin{pmatrix} C_{1,n} & 0 \\ 0 & C_{2,n} \end{pmatrix} + (-i\xi t_M \omega_n) \begin{pmatrix} G_n^r \Gamma_{R,n} G_n^a & -iG_n^a - G_n^r \Gamma_{L,n} G_n^a \\ iG_n^r - G_n^r \Gamma_{L,n} G_n^a & -G_n^r \Gamma_{L,n} G_n^a \end{pmatrix} \right\} \\
 &\equiv \det B_n \det \begin{pmatrix} C_{1,n} & 0 \\ 0 & C_{2,n} \end{pmatrix},
 \end{aligned} \tag{4.90}$$

where we can easily verified that

$$\begin{aligned}
 B_n &= \begin{pmatrix} 1 + a_1 G_n^r \Gamma_{R,n} G_n^a \Gamma_{L,n} & -ia_2 G_n^a \Gamma_{R,n} - a_2 G_n^r \Gamma_{L,n} G_n^a \Gamma_{R,n} \\ ia_1 G_n^r \Gamma_{L,n} - a_1 G_n^r \Gamma_{L,n} G_n^a \Gamma_{L,n} & 1 - a_2 G_n^r \Gamma_{L,n} G_n^a \Gamma_{R,n} \end{pmatrix} \\
 &= \begin{pmatrix} 1 + a_1 G_n^r \Gamma_{R,n} G_n^a \Gamma_{L,n} & a_2 (-iG_n^a \Gamma_{R,n} - G_n^r \Gamma_{L,n} G_n^a \Gamma_{R,n}) \\ a_1 (iG_n^a \Gamma_{L,n} + G_n^r \Gamma_{R,n} G_n^a \Gamma_{L,n}) & 1 - a_2 G_n^r \Gamma_{L,n} G_n^a \Gamma_{R,n} \end{pmatrix} \\
 &\equiv \begin{pmatrix} 1 + a_1 T_1 & a_2 T_{12} \\ a_1 T_{21} & 1 - a_2 T_2 \end{pmatrix} \tag{4.91}
 \end{aligned}$$

and $a_1 = -i\xi\omega_n\hbar(f_{L,n} + \frac{1}{2})$ and $a_2 = -i\xi\omega_n\hbar(f_{R,n} + \frac{1}{2})$.

The important closure relations for T_1 , T_2 , T_{12} and T_{21} can be given as follows

$$T_{12}T_2 = T_1T_{12}, \tag{4.92}$$

$$T_{21}T_1 = T_2T_{21}, \tag{4.93}$$

$$T_{21}T_{12} = T_2(1 - T_2), \tag{4.94}$$

$$T_{12}T_{21} = T_1(1 - T_1). \tag{4.95}$$

The sample proofs for the first and the third relation are given in the followings by repeatedly using $\Gamma_{L,n} + \Gamma_{R,n} = -i(G_n^{r-1} - G_n^{a-1})$, while the remaining relations can be similarly verified. In the sample proof, the subscript n is omitted for convenience.

First, we need to notice that the relation between T_1 and T_2 :

$$\begin{aligned}
 T_1 &\equiv G^r \Gamma_R G^a \Gamma_L = [i(G^r - G^a) - G^r \Gamma_L G^a] \Gamma_L \\
 &= iG^r \Gamma_L - iG^a \Gamma_L - G^r \Gamma_L G^a [iG^{a-1} - iG^{r-1} - \Gamma_R] \\
 &= -iG^a \Gamma_L + iG^r \Gamma_L G^a G^{r-1} + T_2.
 \end{aligned}$$

For the first relation (4.92)

Based on the definition of T_{12} and T_2 , we know

$$T_{12}T_2 = -iG^a\Gamma_R T_2 - T_2^2$$

and on the other hand

$$\begin{aligned}
 T_1T_{12} &= -iT_1G^a\Gamma_R - T_1T_2 \\
 &= -iG^r\Gamma_R G^a\Gamma_L G^a\Gamma_R \\
 &\quad - \left[-iG^a\Gamma_L + iG^r\Gamma_L G^a G^{r-1} + T_2\right] T_2 \\
 &= -i\left\{G^a(\Gamma_L + \Gamma_R)G^r - G^r\Gamma_L G^a\right\}\Gamma_L G^a\Gamma_R \\
 &\quad - \left[-iG^a\Gamma_L + iG^r\Gamma_L G^a G^{r-1}\right] T_2 - T_2^2 \\
 &= \left\{-iG^a(\Gamma_L + \Gamma_R) + iG^r\Gamma_L G^a G^{r-1} + iG^a\Gamma_L - iG^r\Gamma_L G^a G^{r-1}\right\} T_2 \\
 &\quad - T_2^2 \\
 &= -iG^a\Gamma_R T_2 - T_2^2 \\
 &= T_{12}T_2.
 \end{aligned}$$

For the third relation (4.94)

$$\begin{aligned}
 T_{21}T_{12} &= (iG^a\Gamma_L + T_1)(-iG^a\Gamma_R - T_2) \\
 &= (iG^r\Gamma_L G^a G^{r-1} + T_2)(-iG^a\Gamma_R - T_2) \\
 &= G^r\Gamma_L G^a G^{r-1} G^a\Gamma_R - iG^r\Gamma_L G^a G^{r-1} T_2 \\
 &\quad - iT_2 G^a\Gamma_R - T_2^2 \\
 &= G^r\Gamma_L G^a G^{r-1} G^a\Gamma_R - iG^r\Gamma_L G^a (\Gamma_L + \Gamma_R) G^a\Gamma_R \\
 &\quad - T_2^2 \\
 &= G^r\Gamma_L G^a G^{r-1} G^a\Gamma_R - iG^r\Gamma_L G^a i (G^{a-1} - G^{r-1}) G^a\Gamma_R \\
 &\quad - T_2^2 \\
 &= G^r\Gamma_L G^a\Gamma_R - T_2^2 \\
 &= T_2 (1 - T_2).
 \end{aligned}$$

After these preparations and let $t_M \rightarrow \infty$, the CGF of energy transport can be obtained as

$$\ln \mathcal{Z}(\xi) = \sum_{n \geq 1} \ln \left(\frac{1}{\det B_n} \right) \quad (4.96)$$

$$= -\frac{t_M}{2\pi} \sum_{n \geq 1} d\omega_n \ln \det B_n \quad (4.97)$$

$$= -\frac{t_M}{2\pi} \int_0^\infty d\omega \ln \det B[\omega], \quad (4.98)$$

where employing the formula $\det \begin{pmatrix} A & B \\ C & D \end{pmatrix} = \det \{(D - CA^{-1}B)A\}$ and the closure relations for T_1 , T_2 , T_{12} and T_{21} , we get

$$\det B_n = \det \{1 - T_2(a_2 - a_1 + a_1 a_2)\} \frac{\det(1 + a_1 T_1)}{\det(1 + a_1 T_2)}. \quad (4.99)$$

Notice that due to the properties $(G^{r,a})^T = G^{r,a}$ and $\Gamma_\alpha^T = \Gamma_\alpha$, $\alpha = L, R$ and cyclic property of the trace, $\text{Tr} T_1^n = \text{Tr} T_1^{n,T} = \text{Tr} T_2^n$, for all $n \geq 1$. Thus

$$\det(1 + a_1 T_1) = e^{\text{Tr} \ln(1 + a_1 T_1)} \quad (4.100)$$

$$= e^{\text{Tr} \ln(1 + a_1 T_2)} \quad (4.101)$$

$$= \det(1 + a_1 T_2). \quad (4.102)$$

Finally, the CGF of energy transport can be simplified to be

$$\ln \mathcal{Z}(\xi) = -\frac{t_M}{2\pi} \int_0^\infty d\omega \text{Tr} \ln \{1 - T_2 g(\xi)\} \quad (4.103)$$

$$g(\xi) \equiv (i\xi) \hbar\omega (f_L - f_R) + (i\xi)^2 (\hbar\omega)^2 \left(f_L + \frac{1}{2}\right) \left(f_R + \frac{1}{2}\right). \quad (4.104)$$

The first two cumulants can be immediately given as

$$\begin{aligned} I_{\text{steady}} &= \frac{1}{t_M} \frac{\partial \ln \mathcal{Z}(\xi)}{\partial (i\xi)} \Big|_{\xi=0} \\ &= \frac{1}{2\pi} \int_0^\infty d\omega \text{Tr} T_2 \hbar\omega (f_L - f_R) \end{aligned} \quad (4.105)$$

and

$$\begin{aligned} \langle\langle Q_L^2 \rangle\rangle &= \frac{t_M}{2\pi} \int_0^\infty d\omega (\hbar\omega)^2 \left[\text{Tr} T_2 \left(f_L + f_R + 2f_L f_R + \frac{1}{2} \right) \right. \\ &\quad \left. + \text{Tr} T_2^2 (f_L - f_R)^2 \right] \end{aligned} \quad (4.106)$$

$$= \text{correct quantum one} + \frac{t_M}{2\pi} \int_0^\infty d\omega \frac{(\hbar\omega)^2}{2} \text{Tr} T_2 [\omega]. \quad (4.107)$$

Where the ‘correct quantum one’ term comes from the pure quantum-mechanical result, see Eq. (4.65). Based on the first two cumulants, we realized that for ballistic systems the QMD can give exact quantum result for steady current and ‘nearly’ correct quantum result for second cumulant with a correction term which does not depend on the temperatures of the heat baths.

Chapter 5

Distribution of energy transport across nonlinear systems

In this chapter, we consider thermal conduction across a general nonlinear phononic junction [45]. Based on two-time consistent quantum histories and the field theoretical/algebraic method, the cumulants of the heat transfer in both transient and steady-state regimes are studied on an equal footing, and a practical formula for cumulant generating function of heat transfer is obtained. As an application, the general formalism is used to study anharmonic effects on fluctuation of steady-state heat transfer across a typical molecular junction with a quartic nonlinear on-site pinning potential. In addition, an explicit nonlinear modification to cumulant generating function exact up to the first order is given. Also, the first three cumulants are numerically demonstrated using both the self-consistent approach and the first-order perturbation approach.

5.1 Model and the general formalism

We still consider the lead-junction-lead model initially prepared in a product state $\rho_{ini} = \Pi_{\alpha=L,C,R} \frac{e^{-\beta_\alpha H_\alpha}}{\text{Tr}(e^{-\beta_\alpha H_\alpha})}$. It can be imagined that left lead (L), center junction (C), and right lead (R) in this model were in contact with three different heat baths at the inverse temperatures $\beta_L = (k_B T_L)^{-1}$, $\beta_C = (k_B T_C)^{-1}$ and $\beta_R = (k_B T_R)^{-1}$, respectively, for time $t < t_0$. At time $t = t_0$, all the heat baths are removed, and couplings of the center junction with the leads $H_{LC} = u_L^T V^{LC} u_C$ and $H_{CR} = u_C^T V^{CR} u_R$ and the interested nonlinear term H_n appearing only in the center junction are switched on abruptly. Now the total Hamiltonian is given by

$$H_{tot} = H_L + H_C + H_R + H_{LC} + H_{CR} + H_n, \quad (5.1)$$

where $H_\alpha = \frac{1}{2} p_\alpha^T p_\alpha + \frac{1}{2} u_\alpha^T K^\alpha u_\alpha$, $\alpha = L, C, R$, represents coupled harmonic oscillators, $u_\alpha = \sqrt{m_\alpha} x_\alpha$ and p_α are column vectors of transformed coordinates and corresponding conjugate momenta in region α . The superscript T stands for matrix transpose.

Recall the discussion in the Sec. 4.2, we can similarly construct a consistent framework consisting of two-time quantum histories to study the heat transfer across arbitrary nonlinear systems in a given time duration. A realization of the quantum history $P_{t_0}^a \odot P_{t_M}^b$ means that the result of the measurement at time t_0 of energy of the left lead associated with the operator H_L is the eigenvalue a of H_L , then the measurement at time t_M yields the eigenvalue b of H_L . Using this consistent quantum framework, we can define the generating function (GF) for heat transfer

in the time duration $t_M - t_0$ to be

$$\begin{aligned}\mathcal{Z}(\xi) &\equiv \sum_{a,b} e^{i(a-b)\xi} \text{Pr}(P_{t_0}^a \odot P_{t_M}^b) \\ &= \langle U_{\xi/2}(t_0, t_M) U_{-\xi/2}(t_M, t_0) \rangle,\end{aligned}\tag{5.2}$$

where $\text{Pr}(P_{t_0}^a \odot P_{t_M}^b)$ stands for the joint probability for the quantum history $P_{t_0}^a \odot P_{t_M}^b$; $U_{-\xi/2}(t_M, t_0)$ means evolution operator associated with the counting-field dependent total Hamiltonian $H_{tot}^{-\xi/2} = e^{i(-\xi/2)H_L} H_{tot} e^{-i(-\xi/2)H_L}$, similarly for $U_{\xi/2}(t_0, t_M)$ and $\langle \dots \rangle$ denotes the ensemble average over the initial state ρ_{ini} .

The first step for the study of the GF is to relate it to the Green's function, by which the closed equation satisfied can be found out. To this end, we generalize the GF to be

$$\mathcal{Z}(\lambda_2 - \lambda_1) \equiv \langle U_{\lambda_2}(t_0, t_M) U_{\lambda_1}(t_M, t_0) \rangle \tag{5.3}$$

$$= \langle e^{i(\lambda_2 - \lambda_1)H_L} U(t_0, t_M) e^{-i(\lambda_2 - \lambda_1)H_L} U(t_M, t_0) \rangle \tag{5.4}$$

$$= \left\langle T_\tau e^{-\frac{i}{\hbar} \int_C d\tau \mathcal{T}_\lambda(\tau)} \right\rangle, \tag{5.5}$$

where, T_τ is a τ -ordering operator arranging operators with earlier τ on the contour C (from t_0 to t_M and back to t_0) to the right. In the second equality we have used the cyclic property of the trace and the commutator relation $[H_L, \rho_{ini}] = 0$; in the third equality we go to the interaction picture with respect to the free Hamiltonian $h = H_L + H_C + H_R$ so that $\mathcal{T}_\lambda(\tau) = \hat{u}_L^{x,T}(\tau) V^{LC} \hat{u}_C(\tau) + \hat{u}_C^T(\tau) V^{CR} \hat{u}_R(\tau) + \hat{\mathcal{H}}_n(\tau)$ with caret put above operators to denote the interaction-picture τ dependence such as $\hat{u}_C(\tau) = e^{\frac{i}{\hbar} h \tau} u_C e^{-\frac{i}{\hbar} h \tau}$, where $\hat{u}_L^x(\tau) = \hat{u}_L(\hbar x_\tau + \tau)$ with $x_\tau = \lambda_1$ (λ_2) with $\tau = t^+$ (t^-) on the upper (lower) branch of the contour C .

Furthermore, we define the adiabatic potential $\mathcal{U}(t, \lambda_2, \lambda_1)$ according to [35]

$$\mathcal{Z}(\lambda_2 - \lambda_1) = e^{-\frac{i}{\hbar} \int_{t_0}^{t_M} dt \mathcal{U}(t, \lambda_2, \lambda_1)}. \quad (5.6)$$

Thus we could apply the nonequilibrium version of the Feynman-Hellmann theorem [73] to get

$$\frac{\partial}{\partial \lambda_1} \mathcal{U}(t, \lambda_2, \lambda_1) = \frac{1}{\mathcal{Z}(\lambda_2 - \lambda_1)} \left\langle T_\tau \frac{\partial \mathcal{T}_\lambda(t^+)}{\partial \lambda_1} e^{-\frac{i}{\hbar} \int_C d\tau \mathcal{T}_\lambda(\tau)} \right\rangle \quad (5.7)$$

$$\equiv \left\langle T_\tau \frac{\partial \mathcal{T}_\lambda(t^+)}{\partial \lambda_1} \right\rangle_\lambda, \quad (5.8)$$

Since

$$\frac{\partial \mathcal{T}_\lambda(t^+)}{\partial \lambda_1} = \hbar \frac{\partial \hat{u}_L^{x,T}(t^+)}{\partial t^+} V^{LC} \hat{u}_C(t^+) \quad (5.9)$$

and introducing contour-ordered Green's functions \tilde{G}_{LC} and \tilde{G}_{CL} defined as

$$\tilde{G}_{LC}(\tau_1, \tau_2) = -\frac{i}{\hbar} \langle T_\tau \hat{u}_L^x(\tau_1) \hat{u}_C^T(\tau_2) \rangle_\lambda \quad (5.10)$$

$$\tilde{G}_{CL}(\tau_1, \tau_2) = -\frac{i}{\hbar} \langle T_\tau \hat{u}_C(\tau_1) \hat{u}_L^{x,T}(\tau_2) \rangle_\lambda, \quad (5.11)$$

we can get

$$\frac{\partial \ln \mathcal{Z}(\lambda_2 - \lambda_1)}{\partial \lambda_1} = \int_{t_0}^{t_M} dt \hbar \frac{\partial}{\partial t'} \text{Tr} \left[\tilde{G}_{LC}^t(t', t) V^{CL} \right] \Big|_{t'=t} \quad (5.12)$$

$$= \int_{t_0}^{t_M} dt \hbar \frac{\partial}{\partial t'} \text{Tr} \left[\tilde{G}_{CL}^t(t, t') V^{LC} \right] \Big|_{t'=t}. \quad (5.13)$$

Notice that the tilde on the Green's functions emphasizes the fact that they are counting field ξ -dependent, and real-time Green's functions can be obtained by specifying the variation range of the time arguments in contour-ordered Green's functions such as

$$\tilde{G}_{LC}(\tau_1, \tau_2) \rightarrow \begin{bmatrix} \tilde{G}_{LC}(t_1^+, t_2^+) & \tilde{G}_{LC}(t_1^+, t_2^-) \\ \tilde{G}_{LC}(t_1^-, t_2^+) & \tilde{G}_{LC}(t_1^-, t_2^-) \end{bmatrix} = \begin{bmatrix} \tilde{G}_{LC}^t(t_1, t_2) & \tilde{G}_{LC}^<(t_1, t_2) \\ \tilde{G}_{LC}^>(t_1, t_2) & \tilde{G}_{LC}^{\bar{t}}(t_1, t_2) \end{bmatrix}.$$

According to the basic analysis of Feynman diagrams, the contour-ordered Green's functions \tilde{G}_{LC} and \tilde{G}_{CL} are given as

$$\tilde{G}_{LC}(\tau_1, \tau_2) = \int_C \tilde{g}^L(\tau_1, \tau) V^{LC} \tilde{G}_{CC}(\tau, \tau_2) d\tau, \quad (5.14)$$

$$\tilde{G}_{CL}(\tau_1, \tau_2) = \int_C \tilde{G}_{CC}(\tau_1, \tau) V^{CL} \tilde{g}^L(\tau, \tau_2) d\tau \quad (5.15)$$

with the shifted bare Greens function for the left lead being

$$\tilde{g}^L(\tau_1, \tau_2) = -\frac{i}{\hbar} \left\langle T_\tau \hat{u}_L^x(\tau_1) \hat{u}_L^{x,T}(\tau_2) \right\rangle, \quad (5.16)$$

where

$$\tilde{G}_{CC}(\tau_1, \tau_2) = -\frac{i}{\hbar} \left\langle T_\tau \hat{u}_C(\tau_1) \hat{u}_C^T(\tau_2) \right\rangle_\lambda \quad (5.17)$$

is the central quantity for the study of the GF of the heat transfer, which we will discuss later. Just now, we use the treatment of symmetrization to simplify $\frac{\partial \ln \mathcal{Z}}{\partial \lambda_1}$ in Eq. (5.13) further according to the time-order version of Eq. (5.14) and Eq. (5.15), *i.e.*,

$$\begin{aligned} \tilde{G}_{LC}^t(t', t) &= \int_{t_0}^{t_M} \tilde{g}_L^t(t', t_1) V^{LC} \tilde{G}_{CC}^t(t_1, t) dt_1 - \int_{t_0}^{t_M} \tilde{g}_L^<(t', t_1) V^{LC} \tilde{G}_{CC}^>(t_1, t) dt_1 \\ \tilde{G}_{CL}^t(t, t') &= \int_{t_0}^{t_M} \tilde{G}_{CC}^t(t, t_1) V^{CL} \tilde{g}_L^t(t_1, t') dt_1 - \int_{t_0}^{t_M} \tilde{G}_{CC}^<(t, t_1) V^{CL} \tilde{g}_L^>(t_1, t') dt_1, \end{aligned}$$

which explicitly means that

$$\begin{aligned} &\frac{\partial \ln \mathcal{Z}(\lambda_2 - \lambda_1)}{\partial \lambda_1} \\ &= \frac{\hbar}{2} \int_{t_0}^{t_M} dt \frac{\partial}{\partial t'} \text{Tr} \left[\tilde{G}_{CL}^t(t, t') V^{LC} + \tilde{G}_{LC}^t(t', t) V^{CL} \right] \Big|_{t'=t} \quad (5.18) \end{aligned}$$

$$\begin{aligned} &= -\frac{\hbar}{2} \int_{t_0}^{t_M} dt dt' \text{Tr} \left[\tilde{G}_{CC}^>(t, t') \frac{\partial \tilde{\Sigma}_L^<(t', t)}{\partial t'} \right. \\ &\quad \left. + \tilde{G}_{CC}^<(t, t') \frac{\partial \tilde{\Sigma}_L^>(t', t)}{\partial t} \right] \quad (5.19) \end{aligned}$$

with the self-energy defined to be $\tilde{\Sigma}_L(\tau_1, \tau_2) = V^{CL} \tilde{g}_L(\tau_1, \tau_2) V^{LC}$. Eq. (5.19) is a generalized Meir-Wingreen formula. In obtaining the second equality we have used the relation $\frac{\partial \tilde{\Sigma}_L^t(t', t_1)}{\partial t'} = -\frac{\partial \tilde{\Sigma}_L^t(t', t_1)}{\partial t_1}$ since $\tilde{\Sigma}_L^t(t', t_1) = \tilde{\Sigma}_L^t(t' - t)$. Essentially we employ the procedure of symmetrization to get rid of the time-ordered version of $\tilde{G}_{CC}(\tau_1, \tau_2)$.

Setting $\lambda_1 = -\xi/2$ and $\lambda_2 = \xi/2$, and noticing that

$$\frac{\partial \tilde{\Sigma}_L^{<, >}(t', t_1)}{\partial t'} = -\frac{1}{\hbar} \frac{\partial \tilde{\Sigma}_L^{<, >}(t', t_1)}{\partial \xi} \quad (5.20)$$

$$\frac{\partial \tilde{\Sigma}_L^{t, \bar{t}}(t', t_1)}{\partial \xi} = 0, \quad (5.21)$$

we can obtain a compact expression for $\frac{\partial \ln \mathcal{Z}}{\partial(i\xi)}$ from the generalized Meir-Wingreen formula Eq. (5.19):

$$\begin{aligned} \frac{\partial \ln \mathcal{Z}}{\partial(i\xi)} &= \frac{1}{2} \int_{t_0}^{t_M} dt \int_{t_0}^{t_M} dt' \text{Tr} \left\{ \begin{pmatrix} \tilde{G}_{CC}^t(t, t') & \tilde{G}_{CC}^{<}(t, t') \\ -\tilde{G}_{CC}^{>}(t, t') & -\tilde{G}_{CC}^{\bar{t}}(t, t') \end{pmatrix} \begin{pmatrix} 0 & \frac{\partial \tilde{\Sigma}_L^{<}(t', t)}{\partial(i\xi)} \\ -\frac{\partial \tilde{\Sigma}_L^{>}(t', t)}{\partial(i\xi)} & 0 \end{pmatrix} \right\} \\ &= \frac{1}{2} \int_C d\tau \int_C d\tau' \text{Tr} \left[\tilde{G}_{CC}(\tau, \tau') \frac{\partial \tilde{\Sigma}_L(\tau', \tau)}{\partial(i\xi)} \right]. \end{aligned} \quad (5.22)$$

If needed, the proper normalization for the CGF, *i.e.*, $\ln \mathcal{Z}(\xi)$, can be determined by the constraint $\ln \mathcal{Z}(0) = 0$.

5.2 Interaction picture on the contour

The nonlinear effects on the GF are completely included in the \tilde{G}_{CC} , for which we try to obtain the closed Dyson equations now.

Recall the discussion on the Heisenberg picture defined on the contour in Sec. (2.2.2).

We can rewrite the \tilde{G}_{CC} from Eq. (5.17) as

$$\tilde{G}_{CC}(\tau_1, \tau_2) = -\frac{i}{\hbar} \left\langle U^S(t_0^-, t_M^-) U^S(t_M^+, t_0^+) T_\tau u_C^H(\tau_1) u_C^{H,T}(\tau_2) \right\rangle \frac{1}{Z}, \quad (5.23)$$

where the evolution operator U^S on the contour is determined by the modified total Hamiltonian $H_{tot}^x(\tau) = e^{ix_\tau H_L} H_{tot} e^{-ix_\tau H_L}$ and remember that $x_\tau = -\xi/2$ ($\xi/2$) with $\tau = t^+$ (t^-) on the upper (lower) branch of the contour C and

$$U^S(\tau_2, \tau_1) = \begin{cases} U_S^+(t_2, t_1), & (\tau_2 = t_2^+) > (\tau_1 = t_1^+) \\ U_S^-(t_2, t_M) U_S^+(t_M, t_1), & \tau_2 = t_2^-, \tau_1 = t_1^+ \\ U_S^-(t_2, t_1), & (\tau_2 = t_2^-) < (\tau_1 = t_1^-) \end{cases} \quad (5.24)$$

with the subscript $+$ ($-$) denoting the upper (lower) branch; the Heisenberg-picture operator such as $u_C^H(\tau_1)$ is defined as

$$u_C^H(\tau_1) = U^S(t_0^+, \tau_1) u_C U^S(\tau_1, t_0^+). \quad (5.25)$$

Now we define the interaction picture on the contour by using the model employed in this chapter as an example.

The modified total Hamiltonian can be split into two parts, *i.e.*,

$$H_{tot}^x(\tau) \equiv e^{ix_\tau H_L} H_{tot} e^{-ix_\tau H_L} = H_0^x(\tau) + H_n \quad (5.26)$$

We define the interaction-picture evolution operator as

$$U_I(\tau_1, \tau_2) = U_0^S(t_0^+, \tau_1) U^S(\tau_1, \tau_2) U_0^S(\tau_2, t_0^+), \quad (5.27)$$

where U_0^S is similar to U^S but determined by $H_0^x(\tau)$. According to the interaction-picture evolution operator, we can define the interaction-picture operator such as

$u_C^I(\tau_1)$ as

$$u_C^I(\tau_1) = U_0^S(t_0^+, \tau_1) u_C U_0^S(\tau_1, t_0^+). \quad (5.28)$$

The relation between the Heisenberg-picture operator and the interaction-picture one turns out to be

$$u_C^H(\tau_1) = U_I(t_0^+, \tau_1) u_C^I(\tau_1) U_I(\tau_1, t_0^+). \quad (5.29)$$

Further, the interaction-picture evolution operator can be expressed as

$$U_I(\tau_1, \tau_2) = T_\tau e^{-\frac{i}{\hbar} \int_{C[\tau_1, \tau_2]} H_n^I(\tau) d\tau} \quad (5.30)$$

for τ_1 succeeds τ_2 and $C[\tau_1, \tau_2]$ denotes the path along the contour C from τ_2 to τ_1 .

Using the interaction picture on the contour, we can rewrite the \tilde{G}_{CC} as

$$\tilde{G}_{CC}(\tau_1, \tau_2) = -\frac{i}{\hbar} \left\langle U_0^S(t_0^-, t_0^+) T_\tau u_C^I(\tau_1) u_C^{I,T}(\tau_2) e^{-\frac{i}{\hbar} \int_C d\tau H_n^I(\tau)} \right\rangle \frac{1}{\mathcal{Z}}, \quad (5.31)$$

which is shown below assuming that τ_1 succeeds τ_2 without loss of generality:

$$\tilde{G}_{CC}(\tau_1, \tau_2) = -\frac{i}{\hbar} \left\langle U_0^S(t_0^-, t_0^+) U_0^S(t_0^+, t_0^+) u_C^H(\tau_1) u_C^{H,T}(\tau_2) \right\rangle \frac{1}{\mathcal{Z}} \quad (5.32)$$

$$\begin{aligned} &= -\frac{i}{\hbar} \left\langle U_0^S(t_0^-, t_0^+) U_I(t_0^-, t_0^+) U_I(t_0^+, \tau_1) u_C^I(\tau_1) U_I(\tau_1, t_0^+) \right. \\ &\quad \left. U_I(t_0^+, \tau_2) u_C^{I,T}(\tau_2) U_I(\tau_2, t_0^+) \right\rangle \frac{1}{\mathcal{Z}} \end{aligned} \quad (5.33)$$

$$= -\frac{i}{\hbar} \left\langle U_0^S(t_0^-, t_0^+) T_\tau u_C^I(\tau_1) u_C^{I,T}(\tau_2) e^{-\frac{i}{\hbar} \int_C d\tau H_n^I(\tau)} \right\rangle \frac{1}{\mathcal{Z}}. \quad (5.34)$$

By introducing $\mathcal{Z}_0 = \left\langle T_\tau e^{-\frac{i}{\hbar} \int_C d\tau (\hat{u}_L^{x,T} V^{LC} \hat{u}_C + \hat{u}_C^T V^{CR} \hat{u}_R)} \right\rangle$, which is the GF when $H_n = 0$, and defining $\mathcal{Z}_n = \mathcal{Z}/\mathcal{Z}_0$, \tilde{G}_{CC} in Eq. (5.31) is written as

$$\tilde{G}_{CC}(\tau_1, \tau_2) = -\frac{i}{\hbar} \text{Tr} \left[\rho_{ini}^I T_\tau u_C^I(\tau_1) u_C^{I,T}(\tau_2) e^{-\frac{i}{\hbar} \int_C d\tau H_n^I(\tau)} \right] \frac{1}{\mathcal{Z}_n}, \quad (5.35)$$

where $\rho_{ini}^I = \rho_{ini} U_0^S(t_0^-, t_0^+) / \mathcal{Z}_0$, ($\text{Tr}(\rho_{ini}^I) = 1$). Notice that ρ_{ini}^I and the interaction-picture operator on the contour, such as $u_C^I(\tau_1)$, after second quantization satisfy the sufficient conditions for the Wick theorem to be valid presented in the appendix 5.5 of this chapter. Physically the key point is that under the interaction picture on the contour the nonlinear interaction is not incorporated into ρ_{ini}^I so that ρ_{ini}^I is still non-interacting, which is inherited from specially chosen initial product state ρ_{ini} .

Observing the structure of Eq. (5.35) and realizing that the denominator \mathcal{Z}_n cancels the disconnected diagrams, we can obtain the Dyson equation for \tilde{G}_{CC} as $\tilde{G}_{CC} = \tilde{G}_{CC}^0 + \tilde{G}_{CC}^0 \tilde{\Sigma}_n \tilde{G}_{CC}$, a symbolic notation of

$$\begin{aligned} \tilde{G}_{CC}(\tau_1, \tau_2) &= \tilde{G}_{CC}^0(\tau_1, \tau_2) \\ &+ \int_C d\tau d\tau' \tilde{G}_{CC}^0(\tau_1, \tau) \tilde{\Sigma}_n(\tau, \tau') \tilde{G}_{CC}(\tau', \tau_2) \end{aligned} \quad (5.36)$$

in terms of

$$\tilde{G}_{CC}^0 = -\frac{i}{\hbar} \text{Tr} \left[\rho_{ini}^I T_\tau u_C^I(\tau_1) u_C^{I,T}(\tau_2) \right] \quad (5.37)$$

and the nonlinear self energy $\tilde{\Sigma}_n$ constructed by the bare propagator \tilde{G}_{CC}^0 , whose vertices are solely due to the nonlinear Hamiltonian H_n .

Going to the interaction picture with respect to the free Hamiltonian $h = H_L + H_C + H_R$, \tilde{G}_{CC}^0 can be written as

$$\tilde{G}_{CC}^0(\tau_1, \tau_2) = -\frac{i}{\hbar} \left\langle T_\tau \hat{u}_C(\tau_1) \hat{u}_C^T(\tau_2) e^{-\frac{i}{\hbar} \int_C d\tau \hat{u}_L^{x,T}(\tau) V^{LC} \hat{u}_C(\tau) + \hat{u}_C^T(\tau) V^{CR} \hat{u}_R(\tau)} \right\rangle \frac{1}{\mathcal{Z}_0} \quad (5.38)$$

so that

$$\tilde{G}_{CC}^0 = g_C + g_C \left(\tilde{\Sigma}_L + \Sigma_R \right) \tilde{G}_{CC}^0, \quad (5.39)$$

where $\Sigma_R(\tau_1, \tau_2)$ is the right-lead version of the ordinary contour-order self energy $\Sigma_\nu = V^{C\nu} g_\nu V^{\nu C}$, $\nu = L, R$, in which $g_\alpha(\tau_1, \tau_2)_{jk} = -\frac{i}{\hbar} \langle T_\tau \hat{u}_{\alpha,j}(\tau_1) \hat{u}_{\alpha,k}(\tau_2) \rangle$ for $\alpha = L, C, R$ are the uncoupled contour-order Green's functions.

Though Eq. (5.36) and Eq. (5.36) are enough for the calculation of \tilde{G}_{CC} , for convenience one can introduce an counting-field independent auxiliary equation $G_{CC}^0 = g_C + g_C(\Sigma_L + \Sigma_R)G_{CC}^0$, and combine it with Eqs. (5.36) and (5.39) to obtain a closed Dyson equation for $\tilde{G}_{CC}(\tau_1, \tau_2)$:

$$\tilde{G}_{CC} = G_{CC}^0 + G_{CC}^0 \left(\Sigma_A + \tilde{\Sigma}_n \right) \tilde{G}_{CC}, \quad (5.40)$$

where the shifted self energy $\Sigma_A \equiv \tilde{\Sigma}_L - \Sigma_L$, which first appears in Ref. [30], accounts for the distribution of heat transfer in ballistic systems.

From now on, for notational simplicity, all the subscripts CC of the Green's functions will be suppressed and the superscript 0 in both \tilde{G}_{CC}^0 and G_{CC}^0 will be re-expressed as a subscript.

Until now, the formalism for studying the distribution of heat transport across general nonlinear junctions has been completely established. As before, the CGF can be used to calculate cumulants of heat transfer. In the case of steady state, one simply set $t_0 \rightarrow -\infty$ and $t_M \rightarrow +\infty$ simultaneously, and technically assume that real-time versions of $\tilde{G}(\tau_1, \tau_2)$ are time-translationally invariant. Then going to the Fourier space, Eq. (5.22) for $\frac{\partial \ln \mathcal{Z}}{\partial(i\xi)}$ in steady state could be rewritten as

$$\frac{\partial \ln \mathcal{Z}}{\partial(i\xi)} = (t_M - t_0) \int_{-\infty}^{\infty} d\omega \frac{\hbar\omega}{2\pi} \text{Tr} \left[\tilde{G}^{<} \Sigma_L^> e^{-i\hbar\omega\xi} \right] \quad (5.41)$$

after taking into account $\tilde{G}^{>}[-\omega] = \tilde{G}^{<}[\omega]^T$ and $\Sigma_L^{<}[-\omega] = \Sigma_L^{>}[\omega]^T$. In the

Fourier space, due to Eq. (5.40) exact result for $\tilde{G}[\omega]$ could be yielded as

$$\tilde{G}[\omega] = \left(G_0[\omega]^{-1} - \Sigma_A[\omega] - \tilde{\Sigma}_n[\omega] \right)^{-1} \quad (5.42)$$

when keeping in mind the convention that the contour-order Green's function such as $\tilde{G}(\tau_1, \tau_2)$ in frequency space is written as

$$\tilde{G}[\omega] = \begin{bmatrix} \tilde{G}^t[\omega] & \tilde{G}^<[\omega] \\ -\tilde{G}^>[\omega] & -\tilde{G}^{\bar{t}}[\omega] \end{bmatrix}. \quad (5.43)$$

5.3 Application to molecular junction

Now we apply the general formalism developed above to study a monatomic molecule with a quartic nonlinear on-site pinning potential, that is, $H_n = \frac{1}{4}\lambda u_{C,0}^4$ in Eq. (5.1). In this case, the nonlinear contour-order self energy exact up to the first order in the nonlinear strength is

$$\tilde{\Sigma}_n(\tau, \tau') = 3i\hbar\lambda\tilde{G}_0(\tau, \tau')\delta(\tau, \tau'), \quad (5.44)$$

where recall that the generalized δ -function $\delta(\tau, \tau')$ is the counterpart of the ordinary Dirac delta function on the contour C introduced in Eq. (2.31). Thus the corresponding frequency-space nonlinear self energy is

$$\tilde{\Sigma}_n[\omega] = 3i\hbar\lambda \begin{bmatrix} \tilde{G}_0^t(0) & 0 \\ 0 & \tilde{G}_0^{\bar{t}}(0) \end{bmatrix}. \quad (5.45)$$

Consequently, exact up to first order in nonlinear strength the CGF for the molecular junction could be given as

$$\begin{aligned} \frac{1}{(t_M - t_0)} \frac{\partial \ln \mathcal{Z}(\xi)}{\partial (i\xi)} &= - \int_{-\infty}^{\infty} \frac{d\omega}{4\pi} \left\{ \frac{\partial \ln D[\omega]}{\partial (i\xi)} - 3i\hbar\lambda \right. \\ &\times \left[\tilde{G}_0^t(0) G_0^t[\omega] - \tilde{G}_0^{\bar{t}}(0) G_0^{\bar{t}}[\omega] \right] \frac{\partial}{\partial (i\xi)} \frac{1}{D[\omega]} \Big\} \end{aligned} \quad (5.46)$$

with

$$\begin{aligned} D[\omega] &\equiv \det \left[I - G_0[\omega] \Sigma_A[\omega] \right] \\ &= 1 - T[\omega] \left[(e^{i\xi\hbar\omega} - 1) f_L (1 + f_R) + (e^{-i\xi\hbar\omega} - 1) f_R (1 + f_L) \right] \end{aligned} \quad (5.47)$$

and $\tilde{G}_0^{t,\bar{t}}(0) = \int_{-\infty}^{\infty} \frac{d\omega}{2\pi} G_0^{t,\bar{t}}[\omega] / D[\omega]$, where $T[\omega] = \text{Tr}(G_0^r \Gamma_R G_0^a \Gamma_L)$ is the transmission coefficient in the ballistic system, and $f_{\{L,R\}} = \{\exp(\beta_{\{L,R\}} \hbar\omega) - 1\}^{-1}$ is the Bose-Einstein distribution function for phonons. Here $G_0^r = G_0^t - G_0^<$ and $G_0^a = G_0^< - G_0^{\bar{t}}$ are retarded and advanced Green's functions, respectively. Also $\Gamma_{\{L,R\}} = i \left[\Sigma_{\{L,R\}}^r - \Sigma_{\{L,R\}}^a \right]$, related to the spectral density of the baths, are expressed by retarded and advanced self energies similarly defined as Green's functions.

One could easily use this CGF in Eq. (5.46) to evaluate cumulants. The steady current out of the left lead is closely related to the first cumulant so that

$$\begin{aligned} I^{ss} &= \frac{d}{dt_M} \left(\frac{\partial \ln \mathcal{Z}(\xi)}{\partial (i\xi)} \Big|_{\xi=0} \right) \\ &= \int_{-\infty}^{\infty} \frac{d\omega}{4\pi} \hbar\omega (1 + \Lambda[\omega]) T[\omega] (f_L - f_R), \end{aligned} \quad (5.48)$$

where $\Lambda[\omega] \equiv 3i\hbar\lambda G_0^t(0) (G_0^a[\omega] + G_0^r[\omega])$ is the first-order nonlinear correction to the transmission coefficient.

The fluctuation for steady-state heat transfer in the molecular junction is obtained by taking the second derivative with respect to $i\xi$, and then setting $\xi = 0$:

$$\begin{aligned} \frac{\langle\langle Q^2 \rangle\rangle}{(t_M - t_0)} &= \int_{-\infty}^{\infty} \frac{d\omega}{4\pi} \left\{ (\hbar\omega)^2 T^2[\omega] (1 + 2\Lambda[\omega]) (f_L - f_R)^2 \right. \\ &\quad + 3\hbar^2 \lambda \omega \left[G_0^{\bar{t}}[\omega] \delta \tilde{G}_0^{\bar{t}} - G_0^t[\omega] \delta \tilde{G}_0^t \right] T[\omega] (f_L - f_R) \\ &\quad \left. + (\hbar\omega)^2 T[\omega] (1 + \Lambda[\omega]) (f_L + f_R + 2f_L f_R) \right\}, \end{aligned} \quad (5.49)$$

where,

$$\delta \tilde{G}_0^{t,\bar{t}} \equiv \left. \frac{\partial \tilde{G}_0^{t,\bar{t}}(0)}{\partial \xi} \right|_{\xi=0} = -i \int_{-\infty}^{\infty} \frac{d\omega}{2\pi} \hbar\omega T[\omega] (f_L - f_R) G_0^{t,\bar{t}}[\omega]. \quad (5.50)$$

Higher-order cumulants can be also systematically given by corresponding higher-order derivatives.

In the following Fig 5.1, we give a numerical illustration to the first three cumulants for heat transfer in this molecular junction using a self-consistent procedure [74], which means that the nonlinear contour-order self energy is taken as

$$\tilde{\Sigma}_n(\tau, \tau') = 3i\hbar\lambda \tilde{G}(\tau, \tau') \delta(\tau, \tau') \quad (5.51)$$

by replacing \tilde{G}_0 with the dressed one \tilde{G} , and \tilde{G} is obtained self-consistently using Eq. (5.40). The immediate physical interpretation is that the dressed interaction is just a screened interaction and the dressed line represents a quasi-particle process.

As shown, the effect of nonlinearity is to reduce the current as well as higher order fluctuations, and the fact that third and higher order cumulants are small but nonzero implies that the distribution for transferred energy is not Gaussian. In this numerical illustration, the Rubin baths are used, that is, K_α , $\alpha = L, R$ in

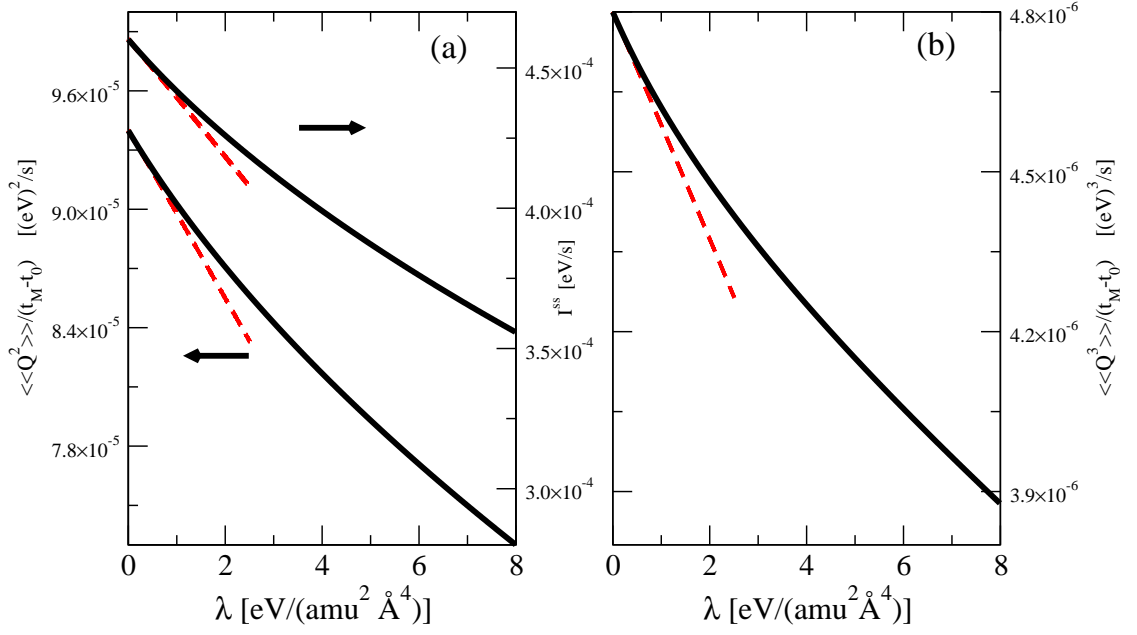


Figure 5.1: The first three steady-state cumulants with nonlinear strength λ for $k = 1 \text{ eV}/(\text{u}\text{\AA}^2)$, $k_0 = 0.1k$, $K_C = 1.1k$, and $V_{-1,0}^{LC} = V_{0,1}^{CR} = -0.25k$. The solid (dotted) line shows the self-consistent (first-order in λ) results for the cumulants.

The temperatures of the left and right lead are 660 K and 410 K, respectively.

Eq. (5.1) are both the semi-infinite tridiagonal spring constant matrix consisting of $2k + k_0$ along the diagonal and $-k$ along the two off-diagonals. And only the nearest interaction $V_{-1,0}^{LC}$ and $V_{0,1}^{CR}$ between the molecular and the two bathes are considered and $H_C = \frac{1}{2}p_{C,0}^2 + \frac{1}{2}K_C u_{C,0}^2$. As expected, for weak nonlinearity the first-order perturbation results, presented as dotted lines, are comparative with the corresponding self-consistent ones.

5.4 Summary

A formally rigorous formalism dealing with cumulants of heat transfer across nonlinear quantum junctions is established based on field theoretical and NEGF methods. The CGF for the heat transfer in both transient and steady-state regimes is studied on an equal footing and useful formulas for the CGF are obtained. A new feature of this formalism is that counting-field dependent full Green's function \tilde{G}_{CC} can be expressed solely through the nonlinear term $H_n^I(\tau)$ with the help of an interaction-picture transformation defined on a contour. Although we focus on the distribution of heat transfer in pure nonlinear phononic systems, there is no doubt that this general formalism can be readily employed to handle any other nonlinear system, such as electron-phonon interaction and Joule heating problems. Up to the first order in the nonlinear strength for the single-site quartic model, the CGF for steady-state heat transfer is obtained and explicit results for the steady current and fluctuation of steady-state heat transfer are given. A self-consistent procedure, which works well for strong nonlinearity, is also introduced to numerically check our general formalism.

5.5 Appendix: The Wick Theorem (Phonons)

In this appendix, we try to give sufficient conditions for the Wick theorem to be valid which covers most of the situation we encounter. The discussion is limited to the case of bosonic operators which is the main interest in this thesis. We mainly follow Gaudin's approach [75]. For an alternative proof, one can resort to the Ref. [76].

First we explain what the Wick theorem is. The Wick theorem says that the average value of a product of creation and annihilation operators is equal to the sum of all complete systems of pairings, mathematically which can be stated as

$$\begin{aligned}
 \text{Tr} \{ \rho^{ini} \beta_1 \beta_2 \cdots \beta_s \} &= \text{Tr} \{ \rho^{ini} \beta_1 \beta_2 \} \text{Tr} \{ \rho^{ini} \beta_3 \beta_4 \cdots \beta_s \} \\
 &+ \text{Tr} \{ \rho^{ini} \beta_1 \beta_3 \} \text{Tr} \{ \rho^{ini} \beta_2 \beta_4 \cdots \beta_s \} \\
 &+ \cdots \\
 &+ \text{Tr} \{ \rho^{ini} \beta_1 \beta_s \} \text{Tr} \{ \rho^{ini} \beta_2 \beta_3 \cdots \beta_{s-1} \}
 \end{aligned} \tag{5.52}$$

and then applying this relation recursively to all of the multiple operator averages until only pairs of operators remain.

Now we explore the sufficient conditions for the Wick theorem to be justified, which simply means that Eq. (5.52) is valid. Suppose the system's degrees of freedom is f , and we define

$$\alpha = \begin{pmatrix} a \\ a^\dagger \end{pmatrix}, \quad \alpha_i = a_i, \quad \alpha_{f+i} = a_i^\dagger, \quad i = 1, 2, \dots, f, \tag{5.53}$$

where a_i and a_i^\dagger are annihilation and creation operators respectively.

Assume

$$\alpha_i \rho^{ini} = \sum_{k=1}^{2f} h_{ik} \rho^{ini} \alpha_k, \quad (5.54)$$

where h_{ik} are c -numbers. We prove the Wick theorem for $\text{Tr} \{ \rho^{ini} \alpha_{i_1} \alpha_{i_2} \cdots \alpha_{i_s} \}$, which is shown below:

$$\begin{aligned} \text{Tr} \{ \rho^{ini} \alpha_{i_1} \alpha_{i_2} \cdots \alpha_{i_s} \} &= \text{Tr} \{ \rho^{ini} [\alpha_{i_1}, \alpha_{i_2}] \cdots \alpha_{i_s} \} + \text{Tr} \{ \rho^{ini} \alpha_{i_2} \alpha_{i_1} \cdots \alpha_{i_s} \} \\ &= \text{Tr} \{ \rho^{ini} [\alpha_{i_1}, \alpha_{i_2}] \cdots \alpha_{i_s} \} + \text{Tr} \{ \rho^{ini} \alpha_{i_2} [\alpha_{i_1}, \alpha_{i_3}] \cdots \alpha_{i_s} \} \\ &\quad + \text{Tr} \{ \rho^{ini} \alpha_{i_2} \alpha_{i_3} \alpha_{i_1} \cdots \alpha_{i_s} \} \\ &= \text{Tr} \{ \rho^{ini} [\alpha_{i_1}, \alpha_{i_2}] \cdots \alpha_{i_s} \} + \text{Tr} \{ \rho^{ini} \alpha_{i_2} [\alpha_{i_1}, \alpha_{i_3}] \cdots \alpha_{i_s} \} \\ &\quad + \text{Tr} \{ \rho^{ini} \alpha_{i_2} \alpha_{i_3} [\alpha_{i_1}, \alpha_{i_4}] \cdots \alpha_{i_s} \} + \text{Tr} \{ \rho^{ini} \alpha_{i_2} \alpha_{i_3} \alpha_{i_4} \alpha_{i_1} \cdots \alpha_{i_s} \} \\ &= \cdots \\ &= \sum_{j=2}^s [\alpha_{i_1}, \alpha_{i_j}] \text{Tr} \{ \rho^{ini} \overset{\circ}{\alpha}_{i_1} \alpha_{i_2} \cdots \overset{\circ}{\alpha}_{i_j} \cdots \alpha_{i_s} \} \\ &\quad + \text{Tr} \{ \alpha_{i_1} \rho^{ini} \alpha_{i_2} \alpha_{i_3} \cdots \alpha_{i_s} \} \\ &= \sum_{j=2}^s [\alpha_{i_1}, \alpha_{i_j}] \text{Tr} \{ \rho^{ini} \overset{\circ}{\alpha}_{i_1} \alpha_{i_2} \cdots \overset{\circ}{\alpha}_{i_j} \cdots \alpha_{i_s} \} \\ &\quad + \sum_{k=1}^{2f} h_{i_1 k} \text{Tr} \{ \rho^{ini} \alpha_k \alpha_{i_2} \alpha_{i_3} \cdots \alpha_{i_s} \} \end{aligned} \quad (5.55)$$

where the circle over the operator means that this operator is omitted. Then

$$\sum_{k=1}^{2f} (1-h)_{i_1 k} \text{Tr} \{ \rho^{ini} \alpha_k \alpha_{i_2} \cdots \alpha_{i_s} \} = \sum_{j=2}^s [\alpha_{i_1}, \alpha_{i_j}] \text{Tr} \{ \rho^{ini} \overset{\circ}{\alpha}_{i_1} \alpha_{i_2} \cdots \overset{\circ}{\alpha}_{i_j} \cdots \alpha_{i_s} \}$$

Multiply by the inverse matrix $(1-h)^{-1}$, we can get

$$\begin{aligned} &\text{Tr} \{ \rho^{ini} \alpha_{i_1} \alpha_{i_2} \cdots \alpha_{i_s} \} \\ &= \sum_{j=2}^s \left\{ \sum_{k=1}^{2f} (1-h)_{i_1 k}^{-1} [\alpha_k, \alpha_{i_j}] \right\} \text{Tr} \{ \rho^{ini} \overset{\circ}{\alpha}_{i_1} \alpha_{i_2} \cdots \overset{\circ}{\alpha}_{i_j} \cdots \alpha_{i_s} \} \end{aligned} \quad (5.56)$$

After considering the special case

$$\text{Tr} \{ \rho^{ini} \alpha_{i_1} \alpha_{i_j} \} = \sum_{k=1}^{2f} (1-h)_{i_1 k}^{-1} [\alpha_k, \alpha_{i_j}], \quad (5.57)$$

we obtain from Eq. (5.56)

$$\text{Tr} \{ \rho^{ini} \alpha_{i_1} \alpha_{i_2} \cdots \alpha_{i_s} \} = \sum_{j=2}^s \text{Tr} \{ \rho^{ini} \alpha_{i_1} \alpha_{i_j} \} \text{Tr} \{ \rho^{ini} \overset{\circ}{\alpha}_{i_1} \alpha_{i_2} \cdots \overset{\circ}{\alpha}_{i_j} \cdots \alpha_{i_s} \},$$

Assume

$$\beta_j = \sum_{i=1}^{2f} g_{ji} \alpha_i \quad (5.58)$$

where g_{ji} are c -numbers. Then

$$\begin{aligned} \text{Tr} \{ \rho^{ini} \beta_1 \beta_2 \cdots \beta_s \} &= \sum_{i_1} \sum_{i_2} \cdots \sum_{i_s} g_{1i_1} g_{2i_2} \cdots g_{si_s} \text{Tr} \{ \rho^{ini} \alpha_{i_1} \alpha_{i_2} \cdots \alpha_{i_s} \} \\ &= \sum_{i_1} \sum_{i_2} \cdots \sum_{i_s} g_{1i_1} g_{2i_2} \cdots g_{si_s} \sum_{j=2}^s \text{Tr} \{ \rho^{ini} \alpha_{i_1} \alpha_{i_j} \} \\ &\quad \times \text{Tr} \{ \rho^{ini} \overset{\circ}{\alpha}_{i_1} \alpha_{i_2} \cdots \overset{\circ}{\alpha}_{i_j} \cdots \alpha_{i_s} \} \\ &= \sum_{j=2}^s \text{Tr} \{ \rho^{ini} \beta_1 \beta_j \} \text{Tr} \{ \rho^{ini} \overset{\circ}{\beta}_1 \beta_2 \cdots \overset{\circ}{\beta}_j \cdots \beta_s \} \end{aligned}$$

which is just the Eq. (5.52).

In summary, the sufficient conditions for the Wick theorem Eq. (5.52) to be valid are Eq. (5.54) and Eq. (5.58) and implicitly $\text{Tr}(\rho^{ini}) = 1$.

In the following, we try to figure out the form of initial density matrix ρ^{ini} satisfying Eq. (5.54), which turns out to be

$$\rho^{ini} = e^{-\alpha^T A \alpha} \quad (5.59)$$

with A to be a general square matrix. We neglect the normalization constant for $\text{Tr}(\rho^{ini}) = 1$ here. To this end, we split the A to be a symmetrical part and an

anti-symmetrical part, that is

$$A = \frac{1}{2}(A + A^T) + \frac{1}{2}(A - A^T) \quad (5.60)$$

$$\equiv A^s + A^a. \quad (5.61)$$

Let us define

$$\begin{aligned} f_i(t) &\equiv e^{t\alpha^T A \alpha} \alpha_i e^{-t\alpha^T A \alpha} \\ &= e^{t\frac{1}{2}\alpha^T A^s \alpha} \alpha_i e^{-t\frac{1}{2}\alpha^T A^s \alpha}. \end{aligned}$$

In obtaining the second equality, notice that $\alpha^T A^a \alpha$ is a c -number due to $[\alpha, \alpha^\dagger] = \begin{pmatrix} 1 & 0 \\ 0 & -1 \end{pmatrix}$ and $A^{a,T} = -A^a$. Thus

$$\begin{aligned} \frac{df_i(t)}{dt} &= e^{t\frac{1}{2}\alpha^T A^s \alpha} \left[\frac{1}{2} \alpha^T A^s \alpha, \alpha_i \right] e^{-t\frac{1}{2}\alpha^T A^s \alpha} \\ &= - \sum_j (\sigma A^s)_{ij} f_j(t), \end{aligned}$$

where $\sigma \equiv \begin{pmatrix} 0 & -1 \\ 1 & 0 \end{pmatrix}$. So $f_i(t) = \sum_j (e^{-t\sigma A^s})_{ij} \alpha_j$ and $f_i(1) = e^{\alpha^T A \alpha} \alpha_i e^{-\alpha^T A \alpha} = \sum_j (e^{-\sigma A^s})_{ij} \alpha_j$ or equivalently

$$\alpha_i e^{-\alpha^T A \alpha} = \sum_j (e^{-\sigma A^s})_{ij} e^{-\alpha^T A \alpha} \alpha_j. \quad (5.62)$$

More generally, the multiplication of finite number of the form of Eq. (5.59) still satisfies Eq. (5.54), such as

$$\rho^{ini} = e^{-\alpha^T A \alpha} e^{-\alpha^T B \alpha}, \quad (5.63)$$

which is briefly shown below:

$$\begin{aligned}
 \alpha_i \rho^{ini} &= \alpha_i e^{-\alpha^T A \alpha} e^{-\alpha^T B \alpha} \\
 &= \sum_j (e^{-\sigma A^s})_{ij} e^{-\alpha^T A \alpha} \alpha_j e^{-\alpha^T B \alpha} \\
 &= \sum_j (e^{-\sigma A^s})_{ij} e^{-\alpha^T A \alpha} \sum_k (e^{-\sigma B^s})_{jk} e^{-\alpha^T B \alpha} \alpha_k \\
 &= \sum_j \sum_k (e^{-\sigma A^s})_{ij} (e^{-\sigma B^s})_{jk} \rho^{ini} \alpha_k \\
 &= \sum_k (e^{-\sigma A^s} e^{-\sigma B^s})_{ik} \rho^{ini} \alpha_k.
 \end{aligned}$$

Due to the sufficient conditions presented in this appendix, the Wick theorem used in this thesis for the Feynman-diagrammatic analysis is justified. For example, for the case of the interaction picture on the contour, initial density matrix $\rho_{ini}^I = \rho_{ini} U_0^S(t_0^-, t_0^+) / \mathcal{Z}_0 = \Pi_{\alpha=L,C,R} \frac{e^{-\beta \alpha H_\alpha}}{\text{Tr}(e^{-\beta \alpha H_\alpha})} e^{-\frac{i}{\hbar} H_0^x(t^-)(t_0-t_M)} e^{-\frac{i}{\hbar} H_0^x(t^+)(t_M-t_0)} / \mathcal{Z}_0$ is the multiplication of finite number of the form of Eq. (5.59) and $\text{Tr}(\rho_{ini}^I) = 1$. In addition, interaction-picture operator on the contour such as $u_C^I(\tau_1)$ in the Eq. (5.28) can be expressed as the linear transformation of α defined in the Eq. (5.53) according to the similar steps for the calculation of $f_i(t)$.

Chapter 6

Summary and future works

We have considered the energy transport from the consistent-history viewpoint on quantum mechanics using the NEGF method. Using a Heisenberg equation of motion method, the nonequilibrium steady state employed in NEGF has been studied. It is shown that on-site potential is crucial for the dynamical reach of steady-state thermal transport from initial product state by the sudden switch-on of the coupling between the baths. Moreover, we have extended the traditional Caroli formula describing the transmission of the heat in lead-junction-lead systems to the case incorporating the lead-lead coupling. In the coupled left-right-lead quantum systems, the distribution of energy transport has been studied and the analytic expression for the cumulant generating function (CGF) of energy transport in a given time duration is obtained, in terms of which fluctuation symmetry is verified. Also, the effects of the quasi-classical approximation on the CGF of energy transport are studied. Furthermore, by introducing interaction picture on

the contour, the compact formalism for the distribution of energy transport across nonlinear systems is established.

It may be noticed that there are two main lines in this thesis, which are clarified as below. The first line involves the complexity of the quantum histories we used to study the energy transport. Specifically, for the steady-state thermal current we simply employed one-time quantum histories, while for the study of probability distribution of energy transport in a given time duration we employed two-time quantum histories. Naturally, the next step for the future work is to consider the application of multi-time quantum histories on the study of the quantum thermal transport [77–79]. For example, we can use continuous quantum histories to construct a new definition of quantum work since work done is really a processing quantity which depends on the whole process of the quantum history. Based on this new definition, we can check the Jarzynski’s equality reflecting the principal of microreversibility of the underlying dynamics and look at the interplay between time-dependent evolution and quantum measurements. Actually the preliminary work has been already done, see Ref. [80]. But we have to admit that it is not so successful there since the states we used are eigenstates of position operators, which can not be normalized. Thus we have to improve this work such as using the normalizable gaussian wave packet to express the states.

On the other hand, it has been noticed that Kundu *et al.* developed a formalism to calculate the distribution of heat flow in a classical harmonic chain, and more importantly obtained the lowest order correction to the CGF [34]. Therefore, we can try to improve and obtain the correction of the quantum CGF formula we have already got in ballistic systems, which turns out to be much more challenging.

Before that, in order to appreciate the quantum correction we may use the quasi-classical approximation, which employs quantum heat baths, to partially consider the quantum effects, see the Ref. [72] and the appendix 4.7.

The other line involves the complexity of the quantum systems we considered. Specifically, we have extended the study of the probability distribution of energy transport in a given time duration to nonlinear systems from ballistic systems. The future work in this respect is try to use the established formalism to study the experimental setup. For example, a recent shot noise measurement on Au nanowires has demonstrated the pronounced phonon signature in electron noise [81], which involves the effects of electron-phonon interaction on electron transport accompanying the energy transport. As a preliminary step, we can study the probability distribution of the coupled electron-phonon transport in one-dimensional atomic junctions in the presence of a weak electron-phonon interaction [82].

The systematic study of this thesis and the proposed plans may enhance our understanding on quantum thermal transport in nanoscale systems and provide a guideline for optimal design of transport devices in nanoscale systems. In addition, the insights into statistics aspect of the quantum thermal transport are provided by using microphysics models to approach the fluctuation theorem.

References

- [1] K. Schwab, E. A. Henriksen, J. M. Worlock, and M. L. Roukes, *Nature* **404**, 974 (2000).
- [2] C. Flindt, C. Fricke, F. Hohls, T. Novotný, K. Netočný, T. Brandes, and R. J. Haug, *Proc. Natl. Acad. Sci. USA* **106**, 10116 (2009).
- [3] M. L. Roukes, *Physica B*, 263, 1 (1999).
- [4] M. Esposito, U. Harbola, and S. Mukamel, *Rev. Mod. Phys.*, **81**, 1665 (2009).
- [5] M. Campisi, P. Hänggi, and P. Talkner, *Rev. Mod. Phys.*, **83**, 771 (2011).
- [6] L. G. C. Rego and G. Kirczenow, *Phys. Rev. Lett.* **81**, 232, (1998).
- [7] M. P. Blencowe, *Phys. Rev. B* **59**, 4992 (1999).
- [8] D. Segal, A. Nitzan, and P. Hänggi, *J. Chem. Phys.* **119**, 6840 (2003).
- [9] A. Dhar and D. Roy, *J. Stat. Phys.* **125**, 805 (2006).
- [10] A. Dhar, *Adv. in Phys.*, **57**, 457-537 (2008).
- [11] A. Ozpineci and S. Ciraci, *Phys. Rev. B* **63**, 125415 (2001).

References

- [12] J.-S. Wang, J. Wang, and N. Zeng, Phys. Rev. B **74**, 033408 (2006).
- [13] M. Galperin, A. Nitzan, and M. A. Ratner, Phys. Rev. B **75**, 155312 (2007).
- [14] Y. Meir and N. S. Wingreen, Phys. Rev. Lett. **68**, 2512 (1992).
- [15] T. Yamamoto and K. Watanabe, Phys. Rev. Lett. **96**, 255503 (2006).
- [16] C. Caroli, R. Combescot, P. Nozieres, and D. Saint-James, J. Phys. C: Solid St. Phys. **4**, 916 (1971).
- [17] N. Mingo and L. Yang, Phys. Rev. B **68**, 245406, (2003).
- [18] W. Zhang, T. S. Fisher, and N. Mingo, Numer. Heat Transf. Part B, **51**, 333 (2007).
- [19] S. G. Das and A. Dhar arXiv:1204.5595.
- [20] M. Di. Ventra, *Electrical Transport in Nanoscale Systems*, Cambridge University Press, 2008.
- [21] R. J. Rubin and W. L. Greer, J. Math. Phys. **12**, 1686 (1971).
- [22] J.-S. Wang, B. K. Agarwalla, and H. Li, Phys. Rev. B **84**, 153412, (2011).
- [23] L. S. Levitov and G. B. Lesovik, JETP Lett. **58**, 230 (1993).
- [24] W. Belzig and Y. V. Nazarov, Phys. Rev. Lett. **87**, 197006 (2001).
- [25] Y. V. Nazarov and M. Kindermann, Eur. Phys. J. B **35**, 413 (2003).
- [26] K. Schönhammer, Phys. Rev. B **75**, 205329 (2007); J. Phys.:Condens. Matter **21**, 495306 (2009).

- [27] K. Saito and A. Dhar, Phys. Rev. Lett. **99**, 180601 (2007); Phys. Rev. Lett. **101**, (2008) 049902(E).
- [28] J. Ren, P. Hänggi, and B. Li, Phys. Rev. Lett. **104**, 170601 (2010).
- [29] K. Saito and A. Dhar, Phys. Rev. E **83**, 041121 (2011).
- [30] J.-S. Wang, B. K. Agarwalla, and H. Li, Phys. Rev. B **84**, 153412 (2011).
- [31] B. K. Agarwalla, B. Li, and J.-S. Wang, Phys. Rev. E **85**, 051142 (2012).
- [32] Y. Utsumi, D. S. Golubev, M. Marthaler, K. Saito, T. Fujisawa, and G. Schön, Phys. Rev. B **81**, 125331 (2010).
- [33] R. Avriller and A. Levy Yeyati, Phys. Rev. B **80**, 041309 (2009).
- [34] A. Kundu, S. Sabhapandit, and A. Dhar J. Stat. Mech.: Theory Exp. (2011) P03007.
- [35] A. O. Gogolin and A. Komnik, Phys. Rev. B **73**, 195301 (2006).
- [36] R. B. Griffiths, J. Stat. Phys. **36**, 219 (1984).
- [37] R. Omnès, Rev. Mod. Phys. **64**, 339 (1992).
- [38] M. Gell-Mann and J. B. Hartle, *Quantum mechanics in the light of quantum cosmology, in Complexity, Entropy, and the Physics of Information*, W. Zurek, ed., (Addison Wesley, Reading, Massachusetts, 1990), p. 425; also in K. K. Phua and Y. Yamaguchi, eds., *Proceedings of the 25th International Conference on High Energy Physics*, (World Scientific, Singapore, 1990).
- [39] R. B. Griffiths, *Consistent Quantum Theory* (Cambridge University Press, Cambridge, 2002).

- [40] C. Cohen-Tannoudji, B. Diu and F. Laloë, *Quantum Mechanics* (Paris: Wiley-Hermann, 1977).
- [41] Kolmogorov, A. N., Grundbegriffe der Wahrscheinlichkeitrechnung, (Ergebnisse Der Mathematik, 1933) ; translated as Foundations of Probability, (New York: Chelsea Publishing Company, 1950).
- [42] E. C. Cuansing, H. Li, and J.-S. Wang, Phys. Rev. E **86**, 031132 (2012).
- [43] H. Li, B. K. Agarwalla, and J.-S. Wang, Phys. Rev. E **86**, 011141 (2012).
- [44] H. Li, B. K. Agarwalla, and J.-S. Wang, Phys. Rev. B **86**, 165425 (2012).
- [45] H. Li, B. K. Agarwalla, B. Li, and J.-S. Wang, arXiv:1210.2798.
- [46] J. Schwinger, J. Math. Phys., **2**, 407 (1961).
- [47] L. P. Kadanoff and G. Baym, *Quantum Statistical Mechanics* (Benjamin/Cummings, 1962).
- [48] L. V. Keldysh, Sov. Phys. JETP, 20, 1018 (1965).
- [49] J.-S. Wang, J. Wang, and J. T. Lü, Eur. Phys. J. B **62**, 381 (2008).
- [50] J.-S. Wang, B. K. Agarwalla, H. Li, and J. Thingna, Front. Phys. (2013).
- [51] A. L. Fetter and J. D. Walecka, *Quantum Theory of Many-Particle Systems* (McGraw-Hill, 1971).
- [52] C. Niu, D. L. Lin, and T.-H. Lin, J. Phys.:Condens.Matter, **11**, 1511 (1999).
- [53] J. Rammer, *Quantum Field Theory of Nonequilibrium States* (Cambridge 2007).

- [54] J.-S. Wang, N. Zeng, J. Wang, C.K. Gan, Phys. Rev. E **75**, 061128 (2007).
- [55] Y. Xu, J.-S. Wang, W. Duan, B.-L. Gu, and B. Li, Phys. Rev. B **78**, 224303 (2008).
- [56] H. Ness, L. K. Dash, and R. W. Godby, Phys. Rev. B **82**, 085426 (2010).
- [57] H. Haug and A.-P. Jauho, *Quantum Kinetics in Transport and Optics of Semiconductors*, 2nd ed. (Springer, New York, 2008).
- [58] L.V. Keldysh, Sov. Phys. JETP **20**, 1018 (1965).
- [59] J. Rammer and H. Smith, Rev. Mod.Phys. **58**, 323 (1986).
- [60] B. K. Agarwalla, J.-S. Wang, and B. Li, Unpublished.
- [61] L. Zhang, P. Keblinski, J.-S. Wang, and B. Li, Phys. Rev. B **83**, 064303 (2011).
- [62] H. Cramer, *Sur un nouveau théorème limite dans la théorie des probabilités*, in: *Colloque consacré à la théorie des probabilités*, vol. 3, (Hermann, Paris, 1938).
- [63] M.D. Donsker, S.R.S. Varadhan, Comm. Pure Appl. Math. **28**, 1 (1975).
- [64] M.I. Freidlin, A.D. Wentzell, *Random Perturbations of Dynamical Systems*, in: *Grundlehren der Mathematischen Wissenschaften*, (Springer- Verlag, New York, 1984).
- [65] R.S. Ellis, *Entropy, Large Deviations, and Statistical Mechanics*, (Springer, New York, 1985).
- [66] A. Dembo, O. Zeitouni, *Large Deviations Techniques and Applications*, 2nd ed., (Springer, New York, 1998).

References

- [67] H. Touchette, Phys. Rep., **478**, 1 (2009).
- [68] P. Talkner, E. Lutz, and P. Hänggi, Phys. Rev. E(R) **75**, 050102 (2007).
- [69] J. V. Neumann, *Mathematical Foundations of Quantum Mechanics* (Princeton University Press, Princeton, NJ, 1955).
- [70] G. Gallavotti and E. G. D. Cohen, Phys. Rev. Lett. **74**, 2694 (1995).
- [71] H. D. Cornean, P. Duclos, and R. Purice, Ann. Henri Poincaré **13**, 827 (2012).
- [72] J.-S. Wang, Phys. Rev. Lett. **99**, 160601 (2007).
- [73] R. P. Feynman, Phys. Rev. **56**, 340 (1939).
- [74] T.-H. Park and M. Galperin, Phys. Rev. B **84**, 205450 (2011).
- [75] M. Gaudin, Nucl. Phys. **15**, 89 (1960).
- [76] J.-P. Blaizot and G. Ripka, *Quantum Theory of Finite Systems* (Massachusetts: MIT Press, 1986).
- [77] M. Campisi, P. Talkner, and P. Hänggi, Phys. Rev. Lett. **105**, 140601 (2010).
- [78] M. Campisi, P. Talkner, and P. Hänggi, Phys. Rev. E **83**, 041114 (2011).
- [79] B. P. Venkatesh, G. Watanabe, P. Talkner, arXiv: 1309.4139.
- [80] H. Li and J.-S. Wang, arXiv: 1304.6286.
- [81] M. Kumar, R. Avriller, A. L. Yeyati and J. M. V. Ruitenbeek, Phys. Rev. Lett. **108**, 146602 (2012).
- [82] J. T. Lü and J.-S. Wang, Phys. Rev. B **76**, 165418 (2007).